

TR 90-64 ✓

THE GEOLOGY AND ALTERATION-MINERALISATION OF THE  
GAMIGAB TIN PROSPECT, DAMARALAND, NAMIBIA.

by

FELIX CASPAR WALRAVEN

THESIS

Submitted in fulfilment of the requirements  
for the degree: Master of Science

Department of Geology  
Rhodes University, 1989

Grahamstown, South Africa

## ABSTRACT

The stratigraphy at the Gamigab Sn prospect consists of two mainly schistose units separated by a thick marble unit which have been assigned to the Orusewa, the Karibib and the Kuiseb Formations respectively. Four phases of folding affected the lithologies with the south-south-west trending F2 folds defining the main structures in the region. The area underwent low grades of metamorphism. Temperatures were in the range 420° to 500°C and pressures less than 2 kbars. The effects of contact metamorphism are seen in the south-east and south-west. Regional metamorphism outlasted the deformation and contact metamorphism started late during deformation. Two Karoo-age intrusions penetrated the metasediments north of the mineralisation. One is an altered porphyry plug and the other is a weathered dolerite plug, the latter containing xenoliths of undeformed Karoo sediments. Cassiterite is hosted within east-west trending quartz veins that cross-cut previously altered schistose country rocks. The alteration types include sericitisation, tourmalinisation, carbonatisation and ferruginisation. Preliminary Rb/Sr dating on muscovite from the alteration zone suggests an age of  $509 \pm 11$  Ma. Breccias of probable hydrothermal origin are spatially associated with the mineralisation. These hydraulic breccias occur in antiformal structures within the marble and developed in response to a sudden pressure release due to a build up of fluids at the contact between the schistose Orusewa and carbonate Karibib Formations.

## CONTENTS

	PAGE
1. INTRODUCTION	1
1.1. Previous Work in North-Western Namibia	4
1.2. Previous Work at the Gamigab Prospect	5
1.3. Aim and Logistics of the Study at Gamigab	6
1.4. Physiography of the Study Area	6
2. REGIONAL GEOLOGICAL SETTING	8
2.1. General Features of the Damara Orogen	8
2.1.1. Intracontinental branch	9
2.1.2. Coastal branch	11
2.2. History of Sedimentation in the Damara Orogen	13
2.3. Structure	16
2.4. Metamorphism	19
2.5. Damara Magmatism	20
2.6. Post-Damara (Karoo) Rocks	22
2.7. Anorogenic Alkaline Magmatism	24
2.8. Geodynamic Evolution of the Damara Orogen	25
3. GEOLOGY OF THE SOUTHERN KAOKO ZONE	27
3.1. The Damara Sequence	27
3.1.1. Ogden Rocks Domain (ORD)	27
3.1.2. Lower Ugab Domain (LUD)	27
3.1.3. Goantagab Domain (GD)	31
3.2. Damara Granites	32
3.3. Post-Karoo Complexes	33
3.4. Metallogenesis in the Northern SKZ	35
4. THE GEOLOGY OF THE STUDY AREA	36
4.1. Basal Schist Unit	36
4.2. Banded Marble Unit	37

## CONTENTS (Continued)

4.2.1. Calcitic marble	38
4.2.2. Dolomitic marble	39
4.2.3. Streaky marble	40
4.3. Upper Schist Unit	40
4.3.1. Schist	41
4.3.2. Calc-silicate lenses	43
4.3.3. Marble interbeds	43
4.4. Intrusive Rocks	44
4.4.1. Porphyry plug	44
4.4.2. Dolerite plug	46
4.4.3. Dolerite dykes	47
4.4.4. Carbonate dykes	48
4.5. Discussion and Correlation of the Lithologies	49
5. STRUCTURE	54
5.1. Folding	54
5.1.1. F1 structures	54
5.1.2. F2 structures	55
5.1.3. F3 structures	57
5.1.4. F4 structures	58
5.2. Faulting	60
5.3. Summary of the Structural Development at Gamigab	60
5.4. Structural Development around Goantagab	62
5.5. Structural Development in the Goantagab Domain	63
6. METAMORPHISM	65
6.1. Regional Metamorphism	65
6.1.1. Indicator minerals in the metapelites	65
6.1.2. Indicator minerals in calc-silicate lenses	66
6.1.3. Indicator minerals in the marbles	67
6.1.4. P-T estimates for the Gamigab region	68
6.2. Contact Metamorphism	70
6.3. Relationship between Metamorphism and Structure	72

## CONTENTS (Continued)

7. THE EFFECTS OF HYDROTHERMAL ACTIVITY	74
7.1. Alteration-Mineralisation in the Orusewa Formation	74
7.1.1. Quartz veins	74
7.1.2. Vein margins	78
7.1.3. Wall rocks	80
7.1.4. Geochemistry of the alteration	81
7.1.5. Tourmaline composition	84
7.2. Brecciation in the Kariḃib Formation	87
7.2.1. Fragments	87
7.2.2. Matrix	88
7.2.3. Geochemistry of the porphyry plug	90
8. MODEL FOR HYDROTHERMAL DEPOSITS	95
8.1. Magma Characteristics	95
8.2. Hydrothermal Alteration	98
8.3. The Hydrothermal Environment at Gamigab	100
8.3.1. Alteration-mineralisation	100
8.3.2. Brecciation	103
8.3.3. Age of mineralisation	106
9. METALLOGENESIS IN THE SOUTHERN KAOKO ZONE	109
9.1. The Brandberg West Sn-W Deposit	110
9.2. Frans Prospect	112
9.3. Goantagab Mining Area	113
9.4. Discussion	114
9.4.1. Tourmaline composition	115
9.4.2. Fluid inclusion determinations	116
9.4.3. Sulphur isotope measurements	118
9.4.4. Concluding remarks	121

## CONTENTS (Continued)

10. SUMMARY	122
ACKNOWLEDGEMENTS	129
REFERENCES	130
APPENDIX 1	147
APPENDIX 2	149

## LIST OF FIGURES

<u>Figure</u> <u>Number</u>		<u>Page</u>
1	Geographical sketch map of north-western Namibia showing locality of the Gamigab tin prospect.	1
2	Simplified geological map of north-west Namibia showing positions and trends of mineralisation.	2
3	Simplified geological map between Goantagab and the Gamigab tin prospect.	3
4	Areas of previous work in north-west Namibia.	4
5	Reassembly of the Gondwana continent showing distribution of several Pan-African belts.	8
6	Simplified geological map showing the positions of the intracontinental and coastal branches.	10
7	Subdivisions of the Damara Orogen.	11
8	Supposed positions and geometry of rifts during early geosynclinal development of the Damara Orogen.	14
9	Schematic stratigraphic cross-section across the intracontinental branch.	15
10	Direction of vergence of the main structure in the Damara Orogen.	17
11	Metamorphic reaction isograds in the Damara Orogen.	20
12	Distribution of Damara-aged granites in the Damara Orogen.	21

## LIST OF FIGURES (Continued)

13	Generalised geological map at the join between the coastal and intracontinental branches, showing the distribution of Karoo-age sedimentary and volcanic rocks, and pre-, syn- and post-Karoo complexes.	23
14	Distribution of anorogenic alkaline ring complexes of the Damaraland province.	24
15	Geological map of the Southern Kaoko Zone showing the structural/lithological domains as defined by Freyer (in prep.).	28
16	Ages of metamorphism in the Southern Kaoko Zone.	30
17	Photomicrograph of basal quartz-biotite schist.	37
18	Photomicrograph of calcitic marble.	38
19	Photomicrograph of tremolite porphyroblasts in calcitic marble.	39
20	Photomicrograph of dolomitic marble.	40
21	Photograph of streaky marble in outcrop.	41
22	Photomicrograph of upper quartz-biotite-chlorite schist.	42
23	Photograph of cordierite porphyroblasts in upper schist.	42
24	Photograph of porphyry plug and satellite plugs in outcrop.	44
25	Close-up photograph of amygdaloidal and brecciated porphyry plug.	45
26	Photomicrograph of porphyry plug.	46

## LIST OF FIGURES (Continued)

27	Photograph of a minor intrafolial fold in the Karibib Formation.	55
28	Poles to banding and schistosity and measured lineations.	56
29	Photograph of F2 minor fold.	57
30	Schematic sketch showing the difference in trend of the main structures between Goantagab and Gamigab.	58
31	Photograph of kink-folded schist.	58
32	Poles to F4 crenulations and kink-band axial planes.	59
33	Simplified sketch of the structural development at Gamigab.	61
34	P-T diagram showing division between low and medium grades of metamorphism.	69
35	P-T diagram showing the reaction curve for grossularite.	69
36	T-X diagram showing the reaction curve for tremolite.	70
37	Photomicrograph of biotite spot developed in response to thermal metamorphism.	71
38	Geological map of the area around the mineralised quartz veins.	75
39	Geological cross sections through trenches 2 and 3 showing the geology and alteration.	76

## LIST OF FIGURES (continued)

40	Photomicrograph of quartz vein with cassiterite.	77
41	Photomicrograph of growth zoning in cassiterite.	78
42	Photomicrograph of tourmalinised vein margin.	79
43	Geochemical variations from the wall rocks into the vein margins and quartz veins.	83
44	Fe# vs MgO for tourmalines in the schistose vein margins and wall rocks.	86
45	Fe# vs MgO for tourmalines in the schistose vein margin and vein margin in marble.	86
46	Sketch (taken from photograph) of breccia body at Gamigab.	88
47	Photograph of breccia with siliceous matrix.	89
48	Ab-Or-An normative diagram showing distribution of felsic rocks.	93
49	Schematic model of crystallising hydrous magma.	97
50	Idealised paragenetic sequence during alteration.	99
51	Proposed model for breccia formation at Gamigab.	104
52	Photograph of quartz veins in schist damming up at the contact with the marble	105
53	Timing and intensity of the alteration-mineralisation at Gamigab.	107
54	Model for the deposits in the Northern Group.	111

## LIST OF FIGURES (Continued)

- |    |  |     |
|----|--|-----|
| 55 | Variation in tourmaline composition in the deposits of the Northern Group.                 | 118 |
| 56 | Variation in homogenisation and corrected temperatures for the deposits in Northern Group. | 119 |

## LIST OF TABLES

<u>Table</u> <u>Number</u>		<u>Page</u>
I	Subdivisions of the intracontinental branch.	10
II	Stratigraphy of the Lower Ugab area.	29
III	Stratigraphy of the Goantagab Domain.	31
IV	Stratigraphy of the Goantagab Domain as suggested by Hodgson (1972).	49
V	General Stratigraphy of the Goantagab Domain.	51
VI	Lithological and stratigraphic subdivisions of the Damara Sequence in the Goantagab Domain.	53
VII	Major and trace element analyses of wall rock, vein and vein margin.	81
VIII	Partial analyses of tourmalines from the tourmalinised vein margins in altered schist.	85
IX	Partial analyses of tourmalines from the sericitised schist wall rocks.	85
X	Partial analyses of tourmalines from vein margins in altered marble.	85
XI	Major and trace element analyses of carbonate and siliceous breccia matrix.	90
XII	Major and trace element analyses and calculated norms of the porphyry plug.	91
XIII	Average major element analyses and norms for various igneous rocks.	92

## LIST OF TABLES (Continued)

XIV	Results of fluid inclusion work on a sample of cassiterite from Gamigab.	102
XV	Paragenic sequence of hydrothermal events at Gamigab.	107
XVI	Partial analyses of tourmalines from Brandberg West, Frans Prospect and Goantagab.	117
XVII	Results of fluid inclusion work on samples from Frans Prospect and Goantagab.	119
XVIII	Results of $\delta^{34}\text{S}$ measurements on sulphide samples from Brandberg West and Goantagab.	120

## 1. INTRODUCTION

The Gamigab tin prospect is located in north-western Namibia at the intersection of lines of latitude  $20^{\circ} 40'S$  and longitude  $14^{\circ} 30'E$  in the south-eastern corner of the farm Vegkop 528 (Fig. 1). The post-Karoo Brandberg Granite Complex, which forms a prominent topographical feature in the region, is approximately 15 km south of the prospect.

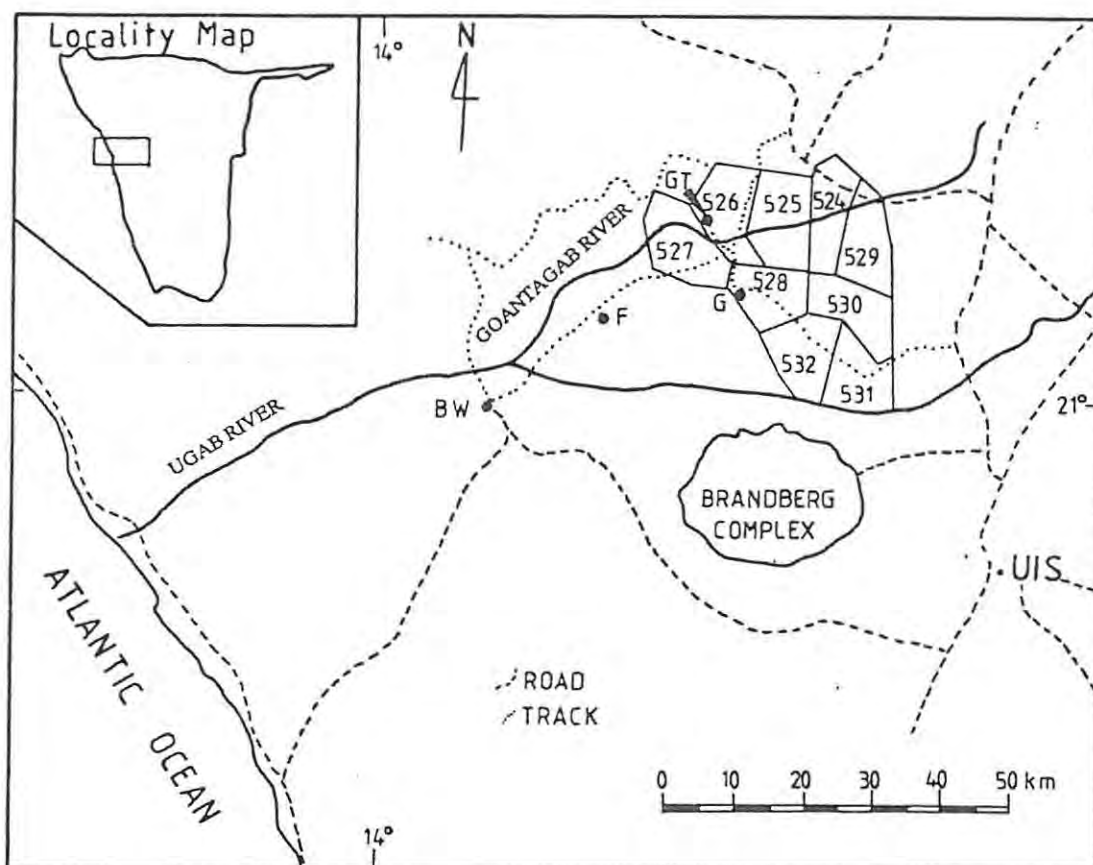
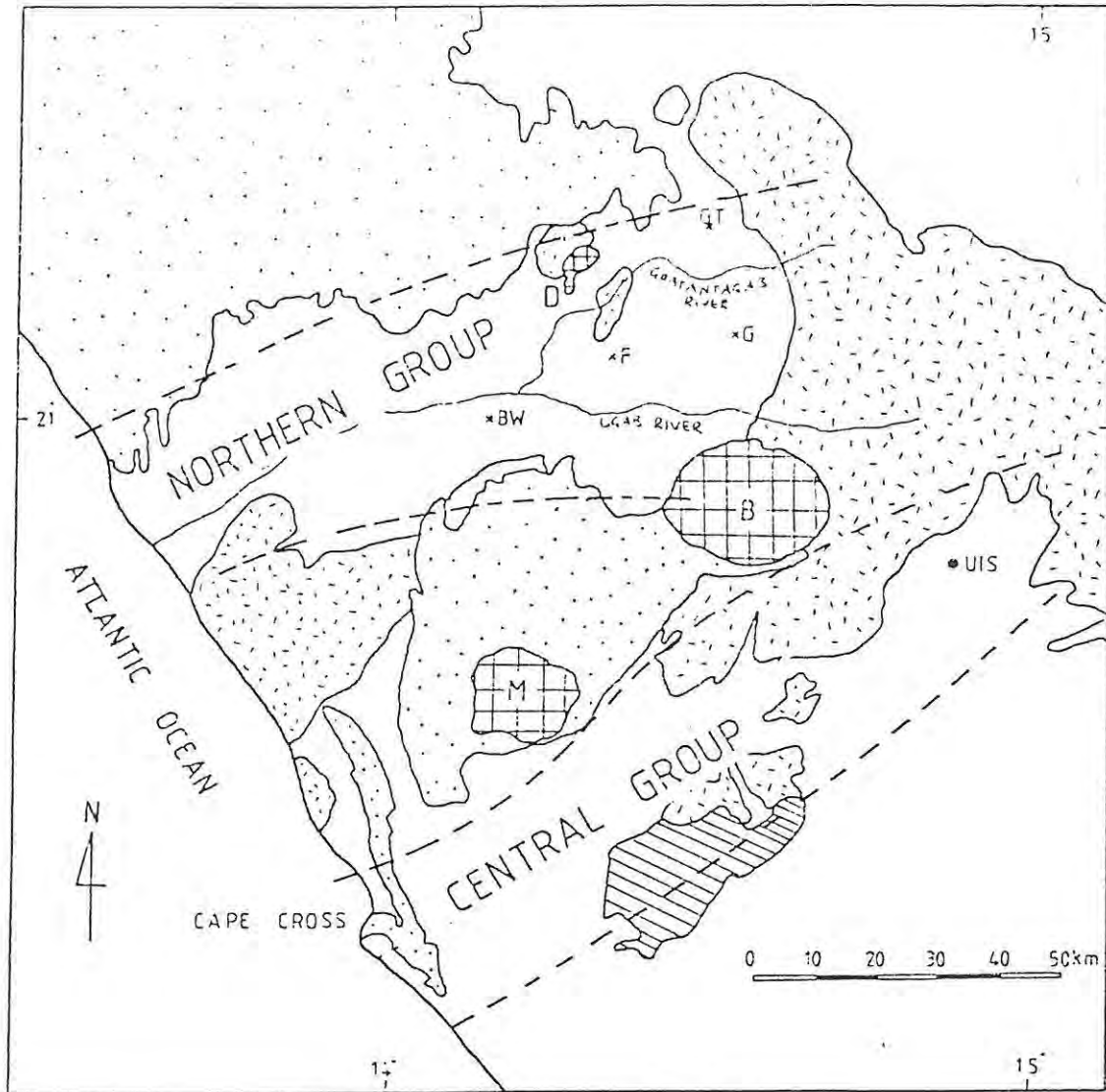


Fig. 1: Geographical sketch map of north-western Namibia showing locality of the Gamigab Sn prospect. BW=Brandberg West; F=Frans Prospect; G=Gamigab; GT=Goantagab. 524-532 denote farm numbers. (Adapted from 1:1 000 000 geological map South West Africa/Namibia).

There are several other Sn-W deposits in the region around Gamigab. Collectively known as the Northern-Group by Pirajno and Jacob (1987a), they occur in an east-north-east trending belt of mineralisation which has a length of some 80 km (Fig. 2). Sn and W mineralisation hosted in quartz veins is



EXPLANATION

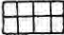

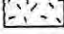

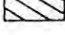
-  Late- to post-Karoo Complexes  
D = Doros, B = Brandberg, M = Messum
-  Karoo Sequence (Lavas and Sediments)
-  Damara Granites
-  Damara Sequence
-  Nosib Group

Fig. 2: Simplified geological map of north-west Namibia showing positions and trends of mineralisation. (Adapted from the 1:1 000 000 geological map of South West Africa/Namibia and Pirajno and Jacob, 1987a)

present at the Brandberg West Mine and at Frans Prospect, approximately 43 km and 20 km south-west of Gamigab respectively. The vein and replacement Sn deposit at Goantagab is 14 km north-north-west of Gamigab (Fig. 3). Some 10 km south of Gamigab is the Ousis pegmatite field consisting of several unzoned, syn- to post-tectonic Sn-bearing pegmatites.

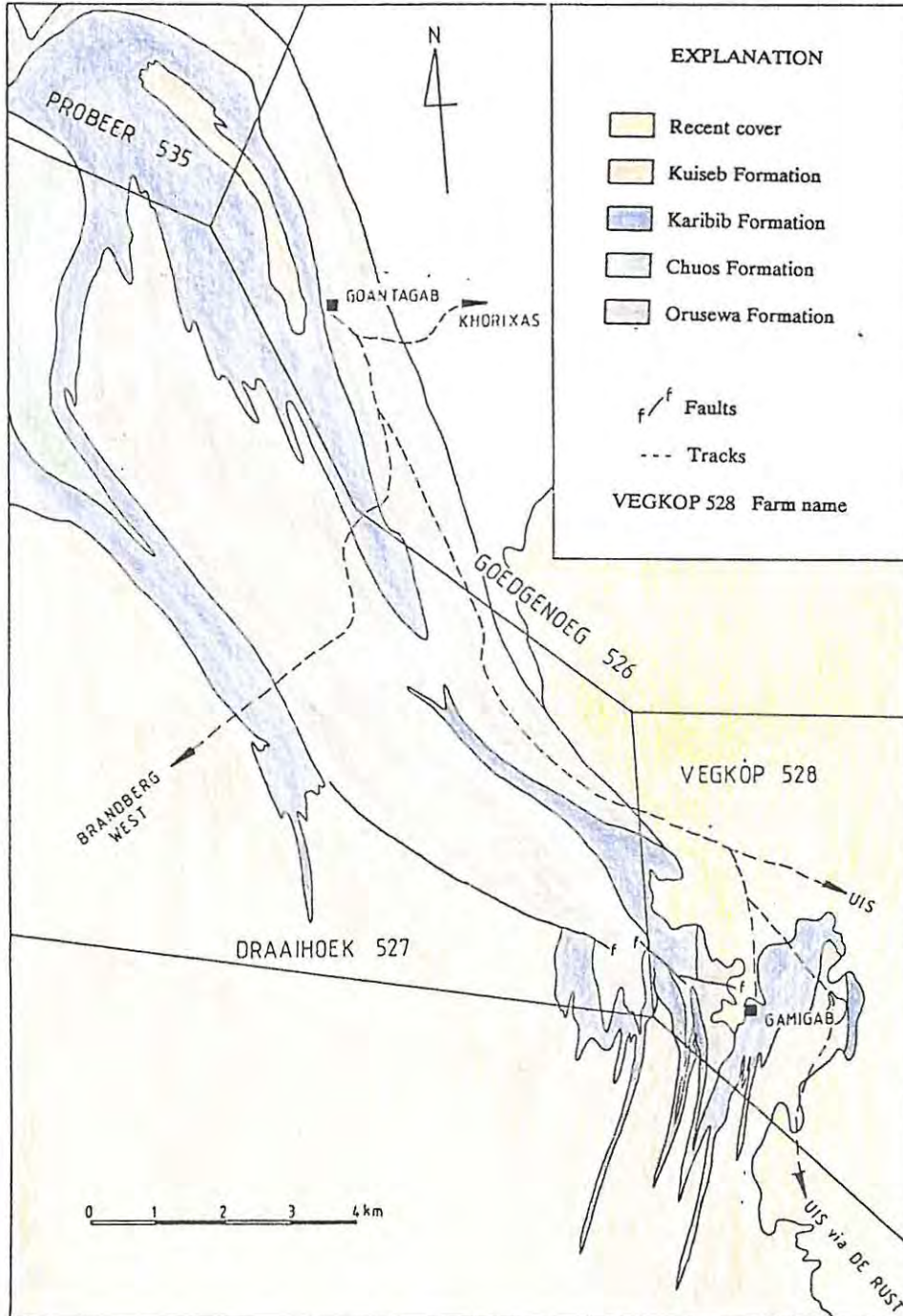


Fig. 3: Simplified geological map between Goantagab and the Gamigab tin prospect.

South-east of the Brandberg Complex is the Strathmore-Uis belt which extends from the coast at Cape Cross in a north-easterly direction (Fig. 2). This band of mineralisation forms part of the Central Group (Pirajno and Jacob, 1987a) and contains unzoned Sn and Ta-bearing, syn- to post-tectonic pegmatites which developed in *en echelon* tension gashes related to the regional deformation in the area (Richards, 1986).

#### 1.1. Previous Work in North-Western Namibia

The areas of previous work in the north-western parts of Namibia are shown in Fig. 4. Jeppe (1952) mapped an area along the course of the Ugab River extending from the lower Ugab region to just north of the Brandberg alkaline complex.

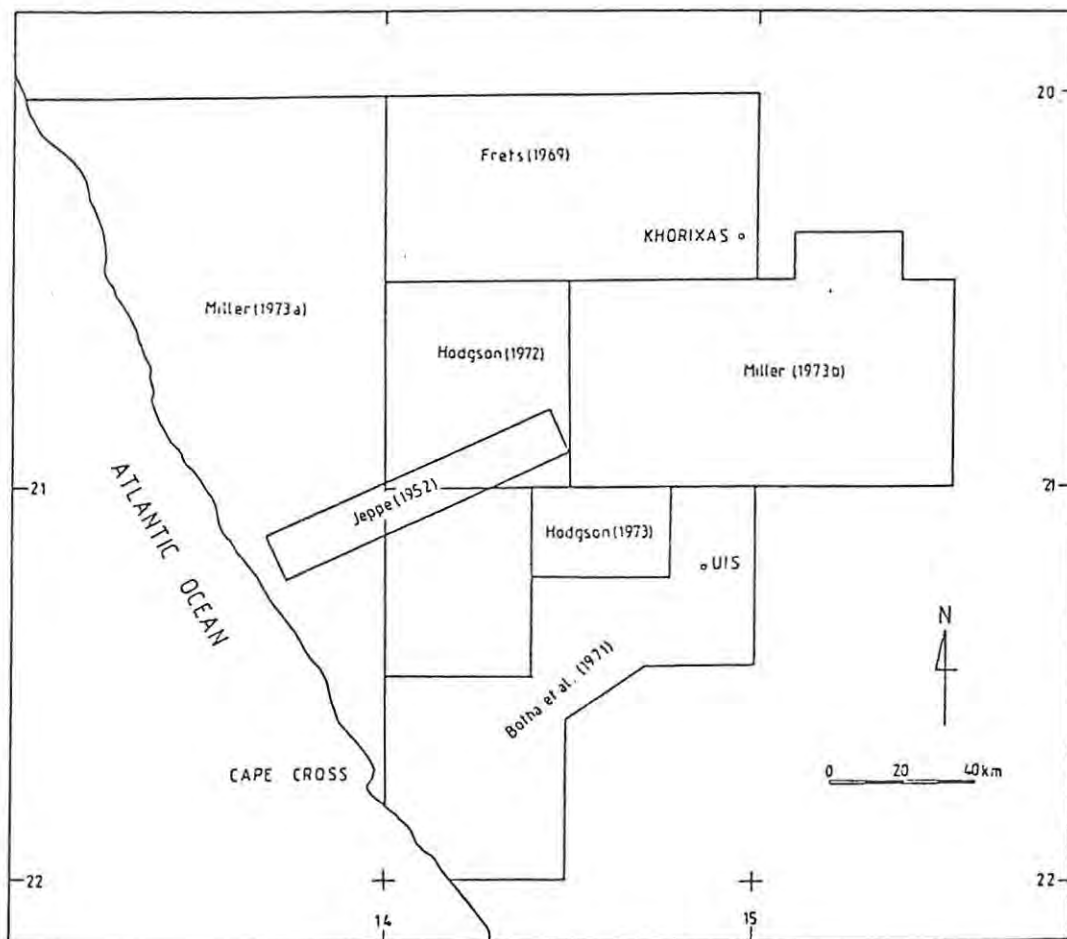


Fig. 4: Areas of previous work carried out in north-western Namibia.

The geology and structure of the Huab-Welwitschia area to the north was investigated by Frets (1969), whereas Hodgson (1972) concentrated on the geology of the Brandberg-Aba Huab area. Hodgson (*op. cit.*) covered the Brandberg complex, the results of which he later published (Hodgson, 1973).

A reconnaissance examination was carried out by Miller (1973a) on an area west of that mapped by Frets (1969) and Hodgson (1972). In a further study Miller (1973b, 1980) investigated the geology of an adjoining area east of that mapped by Hodgson (*op. cit.*). As part of extensive exploration by Gold Fields of Namibia, more detailed geological mapping and structural interpretation of the area around the Goantagab deposit and Gamigab prospect was carried out by Osborn (1985).

#### 1.2. Previous Work at the Gamigab Prospect

The effect of hydrothermal activity at Gamigab was first investigated in 1953 by the South West Africa Company (SWACO). Three exploration trenches were dug perpendicular to the set of mineralised quartz veins. These were subsequently sampled for Sn and W, and geological mapping of the immediate surrounding area was done.

It seems as though the prospect remained untouched for some 29 years when further work was undertaken by the Trekkopje Exploration and Mining Company (a subsidiary of Gold Fields of Namibia). An area of about 0,24 km<sup>2</sup> was mapped by Le Roux (1982); he reported the presence of a felsic volcanic plug some 500 m north-east of the sampling trenches. During this same period a percussion drilling program was undertaken but low Sn and W assays indicated that follow-up diamond drilling was not necessary (Le Roux, *op. cit.*).

### 1.3. Aim and Logistics of the Study at Gamigab

The aim of this study was to evaluate the relationships among the mineralisation, alteration, brecciation, igneous activity and regional structure. Initial field work was started during March 1986 and continued through to July 1986 during which time several mapping exercises were completed:

1. detailed geological mapping on a scale 1:1000 was carried out over of the section mapped by Le Roux (1982) and to the north, east and south covering an area of 1,12 km<sup>2</sup> (Map 1),
2. the region around the prospect was mapped using 1:10 000 orthophotographs and 1:50 000 aerial photographs (Map 2), and
3. the west faces of the sampling trenches were mapped in detail on a scale 1:100 (Fig. 39).

A further month (July 1987) was spent in the field continuing the regional mapping and studying the region between Gamigab and Goantagab in an attempt to elucidate the structural and lithological relationship between the two mineralised areas. Samples for thin-section study, electron-probe analysis and geochemical analysis were collected in the field and analysed at Rhodes University (Appendices 1). Mineral compositions were determined on the Jeol 733 Superprobe (Appendix 2). Whole-rock compositions were determined using a Philips PW 1410 X-ray fluorescence spectrometer with the exception of CO<sub>2</sub> which was determined at the Zimbabwe Geological Survey and Sn and W which were determined at Rocklabs, Johannesburg.

### 1.4. Physiography of the Study Area

The topography in the study area is quite rugged in places. Steep, erosion-resistant marble ridges build the more elevated parts whereas pelitic and semi-pelitic schists underlie the valleys and the low-relief, undulating hills. The drainage

pattern of the region is both lithologically and structurally controlled in that the larger streams are essentially confined to the schist antiforms and synforms. Smaller and more numerous streams feed into the larger streams from the marble ridges producing a trellis-type drainage pattern. The larger streams drain southwards to the Ugab River, which is situated north of the Brandberg and flows westward into the Atlantic Ocean.

The area to the north-east of Gamigab is covered extensively by calcrete and superficial aeolian sand. The area immediately west of the mineralisation is covered by a calcrete terrace (2-3 m thick), which is eroded in places exposing the older rocks. Normally the tracks in the area are negotiable by a 4-wheel drive vehicle.

Daytime temperatures generally span between 30° and 40°C and they seldom vary from this range, although the winter months are somewhat cooler and drier than the summer months. Rainfall is very sparse and is recorded during the months December to March. During the late afternoon a westerly wind may blow; this can bring in an overnight mist providing the much-needed moisture for the vegetation.

Vegetation is generally quite sparse with the Melkbos (*Euphorbia gregaria*) a common feature of the landscape. In the more flat-lying parts a fine desert grass carpets the planes, together with an occasional Welwitschia plant (*Welwitschia Mirabilis*) and Mopane tree (*Colophospermum mopane*), the latter growing along stream courses. Wildlife in the form of kudu, springbok, ostrich and other numerous species of small birds are surprisingly active in the apparently hostile environment. Insect life is abundant and the mopane fly a constant nuisance.

## 2. REGIONAL GEOLOGICAL SETTING

### 2.1. General Features of the Damara Orogen

During late-Precambrian times the African continent experienced several tectono-thermal events which seemed to mark the final episode in a long history of crustal instability (Tankard *et al.*, 1982). These tectono-thermal events affected much of the African continent and adjoining regions (e.g. Brazil, Antarctica, Australia and India) from as early as 1300 Ma ago up until 450 Ma ago (Windley, 1984) (Fig. 5). The orogenic event around the period 500 Ma was given the name *Pan-African Thermo-Tectonic Episode* by Kennedy (1964).

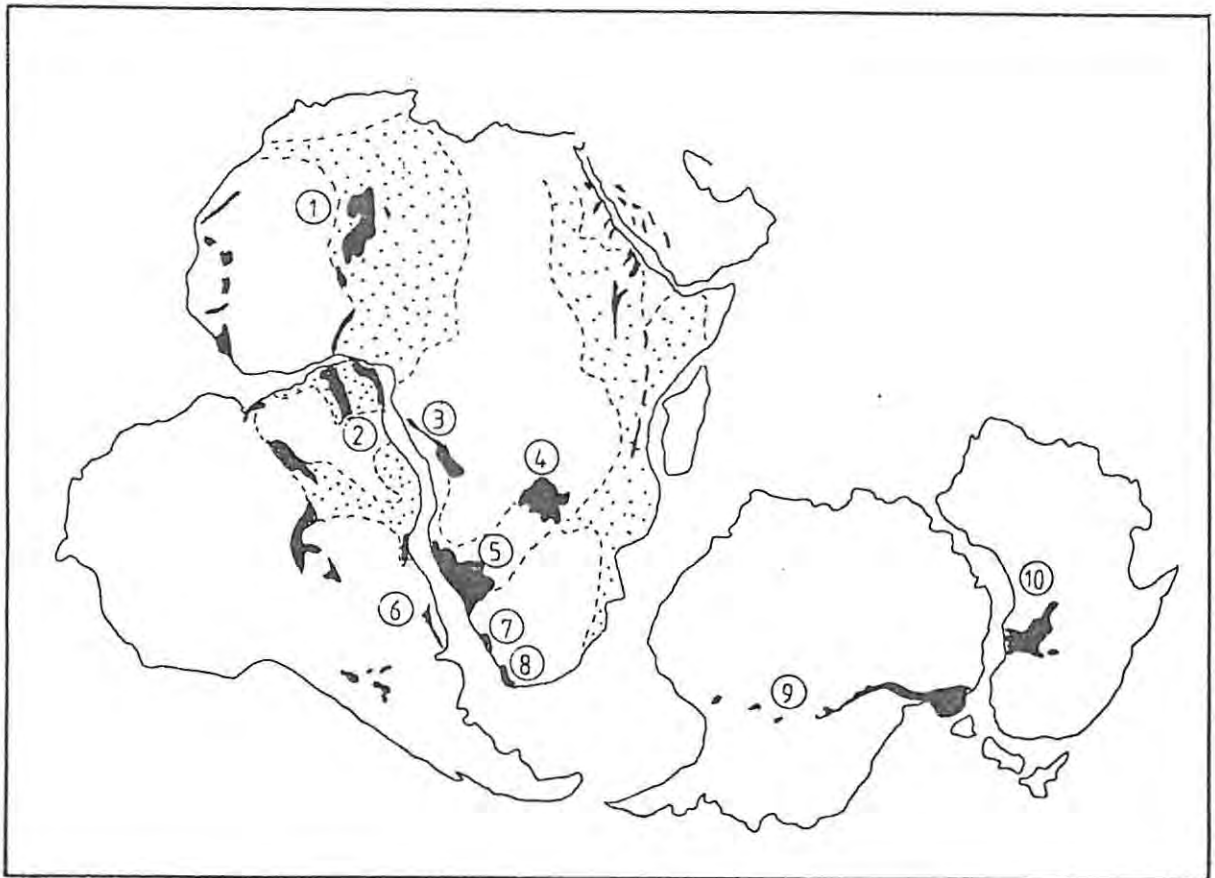


Fig. 5: Reassembly of the Gondwana continent showing distribution of several Pan-African belts. 1=Pharusian; 2= North-eastern fold belt; 3=West Congolian; 4=Katanga Belt; 5=Damara Belt; 6= Ribeira Belt; 7= Gariep Belt; 8= Malmesbury Belt; 9= Transatlantic Belt; 10= Adelaidean (Adapted from Porada, 1985).

The Damara Orogen differs from other similar Pan-African mobile belt systems by its higher metamorphic temperatures and voluminous granitic plutonism (Martin, 1983). It provides for a good understanding of the processes of orogeny because of its triple-junction geometry, its thick geological succession and its high degree of exposure (Tankard *et al.*, 1982). Within the Damara Sequence are numerous basement inliers, approximately 2000 Ma old, consisting of complex associations of granitoid rocks and gneisses, infolded with supracrustal metasediments of the Damara Sequence (Jacob *et al.*, 1983).

The Damara Orogen comprises two main segments, namely the coastal and intracontinental branches (Fig. 6). The coastal branch is at least 150 km in width and trends approximately parallel to the present coastline. The intracontinental branch trends north-east and is approximately 400 km wide. The join of the intracontinental branch and the coastal arm is regarded as a Pan-African triple junction centred off the coast near the town of Swakopmund and is partly seen as a zone of syntaxis south of the Kamanjab inlier (Miller, 1983).

#### 2.1.1 Intracontinental branch

The intracontinental branch has been subdivided into several smaller zones by different authors (Table I). The currently accepted and used tectono-stratigraphic subdivision of the intracontinental branch and flanking areas is that of Miller (1983). Eight zones are recognised on the basis of stratigraphy, structure, grade of metamorphism, plutonic rocks, geochronology and aeromagnetic expression (Fig. 7). The boundaries separating the various zones are defined by faults or thrusts (e.g. the boundaries between the NZ and the CZ and between the SMZ and the SZ), by lineaments (CZ-OLZ), by stratigraphic boundaries (SZ-SMZ), or difference in metamorphic P and T (low pressure OLZ - high pressure SZ). A line of basement inliers, denoting a geanticlinal ridge, separates the NP from the NZ and from the coastal branch.

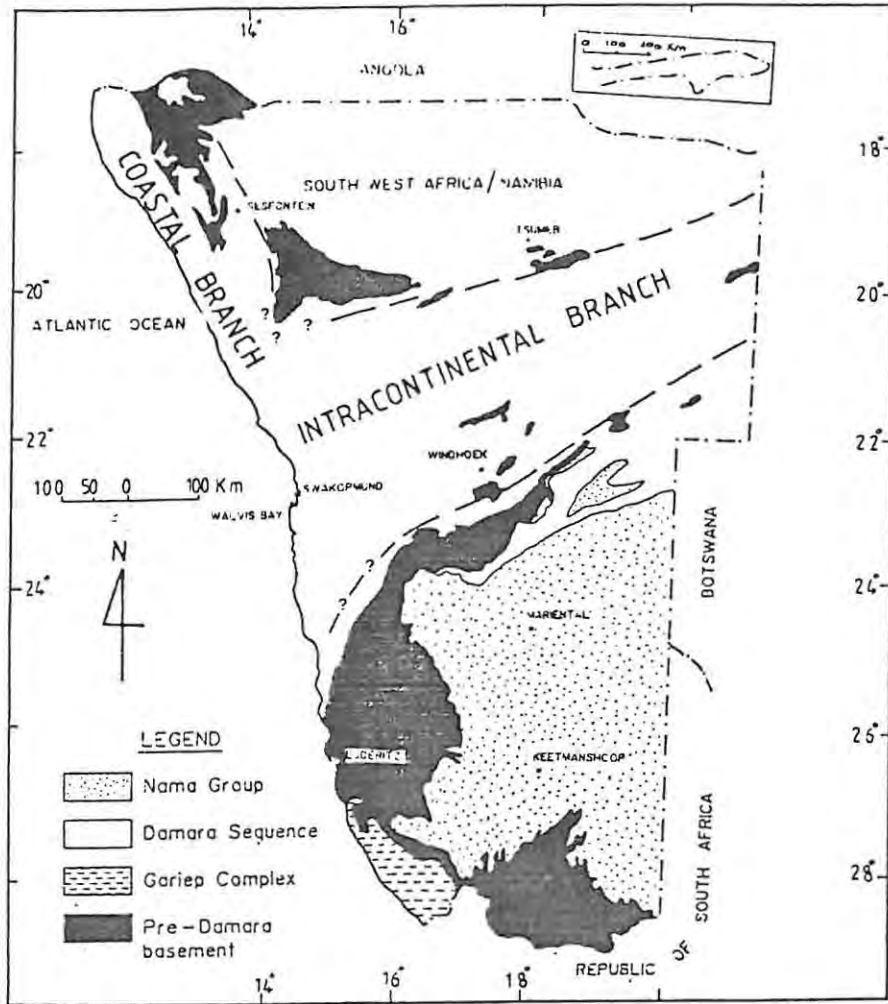


Fig. 6: Simplified geological map of Namibia showing the position of the intracontinental branch and coastal branch.

TABLE I: Subdivisions of the intracontinental branch as suggested by various authors.

MARTIN & PORADA (1977)	MILLER (1983)	PORADA (1985)
NORTHERN PLATFORM	NORTHERN PLATFORM (NP)	
TRANSITIONAL ZONE	NORTHERN ZONE (NZ)	NORTHERN ZONE
CENTRAL ZONE	CENTRAL ZONE (CZ)	CENTRAL ZONE
	OKAHANDJA LINEAMENT ZONE (OLZ)	
	SOUTHERN ZONE (SZ)	
SOUTHERN ZONE	SOUTHERN MARGINAL ZONE (SMZ)	SOUTHERN ZONE
	SOUTHERN FORELAND (SF)	
	SOUTHERN PLATFORM (SP)	

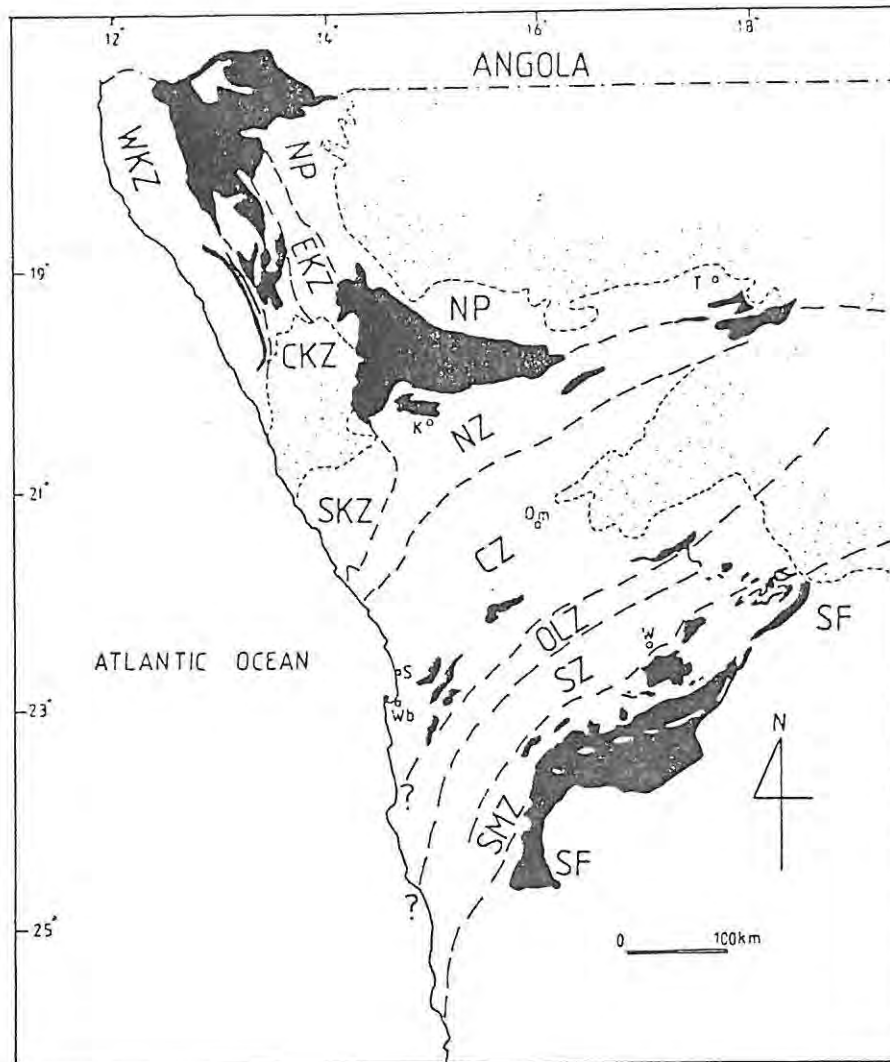


Fig. 7: Subdivisions of the Damara Orogen. W = Windhoek; Wb=Walvis Bay; S=Swakopmund; Om=Omaruru; K=Khorixas; T=Tsumeb (Adapted from Miller, 1983).

Outcrops of the metasedimentary rocks within the intra-continental branch disappear beneath the cover of the Kalahari Basin in north-eastern Namibia. Aeromagnetic traverses over these areas led Reeves (1978) to suggest that the rocks extend beneath the Kalahari cover into the Katanga succession in Zaire and into the south-western parts of Zambia.

#### 2.1.2. Coastal branch

The coastal branch is comprised of two parts; the northern and southern parts. The northern portion is also termed the Kaoko Belt by Hoffmann (1983). The southern extension of the coastal

arm is thought to be represented by the Gariep and Malmesbury provinces in north-western South Africa/southern Namibia (Miller, 1983), whereas a northern extension is in the north-western Congo and possibly further north, represented by the Dahomeyan and Pharusian belts of north-west Africa (Miller, *op. cit.*) (Fig. 5). The western limit is thought to be defined by the Ribeira orogen of Brazil and Uruguay (Porada, 1979). Together with the intracontinental branch they constitute a 3-armed asymmetrical orogenic junction with lithological and structural continuity between each arm (Tankard *et al.*, 1982).

As with the intracontinental branch, the Kaoko Belt is further subdivided (Miller, 1983) (Fig. 7). Rocks of the Western Kaoko Zone (WKZ) are characterised by stratigraphically high level, high temperature low-pressure metamorphism and by the intrusion of syn- and post-tectonic granites. The Purros Lineament, which exhibits similar characteristics to the Okahandja Lineament (Miller, 1979), separates the WKZ from the Central Kaoko Zone (CKZ). The tightly folded CKZ rocks are kyanite-bearing and have been subjected to low-temperature high-pressure metamorphism (Miller, 1983). These rocks have been thrust eastwards along the Sesfontein Thrust (Guj, 1970) over the shelf sediments of the Otavi and Mulden Groups, which make up the Eastern Kaoko Zone (EKZ).

Completing the subdivision, the Southern Kaoko Zone (SKZ) is distinct from the other above-mentioned zones in that it consists entirely of sequences of turbiditic rocks (Miller *et al.*, 1983). These rocks underwent a single phase of intense deformation which produced westerly vergent structures (Jeppe, 1952; Freyer, in prep.). The Gamigab Sn prospect occurs in the eastern parts of the SKZ and it is for this reason that the geology of the SKZ will be dealt with in more depth later.

## 2.2. History of Sedimentation in the Damara Orogen

Rifting of the pre-Damara continental crust some 1000 - 900 Ma ago resulted in the formation of several rift zones within the intracontinental branch and Kaoko Belt (Martin and Porada, 1977; Porada, 1985). Fig. 8 shows their postulated positions and the suggested geometry based on the outcrop of the basal Nosib sediments and the presence of associated volcanic rocks. The rift zones in the northern parts of the orogen are interpreted as full continental grabens whereas those in the southern parts are interpreted as half grabens marginal to a major rift zone, which marks the position of the assumed Khomas trough (Porada, 1985). Although they are shown together, this does not necessarily mean they are of the same age (Porada, *op. cit.*). In regions where these rocks are not exposed on surface, the position of these rift zones during these early times had to be estimated considering factors such as facies differences, thickness changes and indications of igneous activity (Porada, 1985). Kröner (1982) suggests that the current post-tectonic width of the intracontinental branch is some 400 km, and is an indication that the original width could have exceeded some 600 km.

Initial sedimentation in the intracontinental rifts resulted in the deposition of feldspathic to arkosic, locally conglomeratic sediments of the Nosib Group. Igneous activity accompanied the final stages of Nosib deposition, when alkaline to per-alkaline rocks of the Naauwpoort Formation, were extruded onto or intruded into the Nosib sediments along major faults and rift margins (Hawkesworth *et al.*, 1983). Nosib sediments were also deposited in the coastal rifts although were of lesser thickness than the intracontinental rifts (Porada, 1983). Here volcanism started early in Nosib times and continued up until the deposition of the Swakop Group (Porada, *op. cit.*). The turbiditic Swakop Group of the SKZ was deposited in deep-water basins by the end of the Nosib stage (Miller, 1983), implying that rift evolution in the Kaoko Belt was somewhat ahead of the intracontinental branch.

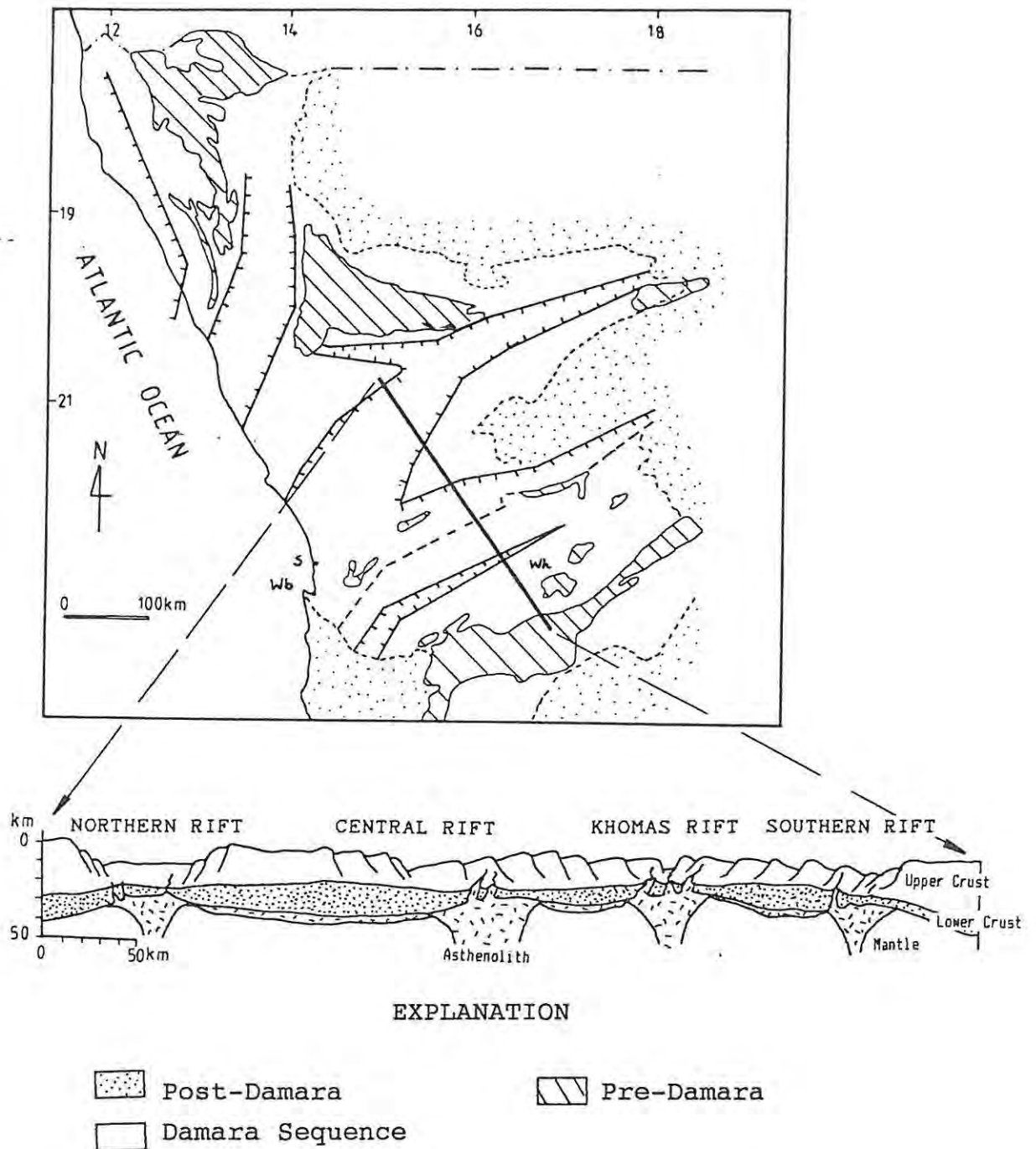


Fig. 8: Supposed positions and geometry of rifts during early geosynclinal development of the Damara Orogen. Wh=Windhoek; Wb=Walvis Bay; S=Swakopmund (Adapted from Porada, 1985).

Around 730 Ma ago further rifting ('passive mantle rifting', Porada, 1985) resulted in general subsidence across the entire geosyncline. The Nosib grabens coalesced and subsequent

sedimentation over-stepped the basement highs (Tankard *et al.*, 1982; Miller, 1983). In the northern parts of the intracontinental branch (Fig. 9) the platform carbonates of the Otavi Group were deposited unconformably on the Nosib sediments on a gently subsiding Congo Craton (Tankard *et al.*, 1982).

The Otavi Group carbonates subsequently underwent gentle folding and erosion, the latter resulting in an erosion surface which cut down into the basement (Tankard *et al.*, *op. cit.*). Molasse-type sediments of the Mulden Group unconformably overlie the Otavi Group.

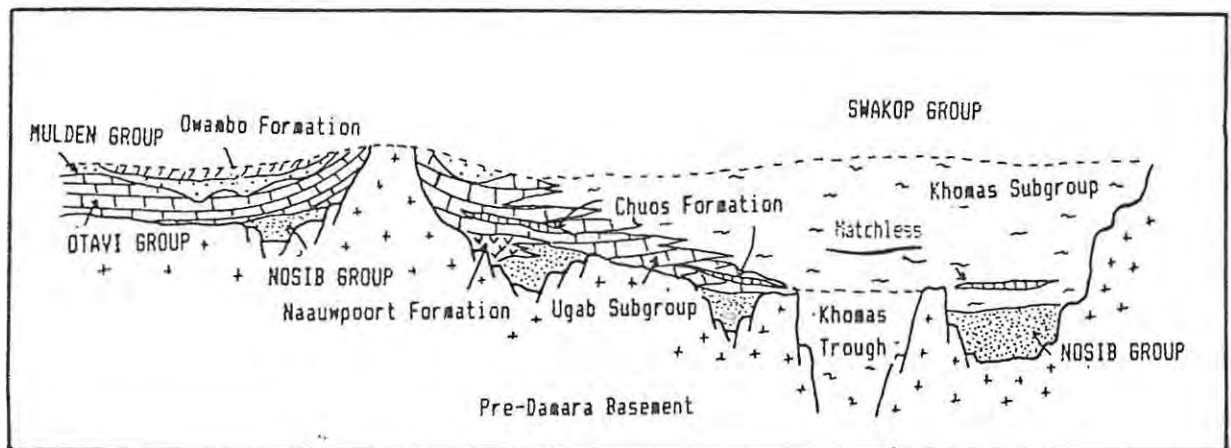


Fig. 9: Schematic stratigraphic cross section across the intracontinental branch (Adapted from Tankard *et al.*, 1982).

In contrast to the shelf environment in the north, the central and southern portions of the orogen developed in a deeper trough setting (Tankard *et al.*, 1982; Martin and Porada, 1977). In the central parts of the intracontinental branch the carbonates and terrigenous sediments of the Ugab Subgroup were sporadically deposited, in many places onlapping the basement (Fig. 9). In the southern parts of the intracontinental branch sediments of the Kudis Subgroup were deposited. Following the deposition of both the Ugab and Kudis subgroups was a period of further rapid differential subsidence during which time the mixtites of the Chuos Formation were deposited.

A proposed glacial origin for the mixtite units (Gevers, 1931; Martin, 1965) is controversial (Miller *et al.*, 1983; Schermerhorn, 1974) although it cannot be ruled out. Schermerhorn (1974) interprets the sediments as mass flow deposits whereas Henry *et al.* (1986) suggest a model invoking re-deposition of glacially derived sediments down the slope of a tectonically active basin margin. Mafic volcanic rocks are intercalated with the rocks of the Chuos Formation in the southern parts of the orogen.

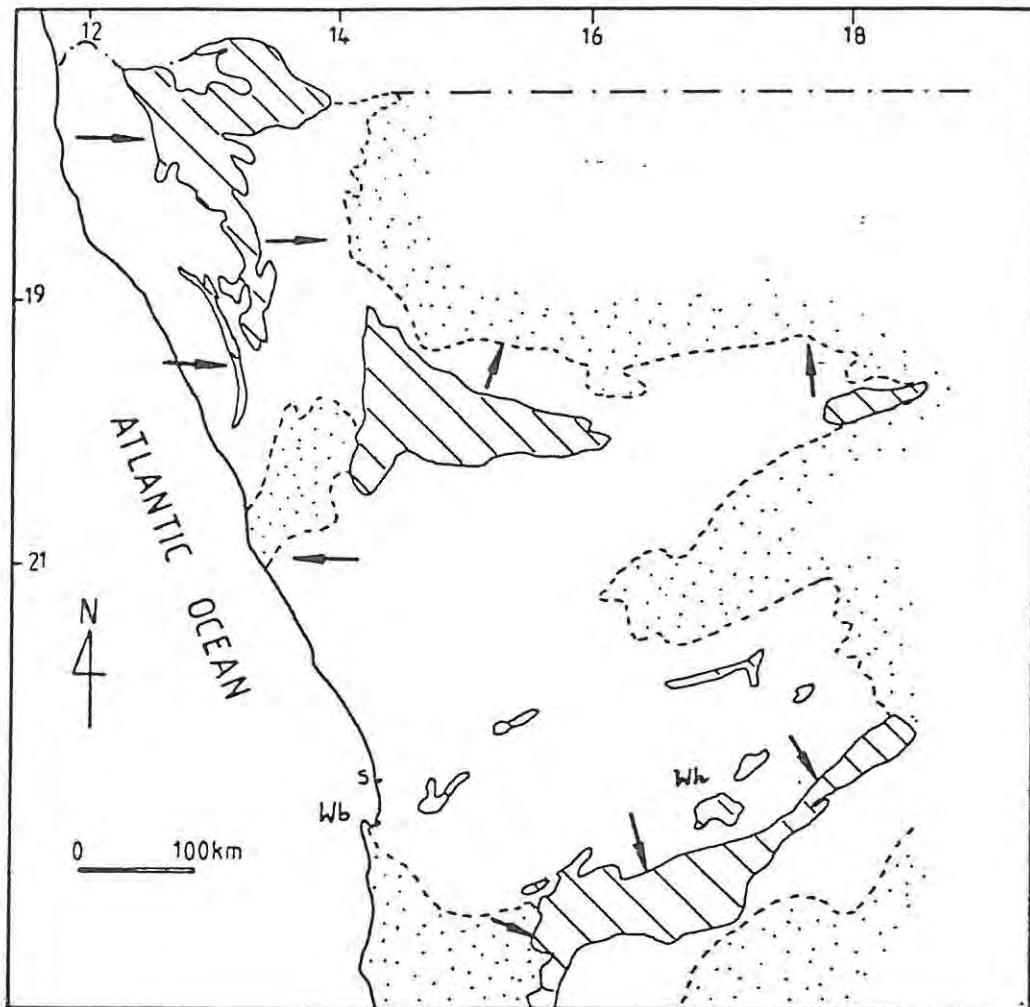
Following on, the platform carbonate rocks of the Karibib Formation were deposited on the Chuos sediments. During deposition of the Karibib sediments in the north, the central regions of the orogen underwent further subsidence and along the basin margins calcareous turbidites (Tinkas turbidites) were transported over the southern edge of the platform and deposited into the subsiding basin (i.e. the Khomas trough; Porada, 1985). Similar turbiditic deposition occurred in the south, in the form of the Chausib turbidites, whose source may have been to the south (Porada and Wittig, 1983).

Sedimentation in the Damara Orogen was terminated by the deposition of the flysch-like sequence of the Kuiseb Formation (Fig. 9). These rocks differ from every other in the Damara Sequence in that they can be traced right across the intracontinental branch (Tankard *et al.*, 1982; Porada, 1985). The Matchless ortho-amphibolite belt occurs within the Kuiseb rocks. With a strike length of some 350 km this north-east trending belt of metavolcanic rocks exhibits ocean-floor characteristics (Finnemore, 1974, 1978; Schmidt and Wedepohl, 1983), and has been dated at approximately 775 Ma (Kröner, 1982).

### 2.3. Structure

Contrasting structural styles and deformation are exhibited in the different zones of the Damara Orogen (Fig. 10). In the intracontinental branch the NP and the NZ are characterised by

relatively simple structures that decrease in intensity northwards (Weber *et al.*, 1983). Structural development in the NZ may have been influenced by the so-called Huab Ridge of Porada *et al.* (1983) and by the rocks of the Naauwpoort Formation (Weber *et al.*, *op.cit.*).



EXPLANATION




-  KAROO AND RECENT
-  DAMARA SEQUENCE  
(including metasediments  
and syn- to post-tectonic  
granites)
-  BASEMENT ROCKS

Fig. 10: Direction of vergence (denoted by arrows) of the main structure in the Damara Orogen (Adapted from Porada, 1979).

More recent work by Swart (in prep) has identified north-west to south-east current directions for the turbidites, which indicates that the presence of the ridge is unlikely. Two periods of deformation have been recognised and interference of the two fold sets produced dome-like, open to tight interference folds (Miller, 1980).

Interference folding in the northern parts of the CZ produced upright, east-trending dome and basin structures (Miller, 1983). In the southern parts of the CZ, the domes become larger and trend north-easterly (Sawyer, 1981). The OL has been described as a large monoclinial downfold which affected all of the rocks of the Damara Sequence, and which also had a major influence throughout the depositional and tectonic history of the Damara Orogen (Miller, 1983). The OLZ which is some 500 - 2000 m in width is characterised by upright structures which become south-easterly vergent toward the SZ. Deformation culminated in intense south-eastward thrusting of cover and basement in the SMZ (Miller, 1983). This deformation strongly affects the northern edge of the SF but fades out some 170 km south-east of the southern edge of the SMZ (Miller, *op. cit.*).

The Kaoko Belt is characterised by complex eastward-vergent folds (Fig. 10) and by eastward thrusting along the Sesfontein thrust (Guj, 1970). Field work revealed the presence of recumbent folds and nappes which override the sediments of the Mulden Group in the EKZ. In the NZ, toward the southern end of the Kamanjab inlier, Frets (1969) recognises five phases of folding. The first phase is related to initial metamorphism and granitisation, which was followed by deformation that produced north-south trending tight folds, which in places were refolded by east-west trending F3 folds producing complex refolded structures. The structural geology of the SKZ differs from the WKZ and CKZ in that the folds are westerly vergent becoming upright toward the east (Miller, 1983).



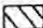
#### 2.4. Metamorphism

Grades of metamorphism vary almost systematically throughout the Damara Orogen (Fig. 11). In the intracontinental branch, studies of mineral reactions have shown that different metamorphic conditions existed on either side of the Okahandja Lineament (Hartmann *et al.*, 1983; Hoffer, 1983; Puhan, 1983). Estimates of the grade of metamorphism in the central parts of the orogen range between 2 - 3 kbar and 580° - 680°C (Hartmann *et al.*, 1983) and 5 kbar and 430° - 590°C (Hoffer, 1983). According to Puhan (1983), an increase in both temperature and pressure of metamorphism in the CZ is indicated by calcite-dolomite geothermometry from 2,6 kbar and 555°C near Karibib to 3,4 kbar and 645°C around Swakopmund.

The number of metamorphic events which affected the rocks in the central and southern parts of the intracontinental branch is a controversial topic. Several authors favour a single metamorphic event (Jacob, 1974; Sawyer, 1981; Hartmann *et al.*, 1983) while others support two metamorphic events (Kasch, 1983a, 1983b, 1986; Miller, 1983), with pressures of the second metamorphic event (M2) being somewhat lower than the first (M1) (Kasch, 1983a). This suggests that M2 was more of a thermal surge without any significant pressure increase (Kasch, 1983b). In the WKZ, Guj (1970) recognised two phases of metamorphism with an increase in grade westward from lower greenschist facies to upper amphibolite facies. Miller (1980) initially suggested a single phase of metamorphism for the NZ with grades increasing from north to south culminating in anatexis and formation of the Salem Suite and Sorris-Sorris granite. However, subject to reinvestigation of the contacts between the granites and country rocks, Miller (1983) has recognised that all Salem-type granites are in fact intrusive. In the SKZ a single phase of low grade metamorphism is suggested with later thermal overprinting in response to syn- to post-tectonic granitic intrusion (Porada *et al.*, 1983). Contact metamorphic effects may be observed in the vicinity of the Salem Suite (Miller, 1980), and the Donkerhuk and other granites in the central zone (Jacob, 1974).



EXPLANATION

-  KAROO AND RECENT
-  DAMARA SEQUENCE  
(including metasediments  
and syn- to post-tectonic  
granites)
-  BASEMENT ROCKS

1.  $\text{Chl} + \text{Plag} = \text{Ga} + \text{Chl} + \text{Qtz} + \text{H}_2\text{O}$
2.  $\text{Ky} + \text{Chl} + \text{Mus} + \text{Qtz} = \text{Cord} + \text{Bi} + \text{H}_2\text{O}$
3.  $\text{And} = \text{Sill}$
4.  $\text{Bi} + \text{Kspar} + \text{Plag} + \text{Qtz} + \text{Cord} = \text{Melt} + \text{Ga}$
5. Main Bi Boundary
6. Thermal Metamorphism, Cord in
7. Feldspar Blastesis in

KEY TO MINERALS:

Chl = Chlorite, Plag = Plagioclase, Ga = Garnet,  
Qtz = Quartz, Ky = Kyanite, Mus = Muscovite,  
Cord = Cordierite, Bi = Biotite, And = Andalusite,  
Sill = Silliminite, Kspar = K-feldspar

Fig. 11: Metamorphic reaction isograds in the Damara Orogen (Adapted from Miller, 1983).

### 2.5. Damara Magmatism

Over 200 syn- to post-tectonic plutons crop out throughout the Damara Orogen (Miller, 1983); they are more abundant in the CZ but also occur in the NZ, OLZ and WKZ (Fig. 12). Together they

form a composite batholith which covers a surface area of some 74 000 km<sup>2</sup>. The plutons vary in size from 5 000 km<sup>2</sup> (Donkerhuk granite) to less than 1 km<sup>2</sup> and their compositions range from gabbroic to granitic. Their emplacement spans a time period of 190 Ma from 650 to 460 Ma (Kröner, 1982; Hawkesworth *et al.*, 1983).

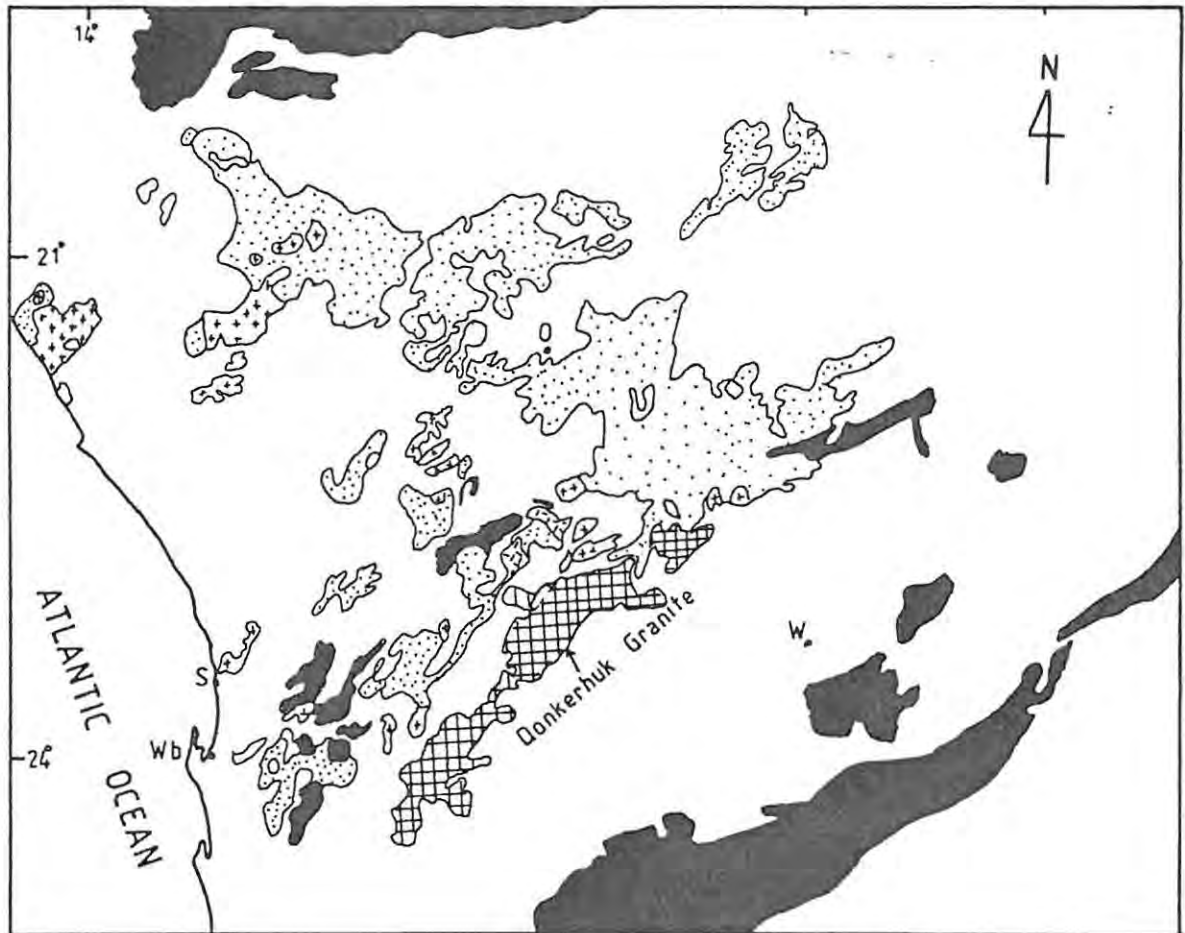


Fig. 12: Distribution of Damara-aged granites in the Damara Orogen. W= Windhoek; Wb= Walvis Bay; S=Swakopmund; O=Omaruru (Adapted from Miller, 1983).

Three major syn- to post-tectonic granite types may be recognised (Miller, 1983):

- 1) Red, medium- to fine-grained granites,
- 2) Coarsely porphyritic biotite monzogranites with which are associated diorites (these constitute the so-called Salem-type granites),
- 3) Fine- to coarse-grained leucogranites, pegmatites and pegmatitic alaskites.

The emplacement history of the granites can be subdivided into three groups according to field evidence and isotopic and geochemical characteristics (Kröner, 1982; Hawkesworth *et al.*, 1983):

- 1) 650 - 540 Ma: gabbroic, dioritic and tonalitic granites with an I-type affinity (i.e. generated during subduction phases of Damaran geodynamic development),
- 2) 580 - 550 Ma: emplacement of syn- to late-tectonic biotite-bearing granitoid suites (Salem type),
- 3) 540 - 450 Ma: continental collision and post-collision activity which produced a range of granitoids with S-type affinities, including two-mica granites.

## 2.6. Post-Damara (Karoo) Rocks

Outcrops of Karoo rocks occur throughout the Kaokoveld and north-western Damaraland (Fig. 13). Pre-Karoo topography and syn-sedimentary faulting has had a pronounced effect on the thickness and stratigraphy of the Karoo sediments (Erlank *et al.*, 1984). Dwyka tillite is only locally preserved, and the base of the succession is represented by the Omingonde

Formation in the east and the Gai-As Formation in the west. The Etjo sandstone marks the top of the sedimentary pile and becomes interbedded with the basaltic rocks of the Etendeka Formation (SACS, 1980).

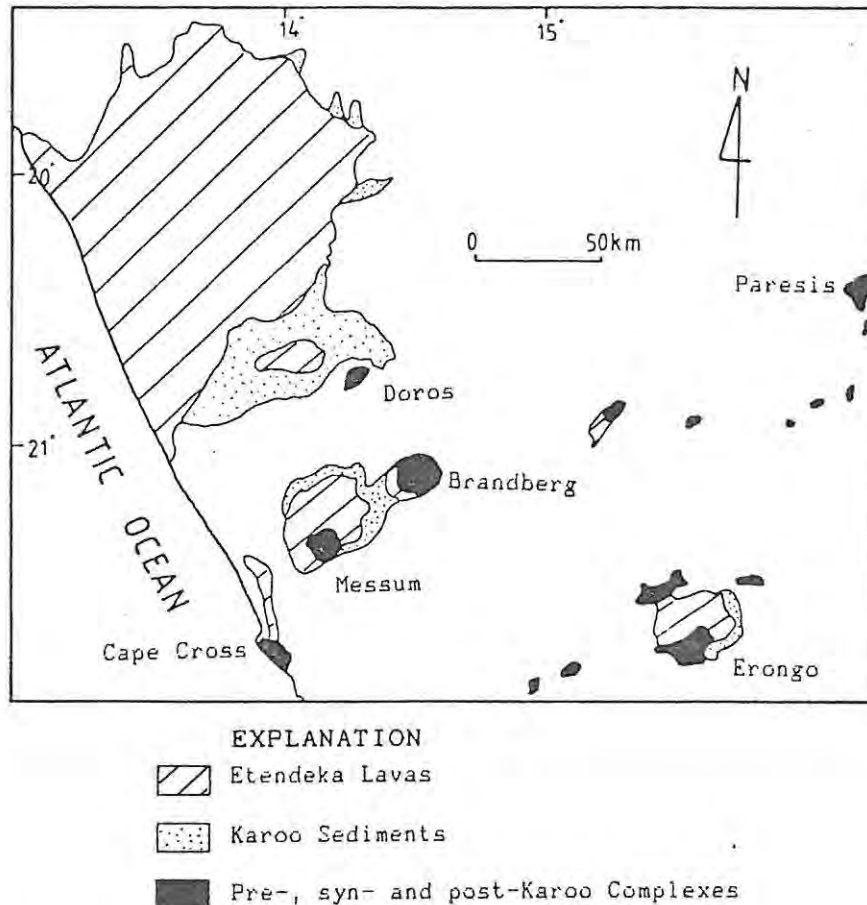


Fig. 13: Generalised geological map at the join between the coastal and intracontinental branches, showing the distribution of Karoo-age sedimentary rocks, volcanic rocks and pre-, syn- and post-Karoo complexes (Adapted from Bristow and Saggerson, 1983).

The Etendeka Formation differs from other Karoo-age volcanic rocks by virtue of its Cretaceous age, stratigraphy, mineralogy, geochemistry, and range in mineralogical, elemental and isotopic compositions for basaltic rocks (Erlank *et al.*, 1984). Covering some 78 000 km<sup>2</sup>, the Etendeka Formation constitutes a suite of basalts and evolved basalts interbedded with quartz latites, small volumes of latite and ash-flow tuffs (Milner, 1988). Present day outcrops are merely remnants of

what was once an extensive lava field (Erlank *et al.*, 1984). The main lava field north of the SKZ has an areal extent of some 12 000 km<sup>2</sup> and attains thicknesses of 880 m in the east around Tafelberg (Milner, 1988).

## 2.7. Anorogenic Alkaline Magmatism

To date some 15 separate alkaline ring-type complexes of Mesozoic age have been recognised (Prins, 1981) (Fig. 14). They occur throughout the Damara Orogen along north-easterly trends which probably correspond to transform directions in the south Atlantic (Marsh, 1973; Prins, 1981).



### EXPLANATION

Alkaline Ring Complexes	Damara Sequence
Karoo Sequence	Pre-Damara
Damara Granite	

Fig. 14: The distribution of the anorogenic alkaline ring complexes of the Damaraland Province, Namibia. D=Doros; B=Brandberg; M=Messum; SK=Spitzkoppe; E=Erongo; KW=Kwaggaspan; OK=Okonjeje; ET=Etaneno; OT=Otjohorong; ON=Ondurakorume; OS=Osongombo; KK=Kalkfeld; P=Paresis; OKR=Okorusu (Adapted from Potgieter, 1987).

The age of the complexes correlates with the early opening of the south Atlantic ocean and it is suggested that, during the Gondwana break-up, Pan-African lineaments were reactivated allowing for the anorogenic emplacement of the complexes (Prins, 1981; Marsh, 1973). Hydrothermal alteration and mineralisation are associated with the complexes (Potgieter, 1987). It has also been suggested that the mineralisation in the Northern Group may be of a similar age (Pirajno and Jacob, 1987a) and therefore possibly related to the emplacement of the complexes.

## 2.8. Geodynamic Evolution of the Damara Orogen

The geodynamic evolution of the Damara Orogen has been intensively studied for more than a decade. The proposed models all infer that subduction of one kind or another was responsible for the geodynamic development of the Damara Orogen. The various proposals are only mentioned here and the relevant references are given.

Martin and Porada (1977) based their model on aulacogen ensialic processes whereby the belt developed as five grabens in response to gravitational instability between a dense subcontinental lithosphere and the underlying less dense asthenosphere. They believed that the Damara never proceeded to the stage of ocean opening but remained as a failed rift which evolved into an aulacogen.

A delamination model proposed by Kröner (1977, 1982) suggests that the basin formed by crustal stretching over a mantle plume. Subsequent closure of the basin was by delamination followed by continental subduction, crustal underthrusting and interstacking. Kasch (1986) suggests that both delamination and suture progradation are able to explain the structural and metamorphic history of the orogen.

Models involving sea floor spreading followed by subduction have also been proposed and vary between those promoting a

limited Wilson-cycle (Miller, 1983) and those promoting a full Wilson-cycle (Hartnady, 1978; Barnes and Sawyer, 1980; Kasch, 1979, 1983b). In his model Kasch (1983b) proposes a four-stage model of continental collision involving a wide ocean, which he refers to as the *pre-collision continental convergence phase*, the *continental collision phase*, the *suture progradation phase* and the *thermal relaxation phase*. Miller (1983) envisages the Damara ocean as being somewhat like the Red Sea where sediments cover an active mid-ocean ridge, which he suggests is indicated by the Matchless Member. Barnes and Sawyer (1980) favour a model which allows for the development of a wide ocean followed by subduction and ocean closure terminating in continental collision.

Coward (1983) proposes a model which incorporates strike-slip faulting coupled with oblique subduction of small pull-apart basins which were partly floored by oceanic crust and acted as traps for the Damara sediments. According to this model, "the Damara Orogen formed at a triple-junction composed of two destructive boundaries (the coastal branches) and a transform fault (the intracontinental branch)" (Martin, 1983; page 937).

Further reviews of the models on the geodynamic evolution of the Damara Orogen are given by Tankard *et al.* (1982), Martin (1983), Hawkesworth *et al.*, (1986) and Porada (1989).

### 3. GEOLOGY OF THE SOUTHERN KAOKO ZONE

The Southern Kaoko Zone (SKZ) is a tectono-stratigraphic unit located in the north-western parts of the intracontinental branch close to the intersection with the coastal arm (Fig. 7). The area is bounded in the south-east and east by the contact between the Damara metasediments and the Damara granites. The Etendeka plateau forms the northern limit of the SKZ and to the west the SKZ is bounded by the Atlantic Ocean. The rock types present in the SKZ consist of metasediments, syn- to post-tectonic granites, alkaline and mafic intrusives, and undeformed sediments and lavas.

#### 3.1. The Damara Sequence

The northern part of the SKZ is an area in which Damara Sequence metasediments predominate. They have been intruded by several syn- to post-tectonic granites (Salem Suite and Sorris-Sorris suite) and the post-Karoo Doros and Brandberg Complexes. Freyer (in prep.) has subdivided the region into three structural/lithological domains, namely the Ogden Rocks Domain (ORD), the Lower Ugab Domain (LUD), and the Goantagab Domain (GD) (Fig. 15).

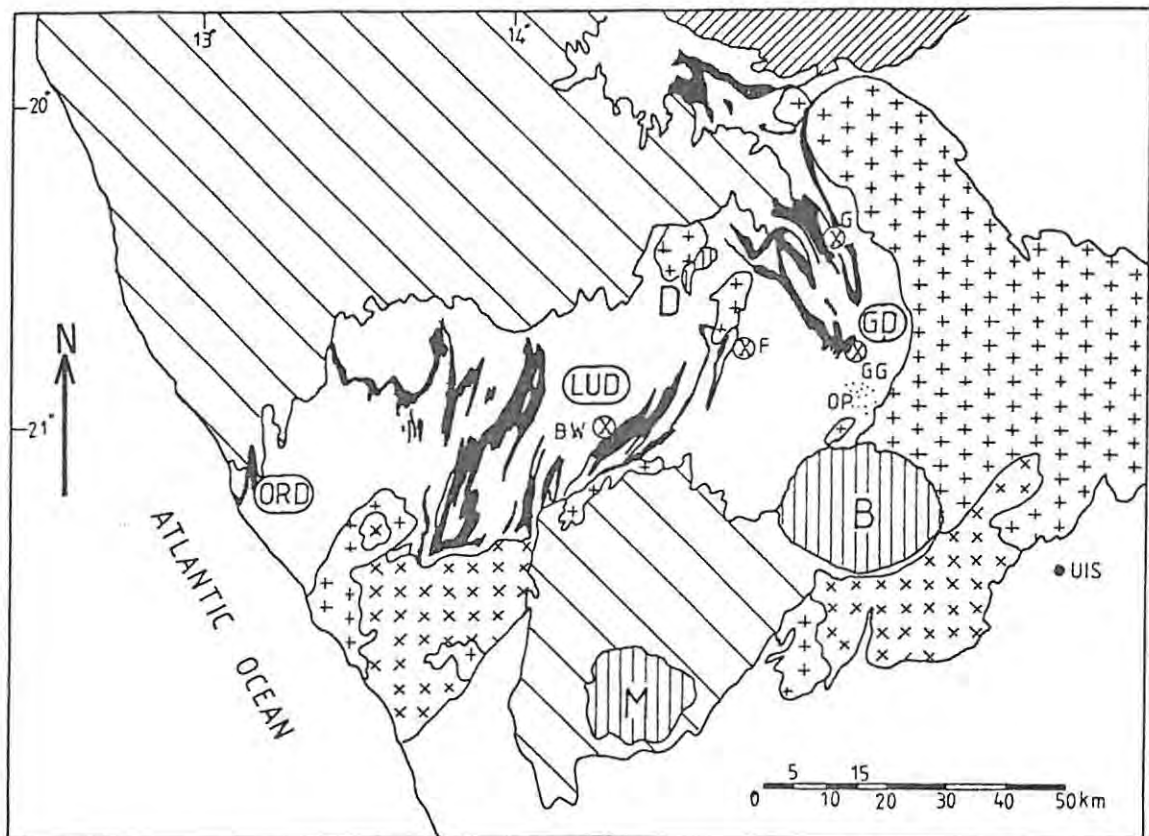
##### 3.1.1. Ogden Rocks Domain (ORD)

The rocks in the ORD have been described as being blastomylonites intercalated with sheared marble bands and phyllonites (Freyer and Hälbich, 1983). The sequence was folded during and after mylonitisation into structures resembling the folds in the LUD (Freyer and Hälbich, *op. cit.*).

##### 3.1.2. Lower Ugab Domain (LUD)

The stratigraphy of the lower Ugab River area is shown in Table II. It consists of a thick succession of mica schist with

two thin, persistent interbedded marble units (Jeppe, 1952; Miller *et al.*, 1983). The succession has been correlated with the Swakop Group (Miller *et al.*, 1983) and interpreted as being turbiditic by Miller *et al.* (*op. cit.*) and Swart (1987). The evidence for the turbidites is the presence of partial to complete Bouma sequences, the regular nature of the bedding, flute clasts, load structures, rip up clasts and graded bedding (Swart pers. comm., 1987).



- |  |   |  |                              |
|--|---|--|------------------------------|
|  | POST-KAROO INTRUSIVE COMPLEXES (B = BRANDBERG; M=MESSUM; D=DOROS) |  |                              |
|  | KAROO LAVAS & SEDIMENTS   |  | SWAKOP GROUP    Black=Marble |
|  | POST-TECTONIC GRANITES  |  | BASEMENT ROCKS               |
|  | SYN/POST-TECTONIC GRANITES  |  |                              |

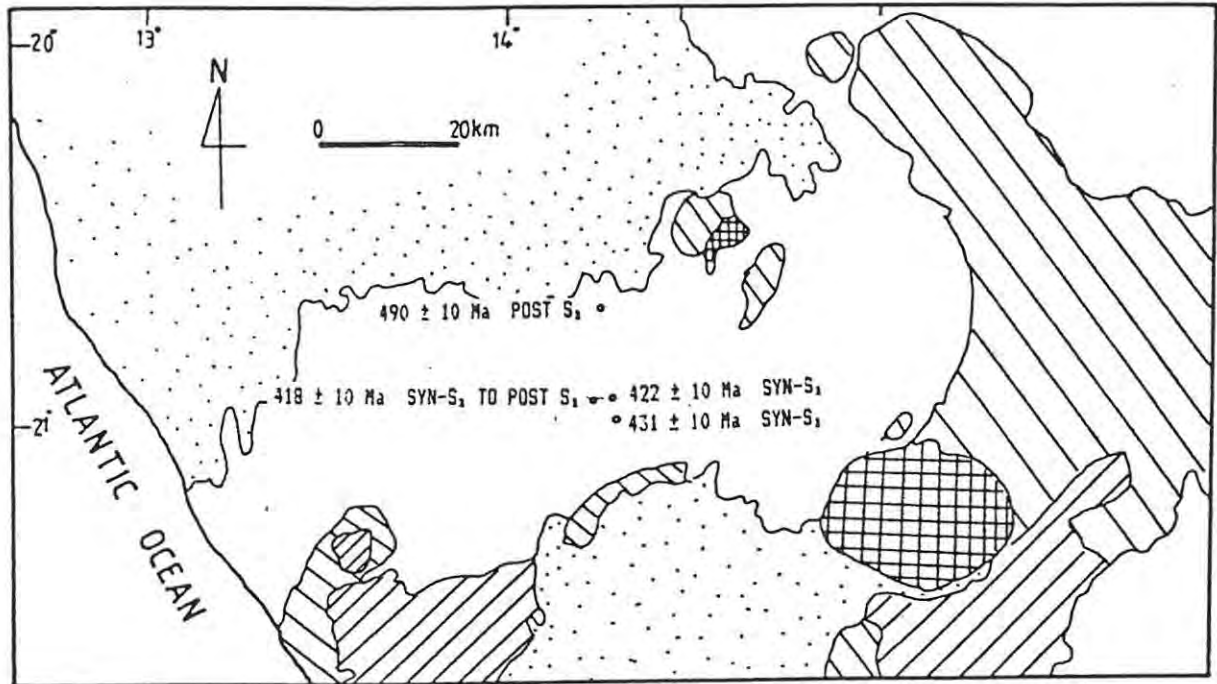
Fig. 15: Geological map of the Southern Kaoko Zone showing the structural/lithological domains as defined by Freyer (in prep). ORD = OGDEN ROCKS DOMAIN; LUD = LOWER UGAB DOMAIN; GD = GOANTAGAB DOMAIN. BW=Brandberg West; F=Frans Prospect; G=Goantagab; GG=Gamigab; OP=Ousis Pegmatites (Adapted from Pirajno and Jacob, 1987a).

TABLE II: Stratigraphy of the Lower Ugab area. (Adapted from Miller *et al.*, 1983).

LITHOLOGY	STRATIGRAPHIC SUBDIVISION		
	Jeppe (1952)	Miller <i>et al.</i> (1983)	
			Correlates
Schistose siliceous turbidites with metagreywacke bases and metapelitic tops.	UPPER SCHIST	Amis River Formation	Kuiseb Formation
Turbiditic limestone, impure limestone and schist.	UPPER MARBLE	Gemsbok River Formation	Karibib Formation
Schistose siliceous turbidites mainly greywacke with local conglomerate.	MIDDLE SCHIST	Brak River Formation	Chuoss Formation
Turbiditic limestone.	LOWER MARBLE	Brandberg West Formation	Rössing Formation
Schistose siliceous turbidites mainly greywacke with local	LOWER SCHIST	Zebraputz Formation	Okonguarri Formation

The schist separating the marble bands is mainly meta-greywacke although it is locally conglomeratic with isolated boulders. This unit has been correlated with the Chuoss Formation (Miller *et al., op. cit.*) and proves to be a useful marker horizon.

The metamorphic grades in the LUD are very-low to low and the mineral assemblages indicate greenschist facies (Porada *et al.*, 1983). The orientation of the biotite indicates a syn-S<sub>1</sub> to post S<sub>2</sub> metamorphism with ages ranging from 418 ± 10 Ma in the west to 430 ± 10 Ma in the central parts and 490 ± 10 Ma in the north (Porada *et al., op.cit*) (Fig. 16). Ahrendt *et al.* (1983) suggest that the K-Ar age of 490 ± 10 Ma represents the peak of regional metamorphism for the area. The effects of contact metamorphism are commonly developed in the vicinity of the syn-tectonic granites along the southern and eastern limits of the SKZ and in the vicinity of the syn-tectonic "Voetspoor" granite north of Frans prospect. Superimposed on the regional metamorphic fabric are biotite and cordierite porphyroblasts in the metapelitic rocks (Porada *et al.*, 1983) and wollastonite and diopside in the marbles and calc-silicate rocks respectively (Hodgson, 1972).



EXPLANATION

- |   |                        |  |                       |
|---|------------------------|--|-----------------------|
|    | Post-Karoo Complexes   |    | Syn-tectonic Granites |
|  | Karoo Sequence         |  | Damara Sequence       |
|  | Post-tectonic Granites |  |                       |

Fig. 16: Ages of metamorphism in the Southern Kaoko Zone.  
(Adapted from Porada *et al.*, 1983).

Three phases of folding have been recognised (Freyer, in prep.). The F1 folds are north-south striking, tight, anisopach folds which generally verge westwards. The term anisopach is introduced by Freyer (in prep.) to describe folds in the SKZ in which the overturned limb is structurally thickened whereas the normal limb is stretched. Associated with these F1 folds is a well developed S<sub>1</sub> platy cleavage. F2 folds are only seen at some localities where the normal limbs of the F1 folds have been kink folded. These folds exhibit a local axial-planar cleavage. Broad, low amplitude, almost east-west striking F3 folds are superimposed on the early folds and produce classical Ramsay-type 2 interference folds (Miller *et al.*, 1983). The westerly vergence of the F1 folds is rather unusual considering that the structures to the north and east verge eastwards (Porada *et al.*, 1983).

3.1.3. Goantagab Domain (GD)

The rocks in the GD are similar to those in the LUD in that two marble units are interbedded with mica schist (Osborn, 1985) (Table III). The rocks have been correlated with the Swakop Group on the basis of a lithological similarity of a mixtite unit which Osborn (*op. cit.*) suggests is equivalent to the Chuos Formation. Detailed local mapping by Groen (1986) in the Goantagab Mining Area indicates that bedding-plane thrusting may have occurred during an early phase of deformation. This suggests that the two marble units seen could be simply the result of repetition by thrusting of an original single marble layer.

TABLE III: Stratigraphy of the Goantagab Domain (Adapted from Osborn, 1985).

<p><b>Kuiseb Formation</b> (Calcareous schists, impure marbles feldspathic quartzites with calc-silicate bands)</p>	<p style="text-align: center;">KHOMAS SUBGROUP</p>	<p>SWAKOP GROUP</p>
<p><b>Karibib Formation</b> (Upper marble generally massive and homogeneous, often black in the lower parts with granitic boulders. Becomes interbedded with schist toward the top. Separated from lower marble by sericite-biotite-quartz schists. Lower marble blue-grey, massive and homogeneous)</p>		
<p><b>Chuos Formation</b> (Tillites &amp; conglomerates)</p>	<p style="text-align: center;">UGAB SUBGROUP</p>	
<p><b>Orusewa Formation</b> (Black schists, biotite-sericite-quartz±graphite schist)</p>		

Several differences occur between the LUD and GD, for instance the absence of Jeppe's (1952) Black Marker, and it is not certain whether the same lithologies in the LUD may be traced continuously across into the GD, or whether there were possibly two unconnected depositional basins now separated by a ductile shear zone (Osborn, 1985) located along the western limit of the GD. Along the shear-zone, a Damara-aged foliated ortho-amphibolitic body is present (Walraven, 1985). The body intruded into the sediments along the faulted contact between the Chuos mixtites and Karibib marbles (Petzel, 1986).

The metamorphic grades in the GD are somewhat higher than in the LUD since biotite is a common phyllosilicate in the schists, and Hodgson (1972) identified cordierite and tremolite as prograde regional metamorphic minerals. Sedimentary structures have been preserved in the rocks in the LUD whereas they are absent from the GD perhaps because of more complete recrystallisation. The structure in the area is somewhat more complicated with possibly, three phases (Osborn, 1985) or four phases of folding (Petzel, 1986).

### 3.2. Damara Granites

The southern and eastern boundaries of the Damara metasediments are marked by syn- to post-tectonic granite intrusions of the Salem Suite, and other post-tectonic granites (Sorris-Sorris granite) (Fig. 15). Smaller intrusions of the Salem-type granite occur south and north of the post-Karoo Doros Crater. The granites forming the Omangambo pluton in the eastern parts are coarse-grained, porphyritic and biotitic with large subhedral to euhedral phenocrysts of microcline (Miller and Burger, 1983). They have been dated at  $589 \pm 40$  Ma (Miller and Burger, *op. cit.*). The intrusion of the Omangambo pluton post-dates two periods of folding and produced a thermal aureole some 15 km wide (Miller, 1980).

The Sorris-Sorris granite is late- to post-tectonic, and intrudes the Omangambo pluton (Miller, 1980). The granite is

medium grained and three varieties are distinguished on the basis of the colours red, pink, and grey.

### 3.3. Post-Karoo Complexes

Included in this group of intrusives are the Brandberg Granite Complex, the Doros Crater and the Messum Complex (Fig. 15). Igneous activity during Karoo and post-Karoo times was responsible for the emplacement of these complexes and this possibly resulted in the Sn ± W mineralisation in the northern parts of the Southern Kaoko Zone.

The Brandberg Complex, located at the south-eastern corner of the SKZ, was intruded along the contact between the Damara schists and the Salem granite suite. Hodgson (1973) recognised five granitic phases of emplacement:

- (1) An initial implacement of a main hornblende granite;
- (2) Injection of aegerine-augite granite;
- (3) Intrusion of red aplite dykes;
- (4) Intrusion of white aplite dykes; and,
- (5) Injection of "Brandbergite" dykes.

According to Hodgson (1973) a period of subsidence followed the intrusion of the white aplite dykes in the south-western parts producing a brecciated zone up to 700 m wide. The collapse of the magma chamber produced the necessary cracks into which the residual melt was able to move, producing the Brandbergite dykes. Until now no age determinations for the Brandberg have been published but in the field it is seen to intrude the Karoo volcanics of the Gobobosebberge (Pirajno, pers. comm., 1988).

More recent work on the complex indicates four main rock types: monzonite-syenite, quartz-syenite, riebeckite-aegerine granite and hornblende granite (Diehl, as cited by Pirajno, 1987b). The Messum Complex, whose geology will be described below, has been dated at  $132 \pm 2,2$  Ma by Allsopp *et al.* (1984) and also intrudes into the same suite of volcanic rocks as the

Brandberg. This may imply that the Brandberg may have a similar age to the Messum complex or is younger than 132 Ma.

The Doros Crater in the north-eastern parts of the SKZ (Fig. 15), is a post-Karoo differentiated mafic complex (Hodgson and Botha, 1974), which has been dated at approximately 125 Ma (Seidner and Miller, 1968). It is pear shaped in plan, with a long axis of some 7 km and width of 3,5 km. As with the Brandberg, the Doros Complex intruded along the contact between the Damara metasediments and Salem granites. The layering in the rocks dip towards the centre of the complex and can be identified macroscopically. Hodgson and Botha (*op. cit.*) identified five magmatic episodes in its evolution:

- (1) Intrusion of gabbroic magma;
- (2) The addition of new gabbroic material and subsequent differentiation;
- (3) Emplacement of chrysolite tillaite;
- (4) Injection of gabbroic pegmatite; and,
- (5) Intrusion of aegerine-bostonite dykes.

The country rocks into which it intruded show only slight evidence of contact metamorphism.

The Messum Complex is a late-Karoo basaltic intrusive (Korn and Martin, 1954), located in the south-western parts of the SKZ approximately 30 km south-west of the Brandberg (Fig. 16). The complex consists of two parts, an inner (core) zone and an outer ring, each delimited by a system of ring faults and represents the site of an ancient volcano (Martin *et al.*, 1960).

Initial igneous activity was characterised by the extrusion of basaltic lavas alternating with acid pyroclastics. Following this was an intrusive event, which may be subdivided into an earlier basic and a later acidic event. After a considerable time period, upwelling of granitic magma resulted in ring fracturing and subsidence, the latter causing reversal of dips. Dolerite dykes subsequently intruded into the radial fractures.

The final episode involved further intrusion (alkaline in character), accompanied by cauldron subsidence and extensive metasomatism, all confined to the inner parts of the complex. Recent dating of the complex reveals an Rb/Sr age of  $132 \pm 2,2$  Ma (Allsopp *et al.*, 1984).

#### 3.4. Metallogenesis In The Northern SKZ

Within the LUD and GD several Sn/W mineralised areas have been discovered and, in places, mined (Fig. 15). The bulk of the mineralisation is hosted in quartz veins and replacement-type bodies, whereas in the south the mineralisation occurs in numerous Sn-bearing pegmatites (Ousis pegmatites).

As part of the suite of quartz vein-hosted deposits the Brandberg West Sn-W deposit occurs in the central part of the LUD about 45 km west of the Brandberg Complex. The Frans Sn ± W deposit is also located within the LUD some 25 km north-west of the Brandberg Complex. The GD hosts two known tin deposits; the Goantagab Mining Area north of the Goantagab River and the Gamigab Sn Prospect approximately 12 km south of the Goantagab River. These deposits together form a region of Sn-W mineralisation which trends for about 80 km in an east-north-east direction, known as the Northern Group (Pirajno and Jacob, 1987a). Chapter 9 deals with the characteristics of each of these deposits.

The Ousis pegmatites south of Gamigab (Fig. 15) are the only reported mineralised pegmatites in these northern parts of the SKZ. Essentially Sn and minor amounts of W mineralisation are associated with these Damara-age pegmatites and they may form part of the Uis pegmatite field which occurs further south.

#### 4. THE GEOLOGY OF THE STUDY AREA

The stratigraphic sequence at Gamigab comprises two schist units separated by a thick banded marble unit. Numerous quartz veins and dolerite dykes together with dolerite and felsic plugs have intruded the folded metasediments (Map 1). Within the banded marble unit are several breccias of various sizes and shapes of probable hydrothermal origin (see section 7.2). Samples of rock specimens collected in the field were cut for thin-section study and where appropriate stained using Alizarin Red S to facilitate the distinction of calcite from dolomite (Wolf *et al.*, 1967).

The following lithological descriptions are in stratigraphic order from the basal schist unit through the banded marble into the upper schist. The dolerite and porphyry plugs are then described and the section ends with a discussion of the probable correlation of the units with regional stratigraphic subdivisions.

##### 4.1. Basal Schist Unit

In outcrop this rock is a well foliated, fine-grained and dark-brown quartz-biotite schist. Toward the contact with the overlying banded marble the schist contains several marble lenses. Thickness of the unit in this area cannot be determined as the lower contact is not present.

Thin-section studies (Fig. 17) show that some 60% of the rock is made up of interlocking, subidioblastic and elongated quartz grains which commonly show strained extinction. The average grain size of the quartz is generally less than 0,25 mm. Approximately 38% of the rock is made up of lepidoblastic laths of biotite whose lath length rarely exceeds 0,5 mm and which defines the foliation. Several of the biotite laths contain zircon inclusions with pleochroic haloes.

Fine-grained plagioclase feldspar makes up the remaining 2%. The grains are elongate to granoblastic in shape and are generally untwinned, although some show the development of polysynthetic twins, characteristic of the plagioclase feldspars. Extinction angle measurements on suitable grains revealed the composition of plagioclase to be andesine. Tourmaline, sphene and opaque oxide are accessory phases.



Fig. 17: Photomicrograph (uncrossed polars) of the basal quartz-biotite schist. *Field of view is 4 mm.*

#### 4.2. Banded Marble Unit

At the base of the unit is a thick ( $\pm 20$  m), blue-grey marble band. Bands of pale yellow, blue-grey, yellow-brown, black and white marble overlie the basal blue-grey marble whose thickness is variable ranging between 1 and 10 m. Toward the middle of the unit are several lenses of "streaky marble", which can be traced for several hundred metres along strike but which eventually pinch out. Lenses of quartz-biotite schist are interbedded toward the top of the unit. Within the banded marble, layers of calcitic-marble and dolomitic-marble can be recognised; these are described in more detail below.

#### 4.2.1. Calcitic marble

In thin section there is no apparent difference between the white, blue-grey and pale yellow marbles, all of which consist almost entirely of equigranular, granoblastic polygonal calcite (Fig. 18). The grains are predominantly 1 mm in size and have been completely recrystallised into unstrained and twinned assemblages. Within the calcitic marble are xenoblastic, fine-grained (0,1 mm) quartz grains which constitute only a few per cent of the rock. Also present in small amounts, usually not more than 1%, is fine-grained subidioblastic dolomite.

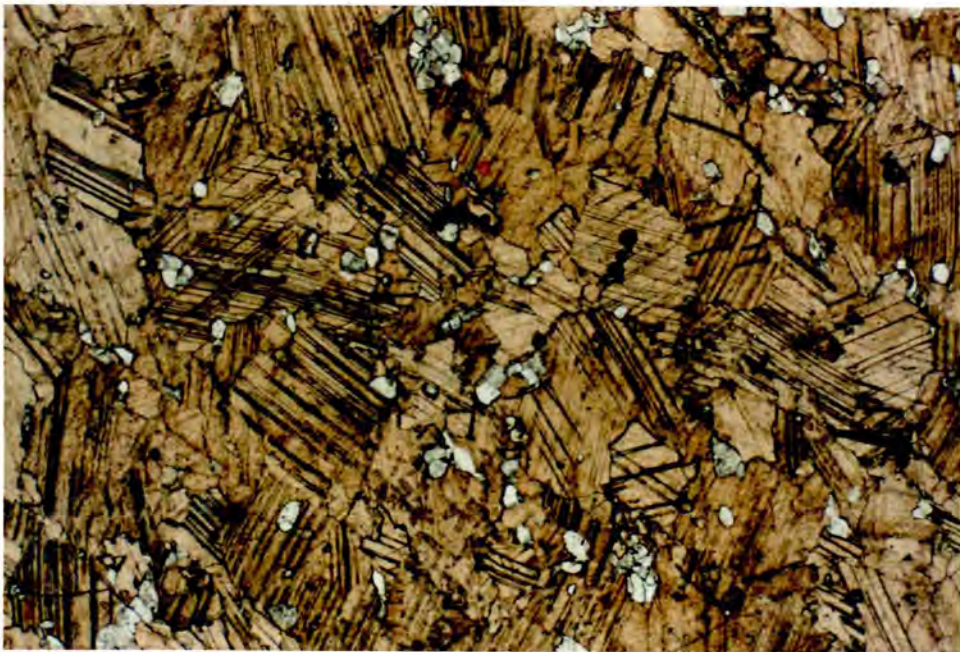


Fig. 18: Photomicrograph (uncrossed polars) of calcitic marble. Calcite has been stained. *Field of view is 4 mm.*

Sieve-textured tremolite porphyroblasts are found within some of the marble bands (Fig. 19). The subidioblastic grains are decussate and replace the early fine-grained assemblage of calcite, dolomite, quartz and colourless mica. The tremolite is usually in lath form, between 2 - 3 mm in length and colourless in plane light. Colourless phlogopite laths are also present. They are less than 0,1 mm in length, and have a distinct preferred orientation.

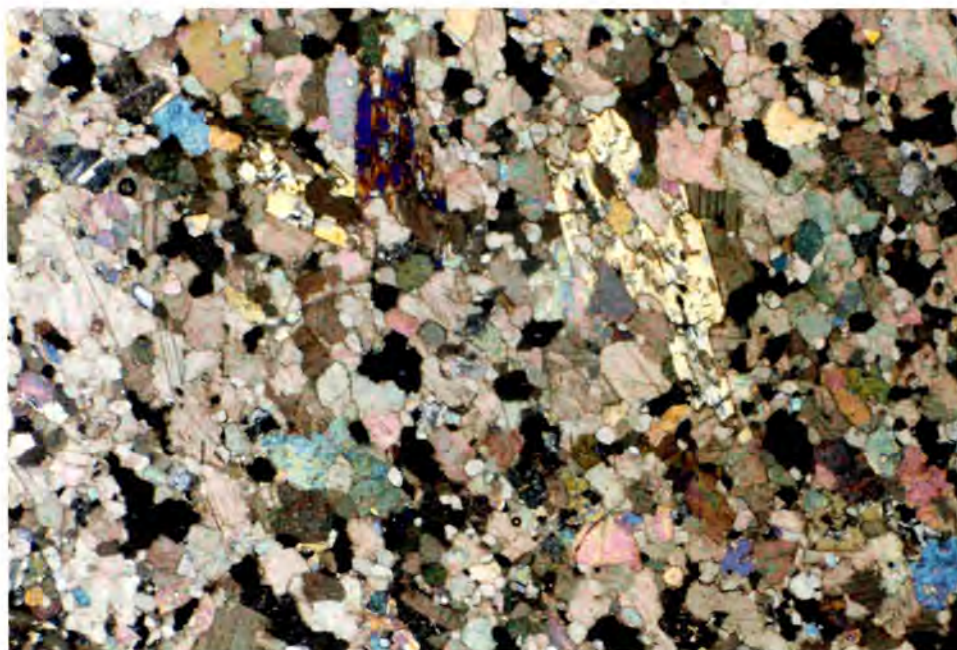


Fig. 19: Photomicrograph (crossed polars) of tremolite porphyroblasts in calcitic marble. *Field of view is 4 mm.*

Small and discontinuous buckled quartz-rich lenses occur in several of the bands. In hand specimen the quartz is very fine grained and when viewed under the microscope is seen to be completely recrystallised. The presence of graphite is responsible for the black colour of the marble and occurs as discrete microscopic flakes or as aggregates forming discontinuous lenses.

#### 4.2.2. Dolomitic marble

The yellow-brown bands are both physically and mineralogically different from the other marble bands; i.e. it is a much finer grained rock which effervesces only slightly on contact with dilute hydrochloric acid. Under the microscope the rock consists almost entirely of dolomite as fine-grained, equigranular and subidioblastic grains (Fig. 20). Small amounts of calcite (1 - 2%) and accessory amounts of fine-grained quartz occur.

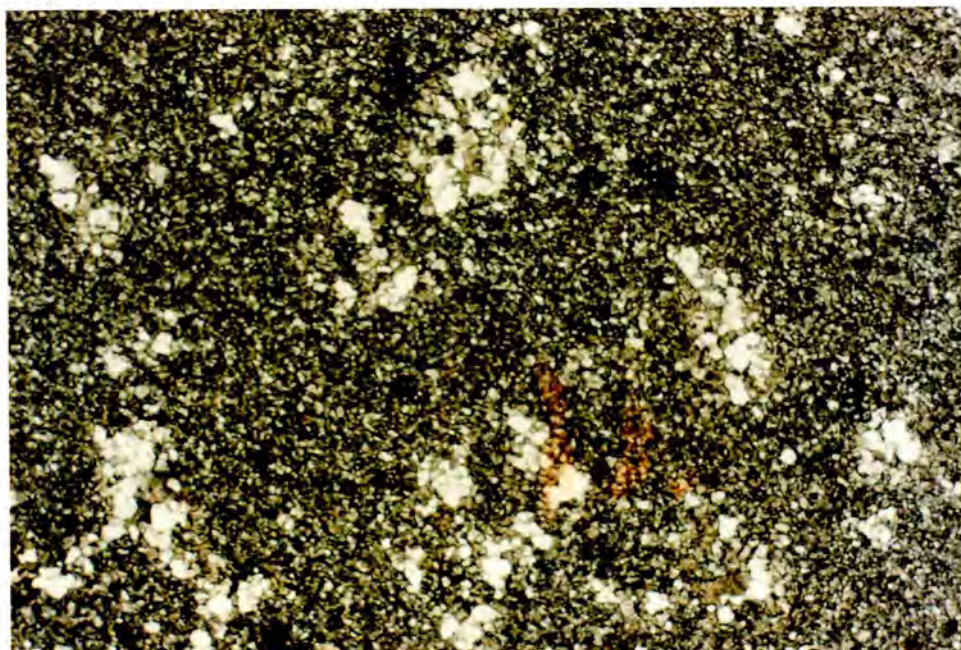


Fig. 20: Photomicrograph (uncrossed polars) of dolomitic marble. *Field of view is 4 mm.*

#### 4.2.3. Streaky marble

The "streaky marble" lenses occur between bands of medium-grained calcitic marble and fine-grained dolomitic marble (Fig. 21). In outcrop the "streaky marble" consists of elongated dolomitic clasts (up to 5 cm in length and 2 - 3 mm in width) cemented together by calcite. Thin sections show that the clasts as well as the calcite matrix are totally recrystallised.

#### 4.3. Upper Schist Unit

This metapelitic sequence is predominantly schistose although calcitic-marble bands and calc-silicate lenses are both widely developed. In hand specimen the schist is a fine grained, well foliated green quartz-biotite-chlorite rock. The strong development of the foliation in the rocks has destroyed evidence of bedding.



Fig. 21: Photograph of streaky marble in outcrop. Note the band of blue calcitic marble on the left and yellow-brown dolomitic marble on the right.

#### 4.3.1. Schist

In thin section the foliation is defined by the alignment of fine-grained (less than 0,5 mm) laths of biotite (40%), chlorite (10%) and muscovite (10%) (Fig. 22). Elongated interlocking xenoblastic quartz grains with an average grain size of less than 0,5 mm constitute approximately 40% of the rock. Medium-grained subidioblastic porphyroblasts of biotite (approximately 1 mm in diameter), which in places has been retrograded to chlorite, are seen to replace the finer grained assemblage.

In outcrop, especially in the eastern parts of the study area, large elongate porphyroblasts of retrograded cordierite were found (Fig. 23). Very few porphyroblasts contain remnant cordierite but consist predominantly of chlorite with biotite and muscovite. In places these porphyroblasts contain a grey core usually 1 - 2 mm in diameter which consists of pinite after cordierite.



Fig. 22: Photomicrograph (uncrossed polars) of upper quartz-biotite-chlorite schist. Coarse biotite flakes developed in response to thermal metamorphism. *Field of view is 4 mm.*



Fig. 23: Photograph of cordierite porphyroblasts in upper schist.

#### 4.3.2. Calc-silicate lenses

Numerous calc-silicate lenses are interbedded with the schist. They normally do not exceed 1 to 2 m in length and vary in width from about 5 cm up to 20 and 30 cm. In hand specimen they have a porphyroblastic texture with porphyroblasts of pink garnet and aggregates of green amphibole which are concentrated more toward the middle of the lenses. The remainder of the rock has a pale colour and consists of plagioclase and quartz.

In thin section the amphibole actinolite is present as radiating, decussate aggregates of slightly poikiloblastic acicular grains approximately 2 mm in length, which in places have cores of chlorite. In some instances a core of carbonate is present. Under plane-polarised light the amphibole is weakly pleochroic from colourless to pale green and when viewed with cross-polars it has an average cleavage to  $\gamma$  extinction angle of 15°. Inclusions of zircon with pleochroic haloes are present in some grains. Sieve-textured garnet porphyroblasts (2 - 3 mm in diameter) are scattered throughout the rock, replacing the finer grained portions and occur in contact with the actinolite.

The lighter coloured portions of the calc-silicate rock are also finer grained although the quartz is coarser than the feldspar. The quartz grains are xenoblastic in form, generally less than 0,25 mm in size and share sutured grain boundaries. The feldspar is much finer grained and few grains show polysynthetic twinning. Very fine-grained actinolite grains occur together with the finer grained feldspar.

#### 4.3.3. Marble interbeds

The marble interbeds are numerous and extend for several hundred metres along strike although in general they are relatively thin ranging between less than 10 cm up to 2 m in thickness. Mineralogically they consist almost entirely of fine- to medium-grained granoblastic calcite with minor amounts

of finer grained subidioblastic quartz. Within some of the marble bands small lenses of recrystallised quartz (5 - 20 cm long) are present as erosion resistant, dark coloured bands.

#### 4.4. Intrusive Rocks

The area mapped in detail contains a number of intrusive bodies including a porphyry plug, a dolerite plug, several dolerite dykes and small carbonate dykes.

##### 4.4.1. Porphyry plug

This igneous intrusion crops out 500 m north-east of the trenches (Map 1). It is red in colour, due to pervasive ferruginisation, and distinctly cuts across the folded meta-sediments with which it shares a sharp contact. The rock is brecciated and a satellite plug, 10 m to the east, is highly amygdaloidal. A second satellite plug crops out 15 m west of the main intrusion (Fig. 24).



Fig. 24: Photograph of porphyry plug and satellite plugs in outcrop.

The breccia fragments are generally small (1 - 2 cm in length), angular in shape, and lighter in colour than the igneous matrix.

In the satellite plug east of the main intrusion the amygdales are generally 2 - 3 mm in diameter (Fig. 25), although one was measured at 3 cm. The amygdales are usually spherical in shape although some are stretched probably in response to flow. Quartz is the usual filling of the amygdales although zeolite and calcite were the final phases to crystallise. Several angular marble fragments have been caught up in the igneous material.



Fig. 25: Close-up photograph of amygdaloidal (on the left) and brecciated porphyry plug.

In thin section this rock shows a distinct porphyritic character, in places exhibiting a glomeroporphyritic texture (Fig. 26). The feldspar phenocrysts are generally untwinned, and sericitised thus making compositional identification difficult. The matrix is microcrystalline and consists of a fine-grained felted mass of feldspar laths. Unfortunately pervasive ferruginisation masks much of the matrix.

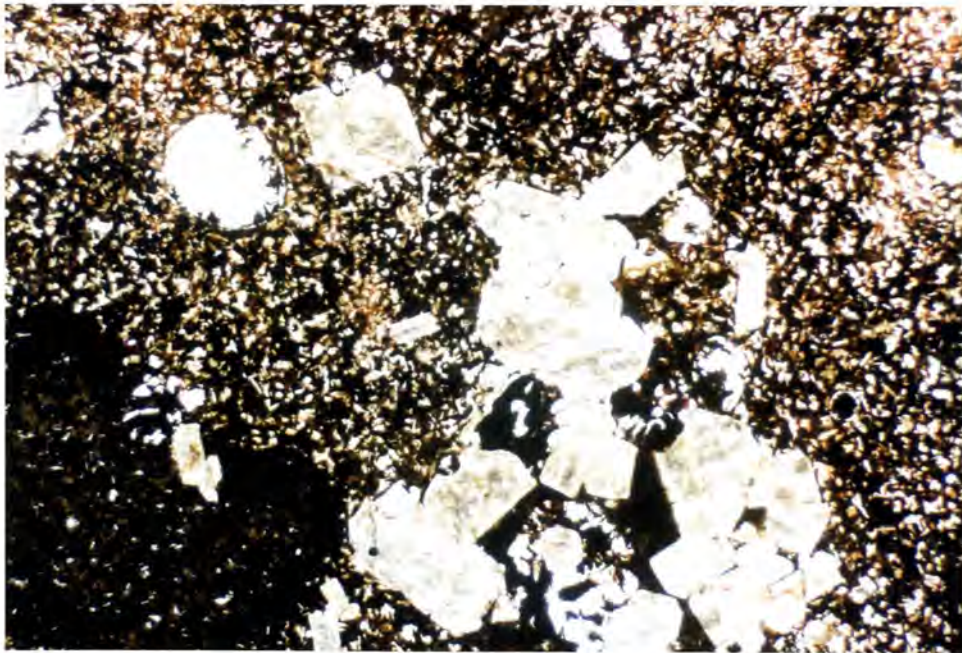


Fig. 26: Photomicrograph (uncrossed polars) of porphyry plug. Note the glomeroporphyritic texture of the feldspar phenocrysts and amygdale in the top left-hand corner. *Field of view is 4 mm.*

#### 4.4.2. Dolerite plug

A dolerite plug containing xenoliths of undeformed sedimentary rock crops out 200 m north of the porphyry plug (Map 1). It is highly weathered making it friable to handle. This intrusion cuts across the folded meta-sediments and much of the contact with the country rocks is obscured by scree cover. In places outcrops of breccia (see section 7.2) appear through the scree cover.

In thin section the dolerite is fine- to medium-grained, and even though it is weathered, it still shows an ophitic texture. Euhedral plagioclase laths (1 - 2 mm long) are partially enclosed by anhedral augite which is largely altered to calcite. The finer grained portions of the rock consist of fine-grained pyroxene and plagioclase.

In the vicinity of peg 70N/24E is a xenolith of undeformed conglomerate (Map 1). The rudaceous rock contains rounded quartz pebbles reaching 7 cm in diameter, set in a fine-grained matrix. The xenolith is small (less than 2 m in diameter) and is totally enclosed within the dolerite host which has a chilled margin developed along the contact. In thin section the quartz pebbles are polycrystalline and well rounded. The matrix cementing the pebbles consists of fine-grained clay and calcite with accessory green tourmaline, zircon and muscovite. The conglomerate is cut by several calcite veinlets.

A second sedimentary xenolith occurs within the dolerite close to peg 66N/24E (Map 1). The xenolith is a red medium-grained sedimentary rock. The contact with the dolerite is not clear but this xenolith is somewhat larger than the conglomerate xenolith (approximately 3 - 4 m in diameter). Thin-section examination shows that the rock is an immature feldspathic greywacke consisting of sub-rounded, angular quartz and feldspar grains (both microcline and plagioclase) set in a fine-grained clay matrix. Grain size is variable ranging from 0,3 mm up to 1 mm in diameter. Accessory green tourmaline and muscovite are present in the matrix.

#### 4.4.3. Dolerite dykes

Several dolerite dykes occur in the Gamigab area and in general they trend N-S sub-parallel to the regional metamorphic fabric. On surface they may be traced for several hundreds of metres along strike transecting the metasediments at a shallow angle. One dyke, south of the detailed mapped area, trends almost east-west.

In outcrop the dolerite is a fine grained, dark coloured, almost black rock which is commonly quite highly jointed. This assists the erosional processes and so in the vicinity of a dyke there is commonly a well developed dolerite scree. At one locality, in the southern parts of the area mapped in detail, a large vug is present in the dolerite. The vug is some 8 cm long by 3 cm wide and is zoned consisting of a rim of coarse quartz crystals followed by a core of very coarse grained, brown calcite. Also in the south, a dolerite dyke cuts a large breccia body in the marble (see section 7.2).

In hand specimen the dolerite appears to be unaltered but several specimens examined under the petrological microscope show alteration effects. A sample of fresh dolerite shows that the mineralogy includes olivine, titanite, plagioclase, hypersthene and sulphide. Together with the olivine, the grains are subhedral in shape and are some 1 - 2 mm in diameter. The plagioclase laths ( $An_{50}$ ) (usually less than 2 mm long) commonly show polysynthetic twinning whereas the coarser varieties show subtle zoning.

Samples of altered dolerite show that the ophitic texture is still recognisable, especially under plane polarised light. The pyroxenes and plagioclases have been altered to a fine-grained carbonate, but in some samples remnants of the original igneous mineral are still identifiable. Associated with these altered dolerites there seems to be an unusual amount of rutile or ilmenite which occurs as reticulate laths usually at a high angle to one another.

#### 4.4.4. Carbonate dykes

Within the detailed mapped area and at one other locality some 800 m east of the mineralised quartz veins are places where the basal blue-grey marble has been intruded by carbonate-rich dykes. The dykes are light brown and distinctly cut across the country rocks.

From thin-section examination, the rock is predominantly calcite and quartz (60% and 37% respectively). The calcite is generally coarser than the quartz (usually 1 mm in size), although both minerals are anhedral in shape. Also present are fine-grained muscovite and weakly pleochroic tourmaline. The muscovite occurs as small (0,1 mm) decussate laths and makes up about 2% of the rock. The tourmaline is present as euhedral and very fine-grained grains (less than 0,1 mm) of dravite and schorl although some seen are slightly larger (0,5 mm).

#### 4.5. Discussion and Correlation of the Lithologies

An initial attempt to correlate the lithologies in the area of the Goantagab Domain was done by Hodgson (1972) who divided the metasediments into two series, the Hakos Series and the Khomas Series, both of which were part of the Swakop Facies of the Damara System (Table IV). Within each series, several stages were recognised and are briefly described.

TABLE IV: Stratigraphy of the Goantagab Domain as suggested by Hodgson (1972).

		DK3	Fine-grained quartz-biotite schists and quartzite.
	Khomas Series		Dark grey calcitic marble.
		DK2	Brown dolomitic-marble. Interbedded marble and schist.
SWAKOP FACIES		DK1	Quartzitic schists.
		DH2	Calcite-marble with minor interbedded schist.
	Hakos Series	DH1	Interbedded quartz-biotite schist and quartzite.

The basal stage of the Hakos Series (DH1; D = Damara; H = Hakos) is described as an interbedded quartz-biotite schist and quartzite which has a thickness of at least 500 m. Overlying this is the DH2 stage which consists of calcite marble with subordinate schist. The marble is variable in colour ranging from grey, yellow, light brown to dark brown. In the vicinity of intrusions, contact effects are seen by the formation of tremolite.

Within the Khomas Series three stages were identified (Table IV). The DK1 stage is schistose and very similar to the DH1 schists although the DK1 metasediments are more quartzitic. The marbles in the DK2 stage, overlying the DK1 stage, too are similar to the marble in the DH2 stage although within this group it is possible to identify three zones (bottom, middle and top zones) along the same lines envisaged by Jeppe (1952). The bottom zone consists of interbedded marble and schist whereas the middle zone is essentially a brown marble. The top zone is described as a dark grey marble.

Within the DK2 stage marbles, dolomitic-marble layers occur, and these together with the calcite-marble layers give the DK2 stage a total thickness between 100 and 170 m. The uppermost stage in the Khomas Series is the DK3 stage which comprises red-brown quartz-biotite schist with quartzite interbeds and is generally a finer grained rock compared to the other schist units.

More detailed work in the Goantagab Mining Area and surrounds was documented by Osborn (1985). He based his correlation of the stratigraphy around a mixtite unit, which he equated with the Chuos Formation. On this basis the metasediments in the area are correlated with the Orusewa Formation, the Chuos Formation, the Karibib Formation and the Kuiseb Formation (Table V). Within the Orusewa Formation, Osborn (1985) recognised a lower black, graphitic schist, a siliceous schist and an upper sericitic schist. It is within the upper parts of the sericitic schist that the Chuos mixtite occurs, which is described as essentially tillitic and/or conglomeratic rocks

TABLE V: General Stratigraphy of the Goantagab Domain (Adapted from Osborn, 1985).

Kuiseb Formation (Metapelitic)	KHOMAS SUBGROUP	SWAKOP GROUP
Karibib Formation (Marble with lenses of schist)		
Chuosi Formation (Mixtite)	UGAB SUBGROUP	
Orusewa Formation (Metapelitic)		

with minor quartz schist, marbles and banded ironstones (Osborn, *op. cit.*). The Karibib Formation, which overlies the Orusewa Formation, consists of two marble units separated by a sericite-biotite-quartz schist. Mineralogically the marbles are calcitic with traces of phlogopite, magnetite and graphite. The upper marble unit contains granitic drop-stones and is interbedded with schist toward the contact with the Kuiseb Formation. The Kuiseb Formation in the area is made up of rhythmically banded, interbedded and generally finely grained sequences of slightly calcareous schists, quartzites and impure marbles. Le Roux (1982) suggests that the prospect is underlain by rocks of the Kuiseb Formation.

Work by the author in the region around the Gamigab Sn-prospect suggests that the lithologies at Gamigab and Goantagab are somewhat different. One such difference is the absence of a mixtite unit at Gamigab. The Karibib Formation at Goantagab is represented by two marble units separated by a schist band whereas the marble at Gamigab is a single marble unit consisting of interbedded calcite and dolomitic marble layers, with lensoid schist.

The Kuiseb Formation in the region west of the Brandberg is represented by schistose siliceous meta-turbidites of the Amis River Formation (Miller *et al.*, 1983). These same rocks are traced across from Brandberg West, eastward until they are

obscured by the superficial sand and calcrete cover east of Gamigab (Miller *et al.*, 1983). According to SACS (1980), the Kuiseb Formation contains lenses of calc-silicate rock. Similar lenses are found in the Gamigab area. Porada (1973) suggests that some of these spindle-shaped lenses in parts of the Damara Orogen are as a consequence of rock deformation.

Continuity of the meta-sediments in the GD is necessary when attempting to correlate the lithologies. Careful study of the aerial photographs in the GD accompanied by follow-up field work indicates that the lithologies in the area around Gamigab may be correlated with those in the area around the Goantagab Mining Area. The Orusewa Formation may be traced all the way from Goantagab to Gamigab and in both places marks the base of the exposed stratigraphy in the GD.

The marble unit at Gamigab, although being somewhat different from that at Goantagab, would therefore be equivalent to the Karibib Formation. The differences between the two areas are probably both sedimentological and structural. This work in the Gamigab area has shown that shearing occurred early during deformation (see section 5.1.1), and work by Groen (1986) has shown the possibility of thrusting in the Goantagab area. In both places this movement occurred in the Karibib Formation but was more pronounced at Goantagab where it may have resulted in some duplication of the lithologies.

The Upper Schist at Gamigab is therefore correlated with the Kuiseb Formation. Table VI shows the relationship in the lithologies between Goantagab and Gamigab, and the suggested correlation.

The cross-cutting nature of the intrusive rocks and the fact that they are not deformed is a clear indication that they are younger than the rocks of the Swakop Group. In general the dolerite dykes in the Gamigab area have an overall general north-south trend which is similar to other dykes in GD classed as Karoo dolerites (Botha and Hodgson, 1976). In places dykes have been altered and the presence of a vug indicates intrusion

to shallow levels. At least some dolerite intrusion post-dated the hydrothermal brecciation since one dyke cross-cuts one of these breccias. The implications of this are very important as it is able to give some indication of the age of the hydrothermal activity and possibly the mineralisation, as will be discussed in section 8.3.2.

TABLE VI: Lithological and stratigraphic subdivisions of the Damara Sequence in the Goantagab Domain.

		OSBORN (1985) GOANTAGAB DOMAIN	THIS WORK GAMIGAB AREA
KHOMAS SUBGROUP	KUISEB FORMATION	Rhythmically interbedded calcareous schist with impure marble, calc-silicate bands and feldspathic quartzite. Basal gritty calcareous schist.	Interbedded marble and schist with calc-silicate bands and basal platy marble and schist.
	KARIBIB FORMATION	Two massive marble units separated by sericite-biotite-quartz schist. Lower blue-grey marble becoming interbedded with schist toward contact with overlying schist. Upper marble contains granitic boulders and becomes interbedded with schist toward contact with Kuiseb Formation.	Single marble sequence consisting of interbedded calcitic and dolomitic marble layers. Lenoid quartz-biotite schist. Marble is blue-grey in colour at the base and at the contact with the Kuiseb Formation.
UGAB SUBGROUP	CHUOS FORMATION	Lenoid mixtite unit with tillite, conglomerate, schist and BIF.	NOT PRESENT
	ORUSEWA FORMATION	Black schist, biotite-sericite-quartz schist.	Quartz-biotite schist with interbedded marble close to contact with Karibib Formation.

## 5. STRUCTURE

### 5.1. Folding

The lithologies in the Gamigab area have been subjected to four phases of folding. The periods responsible for the folding will be termed D1, D2, D3 and D4, whereas the structures produced are termed F1, F2, F3 and F4. Original bedding is labelled  $S_0$ , as distinct from  $S_1 - S_4$  which define the s-surfaces (axial planar foliation) generated during the folding events. Associated lineations are designated  $L_1, L_2, L_3$  and  $L_4$  and the fold axes associated with F1 to F4 will be termed B1, B2, B3 and B4. The refolding of earlier axial planes and axial planar foliation is the evidence used to determine the succession of the fold phases.

#### 5.1.1. F1 structures

The first phase of deformation (D1) in the Gamigab area was a period during which extensive transposition and recrystallisation of the lithologies occurred. This early phase of deformation is represented by an axial planar transpositional banding in the Karibib Formation and the extensive and penetrative regional foliation in the metapelitic rocks ( $S_1$ ). Bedding within the marble and schist has been obliterated but can still be recognised in a few places in the marble as small scale mesoscopic intrafolial  $F_1$  folds (Fig. 27). The fold hinges of these minor folds ( $L_1$ ) plunge steeply and their axial planes lie parallel to the banding in the marbles.

The fabric in the metapelitic units is expressed by the strong parallel alignment of the abundant phyllosilicate minerals biotite, muscovite and chlorite. The penetrative foliation has obliterated any traces of original sedimentary structures and all that remains in outcrop is a highly foliated rock. The contact between the schist and the marble is sharp and lies parallel to the foliation (i.e.  $S_1$  is parallel to  $S_0$ ).



Fig. 27: Photograph of a minor intrafolial fold in the Karibib Formation, within an F2 fold closure.

Shearing within the marble also occurred during an early stage of deformation and is expressed by a 0,5 m thick layer of mylonitic appearance, which is developed in several places between and parallel to, two bands of different mineralogy (ie: calcitic-marble and dolomitic-marble). The sheared band consists of elongated clasts of dolomitic-marble in a matrix of calcitic-marble. These bands of "streaky marble" are persistent over quite long distances along strike (several hundreds of metres) but are seen eventually to pinch out.

#### 5.1.2. F2 Structures

The folds developed during D2 are easily identifiable on aerial photographs. They are represented by megascopic, almost N - S trending folds which plunge between 30° and 50° toward the south. The isoclinal F2 folds are commonly upright although in some instances they are overturned to the west, usually not more than 20°. In cross section the folds have open antiforms but tight synforms so producing "M" shaped folds.

Fig. 28 is a contoured  $\pi$  diagram of poles to foliation and banding in the schists and marbles respectively. The structural data came from the fold limbs as well as the hinge zones. When plotted on the stereonet a high concentration of poles occur around  $110^\circ$  and  $280^\circ$ . The remainder of the data helps define a weak girdle across the stereonet through which a great circle can be drawn. The pole to this great circle defines the fold axis and is indicated as B2 in Fig 28. From the diagram it is evident that the F2 folds trend approximately  $015^\circ$  and plunge  $40-50^\circ$  toward the south.

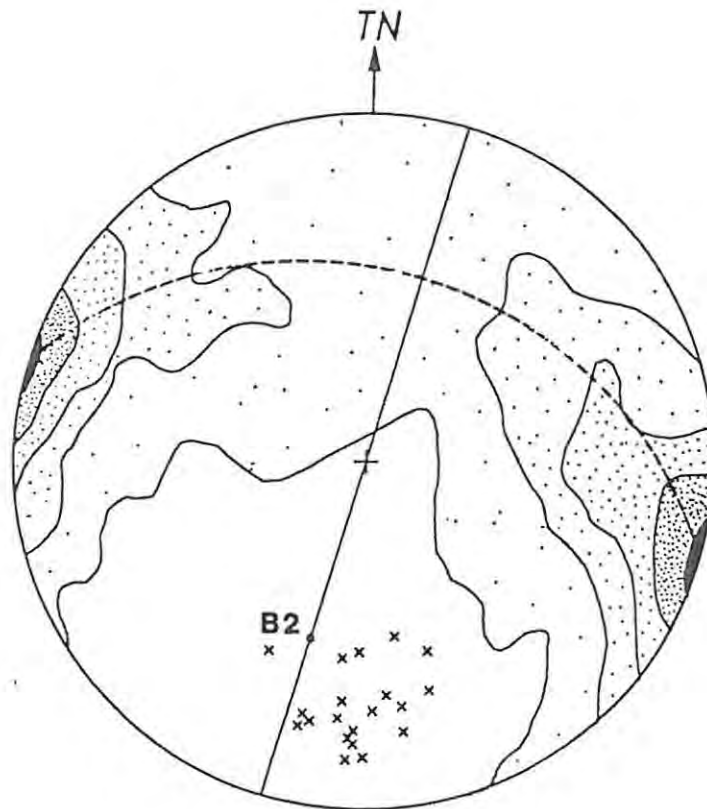


Fig. 28: Poles to banding and schistosity and measured lineations (x). B2 = average plunge of the F2 axis. Contour intervals at 13, 8, 5, 3, 1 per 1% area.  $N > 1000$ .

Lineations associated with this phase of folding are usually in the form of a mineral streaking but more commonly as fold mullions along the F2 limbs because of minor 's' and 'z' folds. The  $L_2$  lineations are only expressed in the marble and even so are not very widespread. They are plotted on Fig. 28 and plot

in the region around B2 as defined previously. No penetrative fabric is associated with the F2 folds, although in several of the F2 fold closures, small scale transposition of the early fabric may be seen (Fig. 29).



Fig. 29: Photograph of F2 minor fold with local transposition into  $S_2$  in the fold closures.

### 5.1.3 F3 Structures

D3 (the third phase of folding) was responsible for the major change in strike of the lithologies between Goantagab and Gamigab. The main structures around Goantagab trend approximately south-south-east whereas those at Gamigab trend south-south-west. Definition of the fold axis on the stereonet is difficult although the drag effect is very distinct on air photographs (Fig. 30).

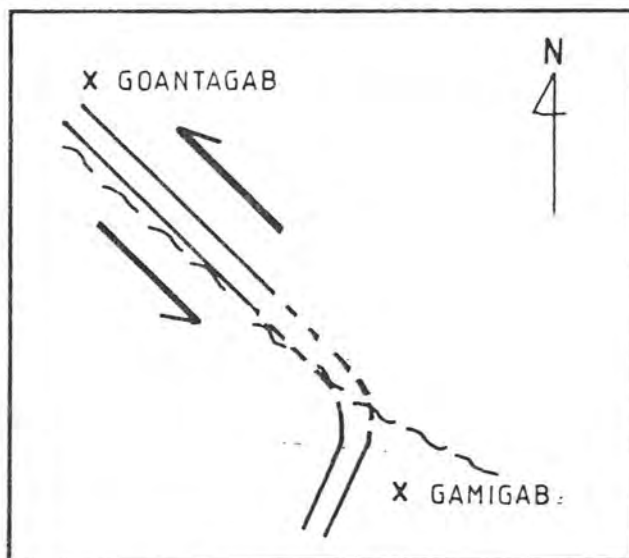


Fig. 30: Schematic sketch showing the difference in trend of the main structures between Goantagab and Gamigab and possible sense of movement during drag folding.

#### 5.1.4. F4 Structures

The fourth phase of folding (D4) was responsible for a flexuring of the earlier structures about an axis trending approximately north-west. Refolding of the earlier structures is expressed on a small scale by tight kink folding in the schists (Fig. 31) and as small open folds in the marble bands (Fig. 29).



Fig. 31: Photograph of kink folded schist.

Fig.32 is a contoured  $\Pi$  diagram of the axial planes of the F4 folds. The steep nature of axial planes of these minor folds is confirmed by the high concentration of points along the circumference around  $030^\circ$  and  $210^\circ$ . The spread of points is due to slight differences in orientation of the crenulations on either side of the B4 axis. Also plotted on Fig. 32 are measured plunges of these crenulations which show that the F4 structures plunge approximately  $45^\circ$  to the north-west. The best lineations associated with the F4 crenulations are well developed fold hinges although at several localities an intersection lineation is present. Since the crenulation cleavage is at a high angle to the regional  $S_1$  foliation (almost  $90^\circ$ ), the resultant intersection of these two surfaces can produce a pencil schist.

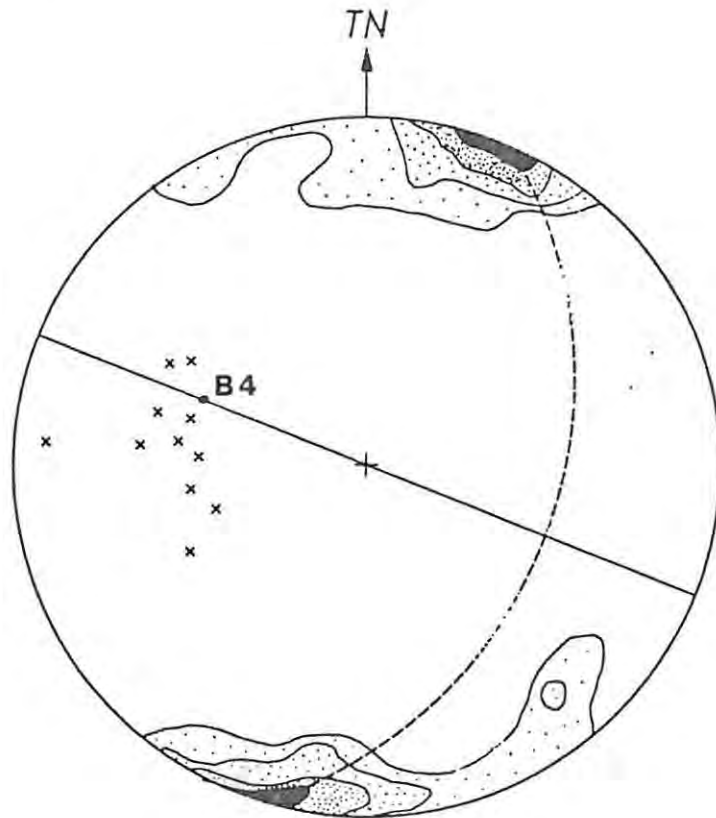


Fig. 32: Poles to F4 crenulation and kink band axial planes, and measured lineations (x). B4 = average plunge of F4 axis. Contour intervals at 20, 15, 9, 3 per 1% area. N = 40.

## 5.2. Faulting

Several faults occur in the Gamigab area. They all strike east-west and postdate the folding. Within the detailed-mapped area, three faults were identified, one to the north of, and two to the east of the mineralised quartz veins. Unfortunately the amount of displacement along the faults is difficult to determine due to the lack of marker horizons and local pervasive ferruginisation.

Two, possibly three, much larger faults occur to the north-west and west of the detailed mapped area. A major fault occurs to the north-west of the prospect, cross-cutting the regional fabric with a north-west trend, and also defining the contact between the basal Orusewa Formation and the uppermost Kuiseb Formation. Alteration and minor quartz veining occurs in the vicinity of this fault. It extends northwards for some considerable distance and disappears beneath the Karoo cover north-west of Goantagab.

## 5.3. Summary of the Structural Development at Gamigab

The structural development in the Gamigab region is shown in Fig. 33. D1 produced the banding in the marbles and the main fabric in the metapelitic sequences. Remnants of F1 are expressed by several minor intrafolial folds in the marbles, but the main F1 fold closures have been totally transposed. The banding and schistosity is refolded during D2 as evidenced in the F2 fold closures. Drag folding during the next phase of deformation resulted in the change of strike of the structures between Gamigab and Goantagab. The final phase of folding resulted in small-scale, brittle kink folding in the schists and open folding in the marbles.

Several faults transect the area and are associated with quartz veining and ferruginous alteration, as a result of the interaction of fluids with the marbles. The origin of the fluids may have been a mixture of hydrothermal fluids and

meteoric waters which were able to permeate to some depth along the fault plane, reacting with the country rocks and precipitating the iron from the fluid or from the crystal lattices of the calcite and/or dolomite. A heat source at depth (a hidden cupola, and source for hydrothermal fluids ?) would have helped in drawing the fluids through the country rocks.

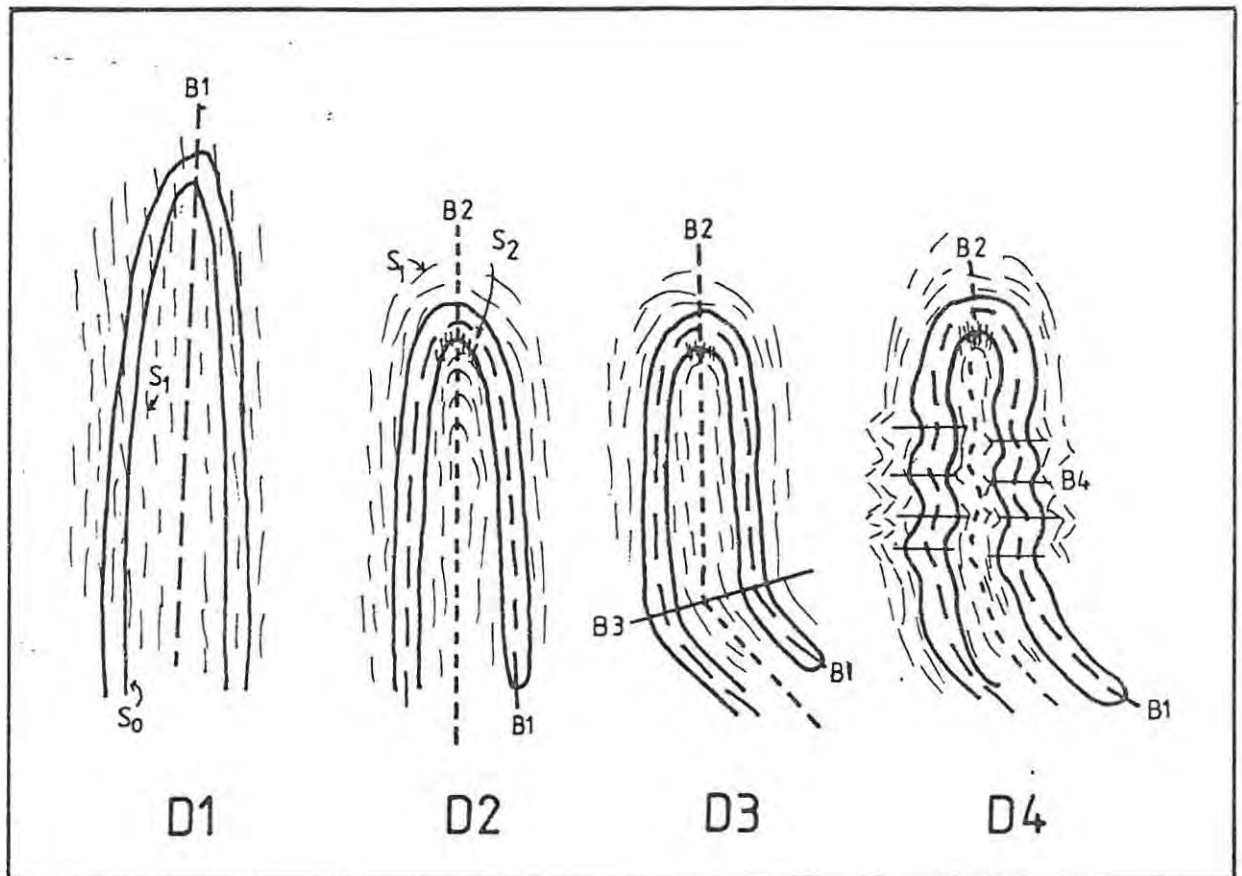


Fig. 33: Simplified sketch of the structural development at Gamigab. D1=tight isoclinal folding with extensive transposition and penetrative  $S_1$  development and minor shearing. D2=refolding of early F1 folds into tight isoclinal south plunging folds with local  $S_2$  developed in fold closures. D3=drag folding with shearing (?), D4=kink folding of earlier structures.

#### 5.4. Structural Development around Goantagab

The structural development around Goantagab is quite complex and is still being assessed, but to date several geologists have made rather different proposals. The main emphasis has been to try and provide a model which adequately explains the localisation of the mineralisation.

Petzel (1984) suggests that three phases of folding produced the upright to westerly vergent structures. The F1 and F2 fold axes are sub-parallel, trending north-north-west. D2 refolded the F1 structures into isoclinal F2 folds which are the main structures in this area. The F3 structures are represented by gentle, north-east trending flexuring of the F1 and F2 axes. Petzel (op. cit.) also mentions a fourth phase of folding, which occurred south of Goantagab, which led to the flexuring of the north-north-west trending structures into south-south-west trending structures in the southern parts of the GD (i.e. the region around Gamigab).

Osborn (1985) also envisages three phases of folding although his ideas are somewhat different to those of Petzel (1984). In his model the F1 structures are tight, isoclinal and north-plunging folds which define the main structure. F2 folds are north-north-west trending, southerly-plunging tight structures whereas D3 was an anticlockwise rotational event causing drag folding along a sinistral shear zone. Interference of F3 with the F1 and F2 structures produced a monoclinial structure but which has subsequently been disproved by drilling.

Groen (1986) presented a model comprising two fold events. The first folds to develop were small and large scale north-north-west trending recumbent folds. During this period, low-angle or bedding plane thrusting accompanied the folding, resulting in the repetition of a postulated one-marble sequence. The evidence for the thrusting is in the form of a strongly tectonised sericite-biotite schist which separates the two marble bands of the Karibib Formation. D2 refolded the F1 structures about axes that were more or less coaxial with the

F1 axes, producing open to tight folds. The large F2 folds form the structures that dominate the area.

#### 5.5. Structural Development in the Goantagab Domain

When comparing the structures that are developed in both the Goantagab and Gamigab areas it is apparent that several similarities exist:

- (i) F2 folds define the main structures;
- (ii) B1 and B2 are parallel;
- (iii) Early shearing occurred; and,
- (iv) Dragging of early structures accompanied by ductile shearing.

Any attempt to relate the structural development of these two areas would require both further detailed structural work in the region between Gamigab and Goantagab and clarification of the complex fold history at Goantagab. No attempt will be made in this study, but suffice to say that at this early stage there are these similarities.

Correlation of the structures between adjacent regions based on orientation alone is a problem although similarities are also seen. In the LUD, Freyer (in prep.) has identified a phase of deformation which produced large scale F3 folds which trend approximately north-east. To the west in the Northern Zone, Miller (1972) also recognises a period of deformation which in places trends north-east, but neither of these can be correlated with any certainty to the drag folding in the GD without further detailed structural work.

In his work in the lower Ugab region, Freyer (in prep) recognises changes in orientation of structures in the vicinity of granite contacts, for example around the 'Voetspoor' granite north-west of Gamigab. Although the region around Gamigab does not have any exposed granite, Freyer (in prep.) suggests that flexuring in the general area could be related to an intrusive

at depth. Possible field evidence for such an intrusion is the presence of elongated biotite porphyroblasts approximately 2 km south of the mineralisation (see section 6.2).

## 6. METAMORPHISM

Rock-forming mineral assemblages are stable only under certain P-T conditions. If these conditions are changed, those assemblages may become unstable, undergo reaction and produce new mineral assemblages that are stable under the changed conditions. In pelitic rocks these controls are essentially temperature and pressure, whereas in carbonate rocks, the variance is greater because the reactions are divariant in that the fluid compositions and pressures (sum of the partial pressures of H<sub>2</sub>O and CO<sub>2</sub> among others) need to be considered.

The most important part of determining the grade of metamorphism in any area is the identification of the minerals and mineral assemblages present. In the determination of the metamorphic conditions, the concept of metamorphic grades as defined by Winkler (1979) will be used. The sub-sections below contain a brief description of the rocks but the reader is referred to Chapter 4 for more comprehensive details.

### 6.1. Regional Metamorphism

#### 6.1.1. Indicator minerals in the metapelites

The schists in the Gamigab area consist predominantly of quartz, biotite, muscovite, plagioclase feldspar and chlorite. In the Orusewa Formation chlorite is absent but it is both a prograde and retrograde mineral in the rocks of the Kuiseb Formation. The lepidoblastic texture of the schists is due to the parallel alignment of the fine-grained (less than 0,5 mm) phyllosilicates (essentially biotite) which form the pre-penetrative S<sub>1</sub> foliation.

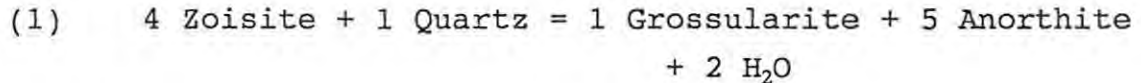
Quartz is a common mineral in the metapelitic assemblages and occurs as xenoblastic and slightly elongated grains which display undulose or strained extinction. It is present in the Kuiseb schists in stable contact with muscovite. Plagioclase is also present and is sometimes twinned and has an andesine

composition.

#### 6.1.2. Indicator minerals in the calc-silicate lenses

The calc-silicate lenses, which are widely developed in the Kuiseb Formation, commonly contain the assemblage: actinolite - plagioclase - grossularite - quartz  $\pm$  zoisite.

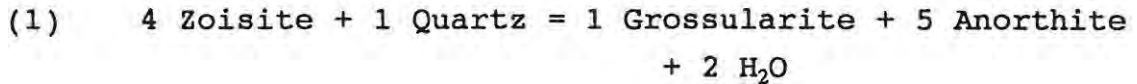
Zoisite is a common mineral at very low-grades of regional metamorphism and the reactions responsible for its formation include the breakdown of lawsonite (Winkler, 1979). If quartz is absent from the assemblage zoisite becomes unstable and breaks down in a CO<sub>2</sub>-rich environment (i.e. if XCO<sub>2</sub> is increased) to produce anorthite and calcite (Storre and Nitsch, 1983). In the presence of quartz the breakdown of zoisite is somewhat different and grossularite can form (Storre and Nitsch, *op. cit.*) as shown by the reaction below:



Grossularite can also form from other reactions and include the breakdown of prehnite (Winkler, 1979).

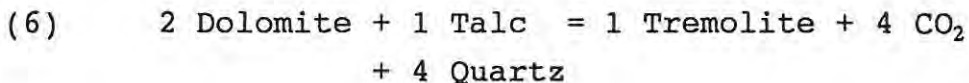
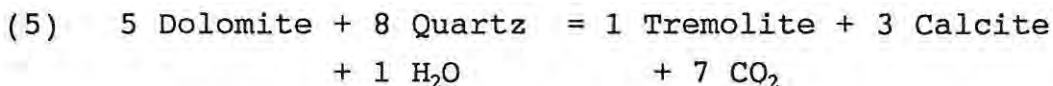
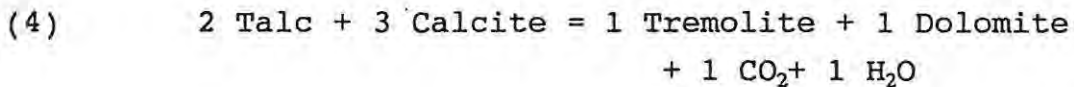
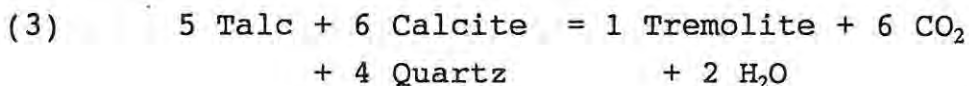
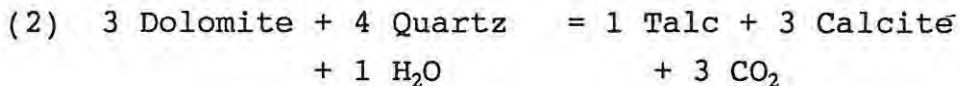
Experiments by Gordon and Greenwood (1971) have shown that grossularite may, under conditions of increased XCO<sub>2</sub>, breakdown during high-grade metamorphism into calcic-plagioclase and wollastonite.

In the calc-silicate lenses, grossularite is present as sieve-textured grains which replace the finer grained quartz - feldspar  $\pm$  zoisite assemblage. Inclusions in the garnet are mainly quartz but no zoisite was observed as inclusions within, or as grains close to, the grossularite. However a single zoisite grain was seen in stable contact with an actinolite cluster. This suggests that the grossularite forming reaction may be given by:



### 6.1.3. Indicator minerals in the marbles

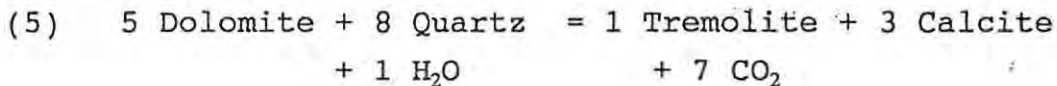
The marbles in the Gamigab area consist predominantly of calcite with lesser amounts of quartz and dolomite and trace amounts of phlogopite. However, within the dolomitic layers fine-grained dolomite is more abundant than calcite. Idioblastic, twinned and coarse-grained tremolite grains are present within some of the marbles, replacing the finer grained calcite, quartz and dolomite assemblages. Talc may also form in these rocks as indicated in the reactions below. Several reactions have been suggested for the formation of tremolite (Metz and Tromsdorff, 1968; Metz, 1970; Puhan and Hoffer, 1973; Slaughter *et al.*, 1975; Winkler, 1979):



Tremolite can form from the reaction between dolomite and quartz in the presence of H<sub>2</sub>O (reaction 5). At even higher temperatures then diopside and forsterite can form generally from the reactions of combinations of tremolite, calcite, dolomite, quartz and talc (Metz, 1970) but this has not

occurred in the Gamigab area. If either of the two minerals were present it would indicate metamorphic conditions of at least amphibolite facies (Winkler 1979).

In samples where tremolite was observed, dolomite and quartz were not found in contact with each other. Talc is not present in the Gamigab area and is barely present at Goantagab and so probably does not appear in the formation of tremolite. Hence the tremolite-forming reaction is:



#### 6.1.4. P-T Estimates for the Gamigab region

An accurate determination of the conditions which prevailed during metamorphism is not possible from only studying mineral relationships, although a reliable estimate can be made.

The mineral assemblages in the schists are typical of the greenschist facies, above the reaction-isograd stilpnomelane + muscovite out/biotite + muscovite in, which according to Winkler (1979) occurs at temperatures greater than 420°C at 1 kbar (Fig. 34).

The grossularite in the calc-silicate lenses of the Kuiseb Formation formed through the reaction of zoisite and quartz. The pressure-temperature dependency of this reaction is shown in Fig. 35 and as can be seen from the curve the reaction can take place at higher temperatures with an accompanying increase in pressure. The mineral assemblages in the schists suggest temperatures less than 500°C and if this is then applied to Fig. 35, pressures of less than 2 kbar are estimated for the Gamigab area.

The thermodynamic study of the CaO-MgO-SiO<sub>2</sub>-H<sub>2</sub>O-CO<sub>2</sub> system by Slaughter *et al.* (1975) shows that at pressures of 1 kbar the tremolite-forming reaction occurs between 400°C and 450°C for

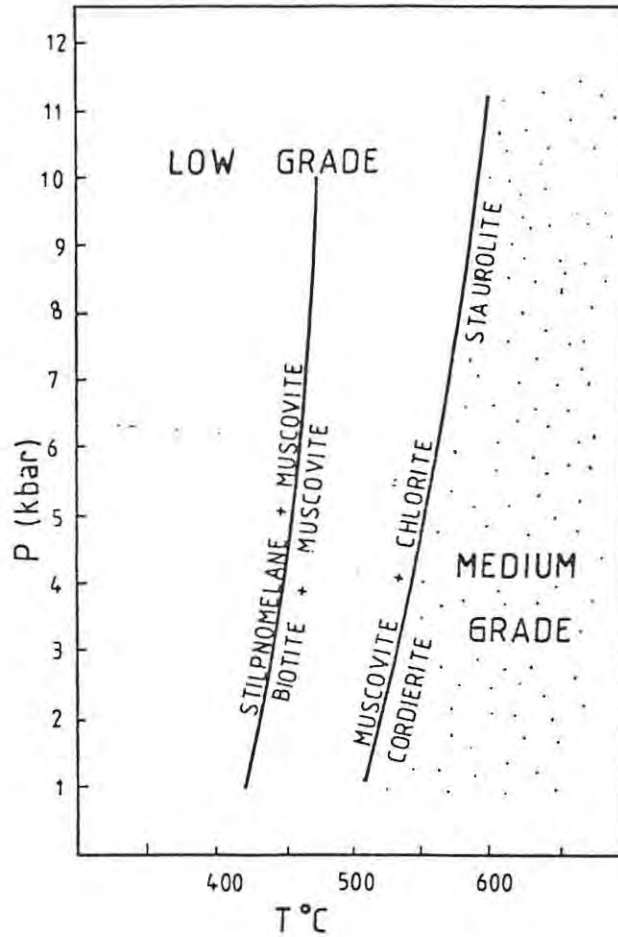


Fig. 34: P-T diagram showing the division between low and medium grades of metamorphism (Adapted from Winkler, 1979).

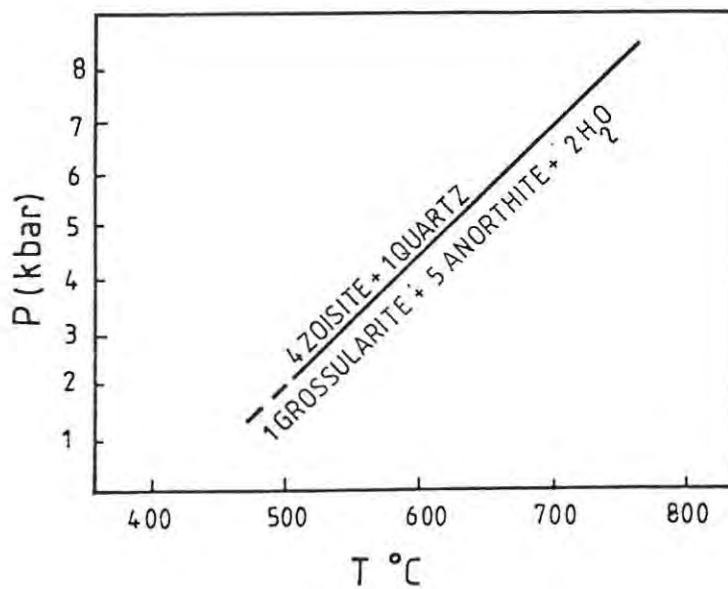


Fig. 35: P-T diagram showing the reaction curve for grossularite (Adapted from Storre and Nitsch, 1983).

$X_{CO_2}$  values greater than 0,7 (Fig. 36). Consider now the pressure at 2 kbar for the same reaction. The results from the work of Slaughter *et al.*, (*op. cit.*) suggest that the reaction can start at slightly higher temperatures ( $\pm 440^\circ C$ ) and persist up to temperatures of  $490^\circ C$ .

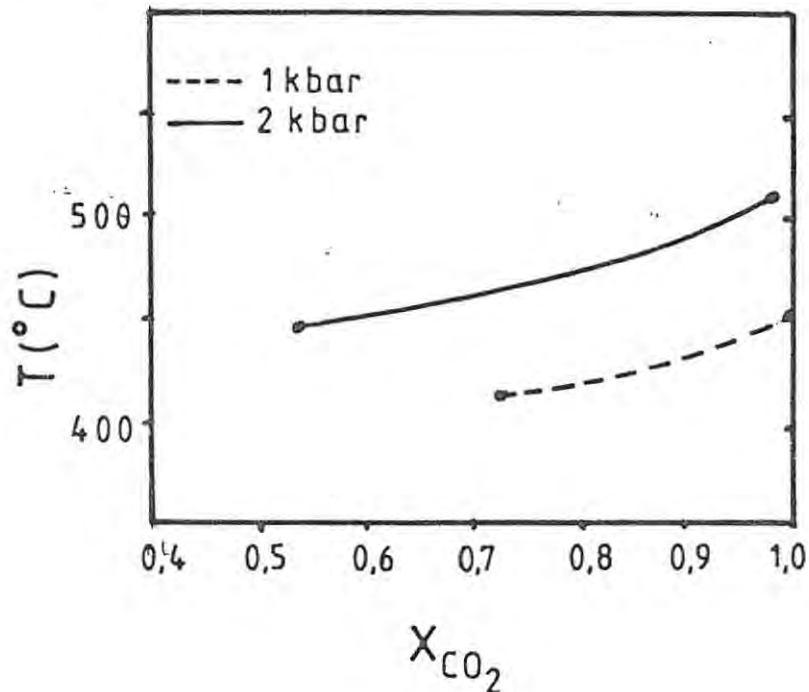


Fig. 36: T-X diagram showing the reaction curve for tremolite at 1 and 2 kbars (Adapted from Slaughter *et al.*, 1975)

From the petrographic study of the metamorphic assemblages the rocks in the Gamigab area underwent low-grades of regional metamorphism. Temperatures were probably ranged between  $420^\circ C$  and  $500^\circ C$  and pressures were less than 2 kbar. This deduction agrees with that of Hodgson (1972) who determined the same conditions of  $500^\circ C$  and 2 kbar in the GD on the basis that tremolite and cordierite (in the marbles and schists respectively) are products of regional metamorphism.

## 6.2. Contact Metamorphism

The effects of contact metamorphism are seen both east of, and west of Gamigab. In the eastern parts, contact effects (probably related to the Omangambo pluton) are seen in the form

of oval shaped pseudomorphs of cordierite. The nodules are 2-3 cm in length and lie in the foliation and are generally randomly orientated. In thin section the porphyroblasts consist of biotite, chlorite and muscovite as retrograde products from the breakdown of cordierite. The retrograde minerals are finer grained than the phyllosilicates which make up the rest of the rock. However, dispersed throughout the rest of the rock and also within the cordierite pseudomorphs are decussate biotite laths which replace the finer grained fabric.

Some 2 km west of Gamigab there is biotite spotting in the Kuiseb schists. In thin section the spots are seen to consist of a coarse-grained, unstrained core of quartz wrapped around by biotite laths which are also unstrained (Fig. 37). These quartz-biotite spots overprint the finer grained  $S_1$  phyllosilicates and in places the coarse biotite laths appear to lie parallel to the  $S_4$  direction.

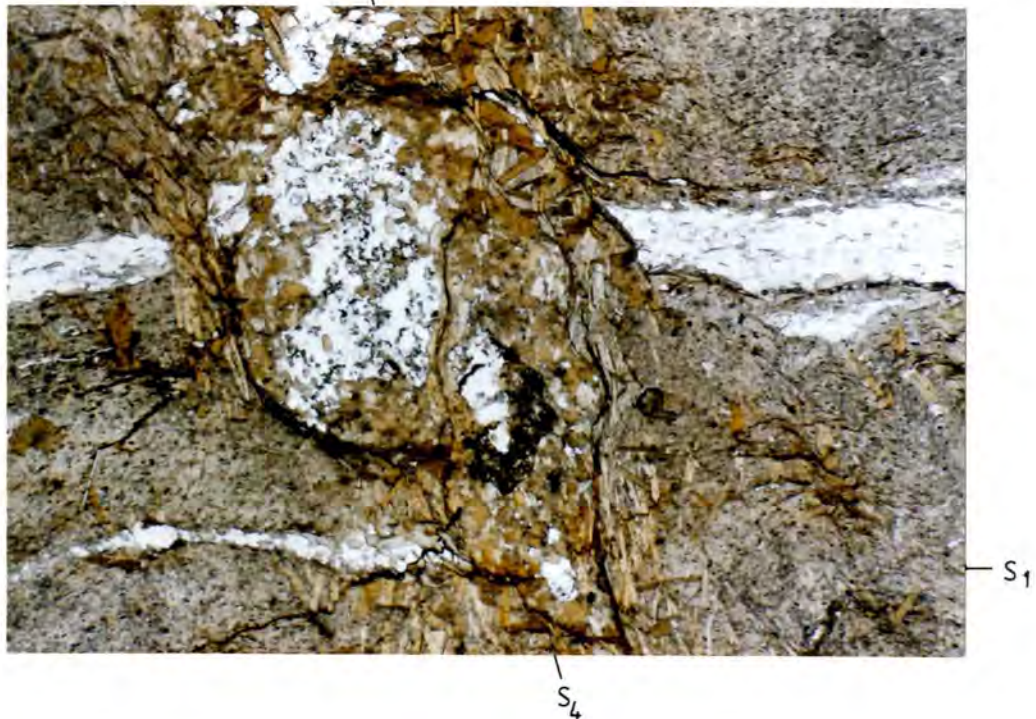


Fig. 37: Photomicrograph (uncrossed polars) of biotite spot developed in response to thermal metamorphism. Field of view is 4 mm.

Similar contact metamorphic-type effects have been noted and documented (Miller, 1973b; Porada *et al.*, 1983). In his work east of the Omangambo Pluton, Miller (1973b) reports the occurrence of poikiloblastic cordierite in the pelitic rocks adjacent to the Salem granite. He suggests that the reaction between biotite, muscovite and quartz produced the cordierite and potash feldspar. Cordierite has also been found by Porada *et al.* (1983) in the vicinity of the "Doros Granite" and along the southern boundary of the LUD.

### 6.3. Relationship Between Metamorphism and Structure

The strong parallel alignment of the micas in the schist indicates that mineral growth occurred syn-tectonically during the early stages of deformation. During F2 this S<sub>1</sub> surface was refolded and in places locally transposed into an S<sub>2</sub> fabric. The crenulation cleavage generated during the last period of deformation (F4) is sporadically developed along the limbs of the F2 folds.

The marbles have been completely recrystallised into an unstrained calcite ± quartz ± dolomite assemblage and the tremolite porphyroblasts are decussate and show no indication of having been affected by further deformation. This suggests that the tremolite formed post-tectonically.

The actinolite clusters in the calc-silicate lenses are however bent and display strained extinction. The grossularite porphyroblasts replace the actinolite-plagioclase-quartz-zoisite assemblage and do not show evidence of rotation or contain rotated or deformed inclusions. Hence, the conditions of metamorphism prevailed after deformation and allowed the formation of the grossularite.

The cordierite pseudomorphs south-east of Gamigab show an alignment in the S<sub>1</sub> foliation but are also decussate, implying that thermal metamorphism in this area started during the late stages of deformation and continued after the cessation of

deformation.

The sub-parallel alignment of part of the quartz-biotite spots in the  $S_4$  direction indicates that thermal metamorphism started in the south-western parts during the final stages of D4. This thermal metamorphism continued on after D4 and produced the overprinting coarse biotite laths also associated with these spots.

In summary, regional metamorphism in the Gamigab area started during deformation and continued for some period afterwards. Thermal metamorphism affected the rocks south-east and south-west of the mineralisation, and also started toward the end of the deformation, continuing after deformation ceased.

When comparing the metamorphic history between the Goantagab Domain and the Lower Ugab Domain, it appears that regional metamorphic grades in the GD were somewhat higher than in the LUD. Hälbig and Freyer (1985) indicate two periods of regional metamorphism in the LUD, whereas this initial work in the GD indicates possibly one period of regional metamorphism. The effects of contact metamorphism are also evident in the LUD in the metapelitic rocks adjacent to intrusive granites.

## 7. THE EFFECTS OF HYDROTHERMAL ACTIVITY

The movement of hydrothermal fluids through the lithologies has had varying effects in the different rock types. Mineralisation and quartz veining with associated wall rock alteration, is seen at several localities within the schistose Orusewa Formation. Wall rock alteration is also closely associated with numerous breccias which, in contrast, are only found within the Karibib marbles.

The alteration associated with the quartz veins is zoned. On either side of the vein is a zone of pervasively tourmalinised wall rock which is termed the *vein margin*. The vein margin is flanked by pervasively sericitised country rocks which are termed *wall rocks* to distinguish them from the vein margin.

In the text that follows, the quartz veins, vein margins, wall rocks and the accompanying geochemical variations from the vein into the wall rocks will be described. This is followed by a section dealing with the breccias.

### 7.1. Alteration-Mineralisation in the Orusewa Formation

#### 7.1.1. Quartz veins

Much of the alteration-mineralisation in the region is located in a southerly plunging, antiformal structure, where a single set of quartz veins was emplaced into the underlying schists of the Orusewa Formation. Unfortunately much quartz scree and rubble discarded by Damara miners obscures the majority of the surface outcrop, although, according to maps compiled by the South West Africa Company (SWACO, 1953), approximately 20 large quartz veins crop out on surface (Fig. 38). Additional quartz veins occur to the east, west and south of the main mineralised centre. As part of the evaluation of the prospect SWACO dug three exploration trenches, two of which were mapped for this project (trenches 2 and 3) (Fig 39). The third smaller trench (trench 1) is unfortunately obscured by overburden and rubble.

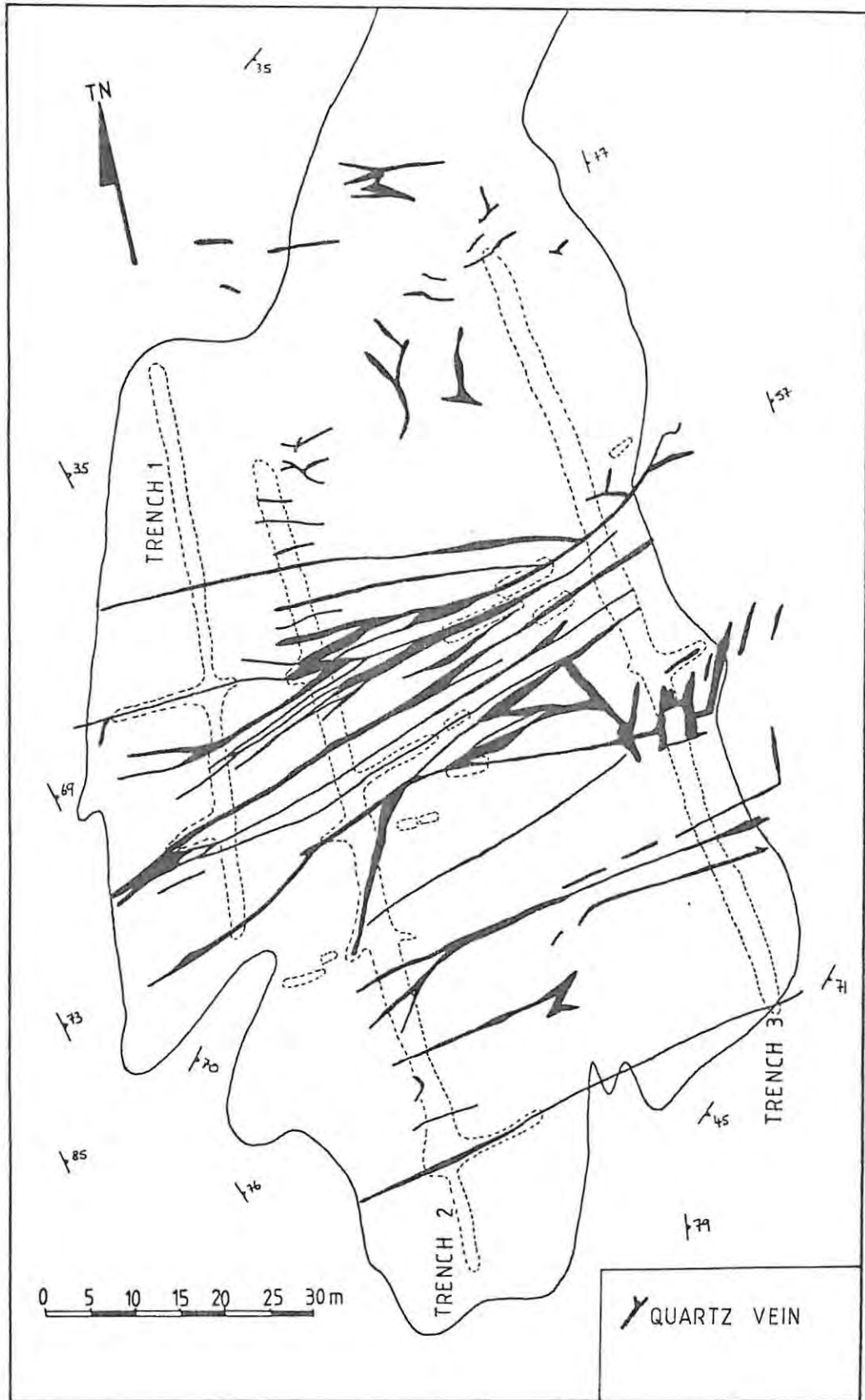
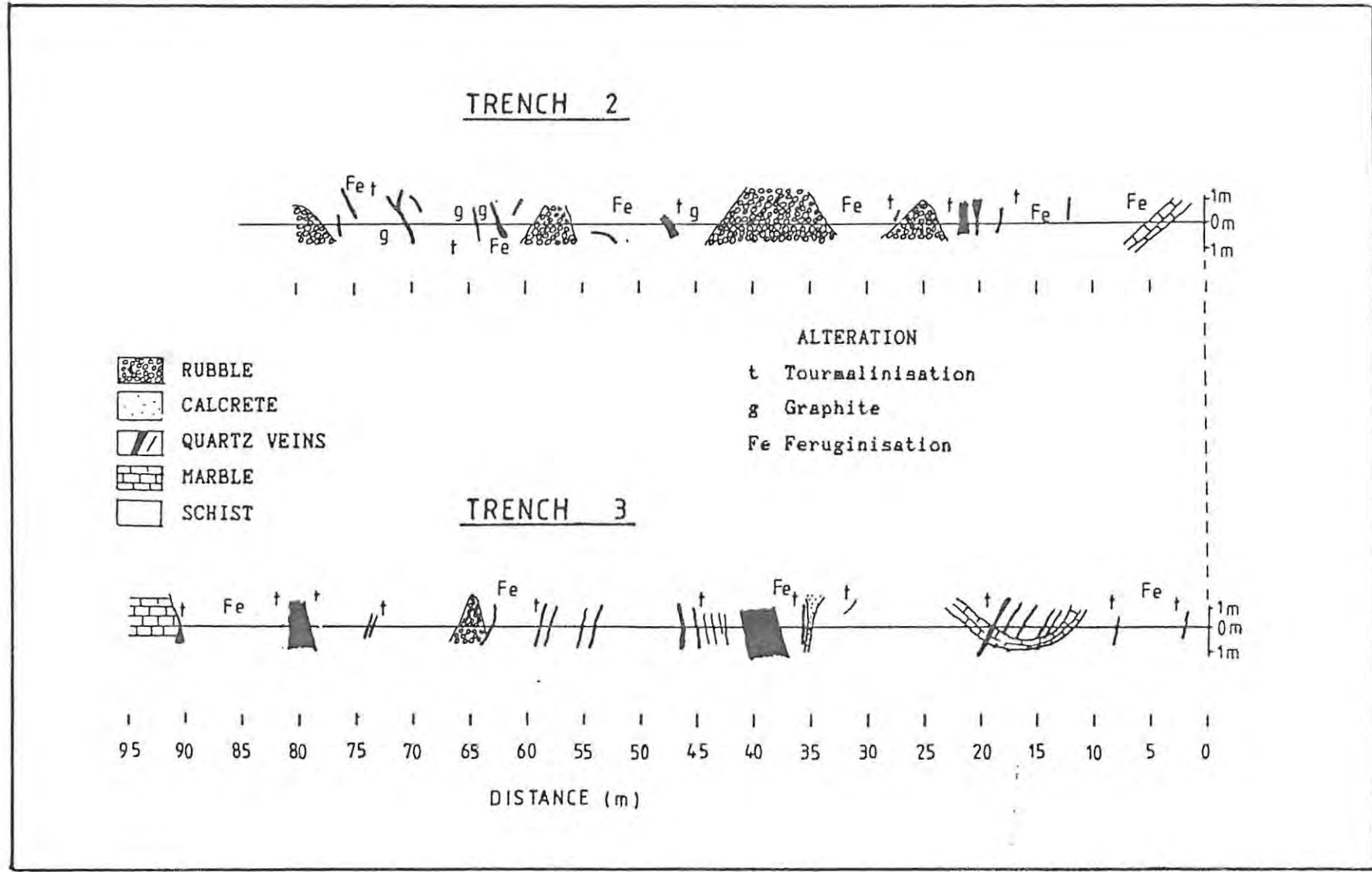


Fig. 38: Geological map of the area around the mineralised quartz veins. Diagram compiled from information from SWACO (1953) and this study.

Fig. 39: Geological cross sections through trenches 2 and 3 showing the geology and alteration.



In general the veins trend almost east-west and are sub-vertical, dipping steeply either to the north or south. Vein thickness is variable, ranging between 10 cm and 3 m, and in most instances the veins have been fractured and these fractures infilled with calcite, and/or siderite and hematite (Fig. 40). In outcrop, the quartz is generally a milky white colour, and has a distinctive "wet-look" appearance. "Wet-look quartz" is a term that was apparently introduced by early prospectors to describe ore-bearing quartz (Pirajno, pers. comm., 1986). The veins are almost totally hosted within the schist, with one intruding for a small distance into the overlying marble.

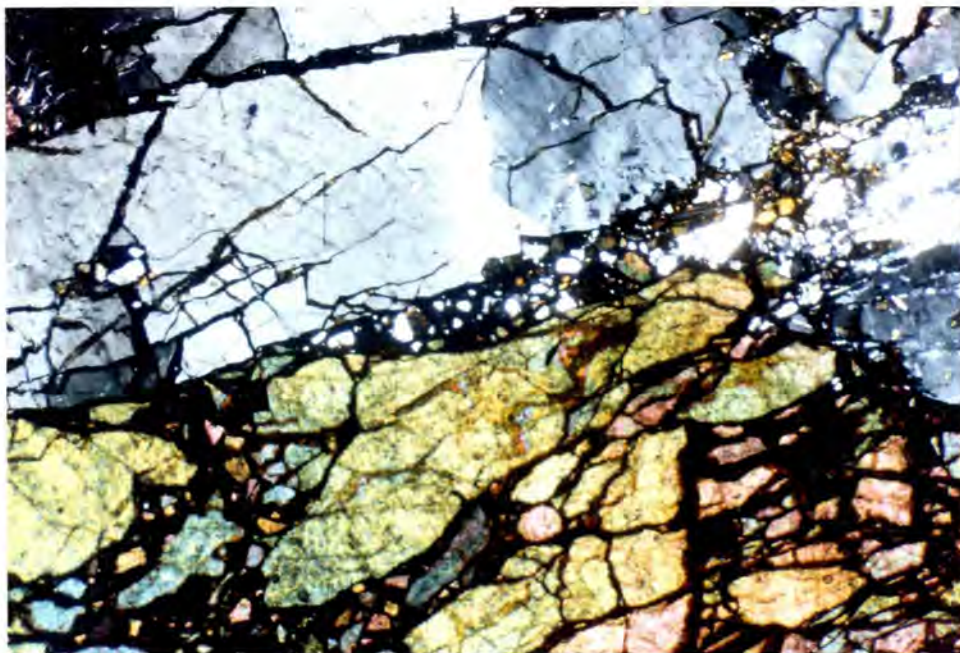


Fig. 40: Photomicrograph (crossed polars) of quartz vein with cassiterite. *Field of view is 4 mm.*

Cassiterite ( $\text{SnO}_2$ ) is the main ore mineral present, with accessory pyrite and chalcopyrite. The cassiterite is found wholly within the veins as fractured and brecciated grains (Fig. 40) ranging in size from a few millimetres to several centimetres in diameter. It displays good euhedral form and distinctive growth zoning (Fig. 41).

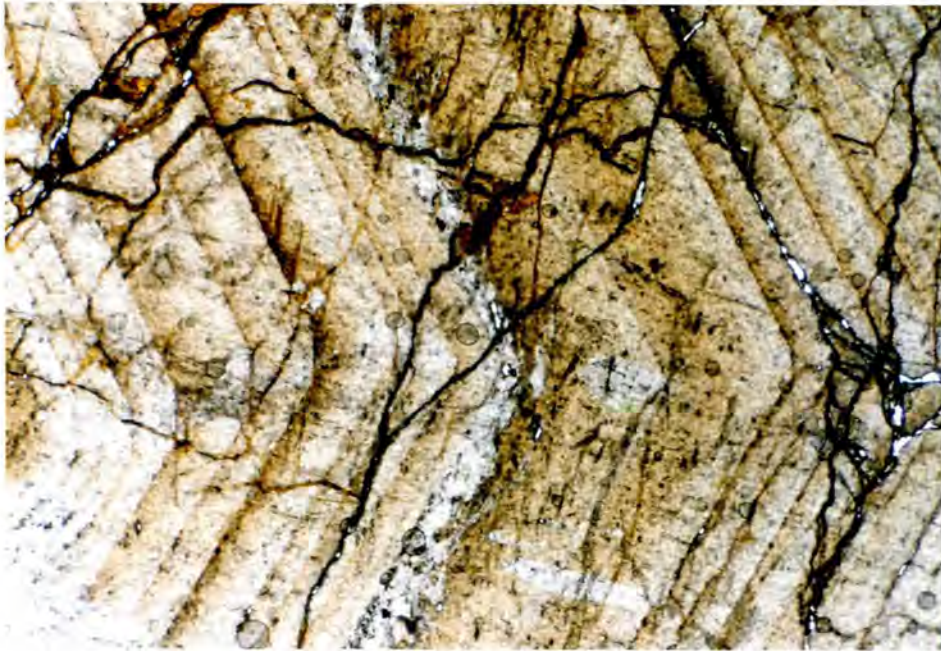


Fig. 41: Photomicrograph (uncrossed polars) of zoned cassiterite ( $\text{SnO}_2$ ). *Field of view is 0,25 mm .*

#### 7.1.2. Vein margins

A common feature adjacent to all the veins is a zone of intensely silicified and tourmalinised wall rock. The width of this zone is variable from less than 10 cm up to 50 cm and does not appear to be controlled by the thickness of the vein. In outcrop, the quartz-tourmaline rocks are dark and fine grained and do not exhibit any metamorphic fabric. Graphite is found in the vein margins both as an alteration product and along joint planes.

Thin sections of the vein margins show that the quartz is present as a recrystallised, fine-grained and unstrained mosaic. Grain size is variable from very fine-grained up to 0,3 mm in diameter. The tourmaline is present as fine-grained laths (0,2 mm - 1 mm) overprinting the quartz mosaic (Fig. 42). The tourmaline grains are pleochroic from a yellow-brown to almost colourless and in some of the larger grains a zoning is evident with darker yellow-brown cores. Although in hand specimen a metamorphic texture is not apparent, thin sections

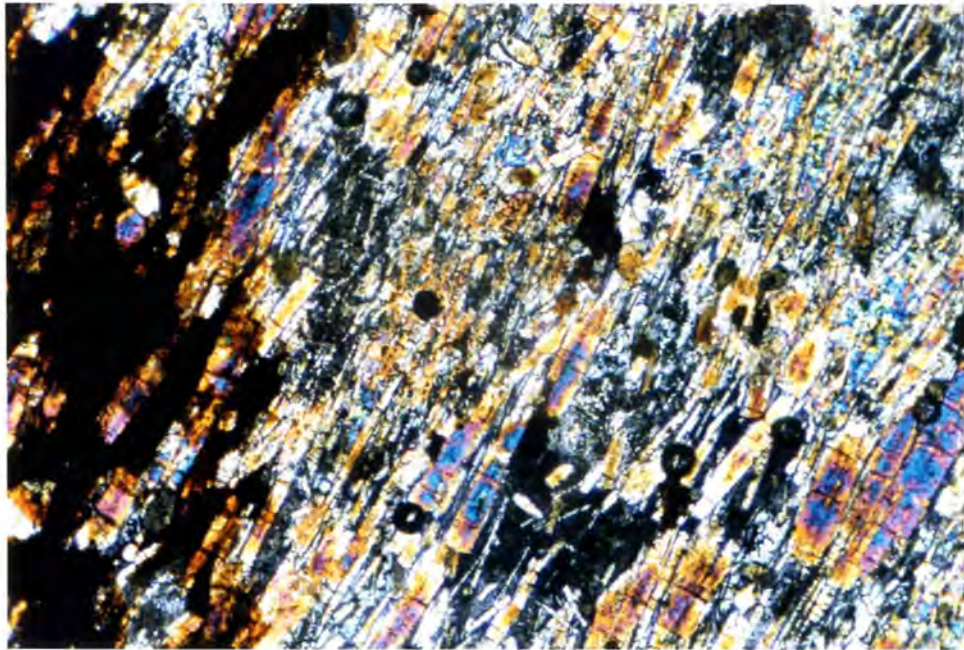


Fig. 42: Photomicrograph (crossed polars) of tourmalinised vein margin. *Field of view is 0,25 mm.*

show the tourmaline to have a parallel alignment in a preferred direction, probably parallel to  $S_1$ , with only a few grains cross-cutting the alignment at a shallow angle. Quartz veinlets cross-cut the rocks in places and adjacent to these veinlets the tourmalines are bent and sometimes fractured.

In some thin sections sphene is present in amounts less than 1% and in places contains inclusions of tourmaline and quartz. Calcite is also present in small amounts surrounding and cross-cutting the tourmaline laths. Where developed, the graphite occurs as opaque flakes which are essentially confined along the tourmaline grain boundaries with a few flecks developed within the tourmaline itself. Red hematitic patches are sometimes developed with the hematite commonly enclosing some tourmaline laths. Elsewhere the hematite occurs together with calcite and is especially developed in calcite veinlets cross-cutting the rocks.

### 7.1.3. Wall rocks

The schist within the mineralised area, and in places to the west of the mineralised area, has been pervasively altered to a fine-grained assemblage of predominantly sericite. A red spotting, probably after sulphide, in the fine-grained grey schistose wall rocks is evident almost everywhere. These spots have an average diameter of about 1 mm. Cutting across the rocks are numerous hematite-filled veinlets. The marble interbeds are also quite extensively ferruginised and coarse-grained tourmaline pockets are locally developed. Unfortunately the schist is weathered and can be quite friable to handle.

Thin-section study of samples of the wall rocks show the rock to be a very fine-grained quartz-sericite schist. The fine-grained quartz which is generally less than 0,05 mm in diameter is anhedral in shape and appears to be almost completely recrystallised. The hydrothermal sericite occurs along the grain boundaries of the quartz and lies in preferred orientation mimicking the metamorphic fabric. Replacing the very fine-grained assemblages are unorientated muscovite porphyroblasts. Tiny decussate stubby laths of yellow-brown tourmaline with grain sizes usually less than 0,1 mm replace the quartz-sericite assemblages, and occur as inclusions within the coarser grained muscovite.

In thin section the red spots are seen to consist of patches of recrystallised quartz, whose grain size is slightly larger than the quartz in the quartz-sericite assemblage. Fine-grained hematite and calcite rim the grains and also define the outline of the spot. Hematitisation is also well developed along the edges of calcite veinlets. The alteration extends out from the veinlet into the sericitic schist but decreases in intensity away from the veinlet.

7.1.4. Geochemistry of the alteration

Samples for geochemical analysis of major and trace elements were collected across a selected vein extending from the wall rocks through the vein margins and into the vein. The results are presented in Table VII and are presented diagrammatically in Fig. 43. It must be noted that the changes in the element proportions are relative and not absolute.

TABLE VII: Major and trace element analyses of wall rock at 2m (WR2m), wall rock at 1m (WR1m), vein margin (VM), fractured quartz vein (QVf) and of unfractured vein (QVu). Major elements expressed in percent; trace elements expressed in parts per million.

Sample No.	GC 27F	GC 28F	GC 29F	GC 30F	GC 47F
Rock type	WR(2m)	WR(1m)	VM	QVf	QVu
SiO <sub>2</sub>	60,71	41,85	61,02	61,92	98,14
TiO <sub>2</sub>	0,81	0,52	0,82	0,00	0,00
Al <sub>2</sub> O <sub>3</sub>	16,78	9,79	17,43	1,25	0,44
Fe <sub>2</sub> O <sub>3</sub>	6,20	5,48	5,49	5,17	0,62
MnO	0,07	0,11	0,09	1,25	0,00
MgO	0,14	0,55	4,82	0,46	0,33
CaO	4,12	21,10	4,91	19,34	0,49
Na <sub>2</sub> O	0,12	0,07	0,24	0,04	0,02
K <sub>2</sub> O	1,09	0,47	0,20	0,27	0,00
P <sub>2</sub> O <sub>5</sub>	0,15	0,18	0,09	0,00	0,00
H <sub>2</sub> O <sup>+</sup>	6,90	4,85	3,16	2,12	0,33
CO <sub>2</sub>	2,27	15,13	2,13	8,36	0,08
<b>TOTAL</b>	<b>99,36</b>	<b>100,10</b>	<b>100,40</b>	<b>100,16</b>	<b>100,45</b>
Sr	139	136	393	380	11
Rb	37	19	12	nd	nd
Nb	17	8	16	nd	nd
Y	27	43	38	10	nd
Zr	157	98	136	nd	nd
Sn	11	26	119	13	8
W	6	7	5	7	5

The variation diagrams show that  $\text{SiO}_2$  decreases in the wall rocks adjacent to the vein margin but increases in the vein margin and in the quartz vein, being higher in the unfractured portion compared to the fractured part.  $\text{Al}_2\text{O}_3$  is lower in the wall rocks 1 m from the vein when compared to the wall rocks 2 m from the vein and decreases sharply in both the fractured and unfractured parts of the quartz vein. There is a saw-tooth variation in  $\text{CaO}$  with peaks in the wall rocks adjacent to the vein margin and again in the fractured part of the vein.

The amount of  $\text{MgO}$  is generally low through-out although in the vein margins it increases to about 5%.  $\text{K}_2\text{O}$  decreases steadily from the wall rocks into the vein margin and into the vein itself.  $\text{Na}_2\text{O}$  is also present in low amounts but peaks in the vein margin relative to the wall rocks and vein.  $\text{TiO}_2$  varies slightly through the wall rocks into the vein margin and is absent in both the fractured and unfractured parts of the vein.  $\text{Fe}_{\text{TOTAL}}$  remains relatively constant, decreasing gently through the wall rocks, vein margin and fractured quartz vein but drops rapidly in the unfractured part of the vein.  $\text{MnO}$  is low but constant in the wall rocks and vein margin but is present in slightly higher amounts in the fractured part of the vein.  $\text{P}_2\text{O}_5$  remains constant in the wall rocks decreasing in the vein margin and is absent in the quartz vein.

Considering the trace element variations, it can be seen from Fig. 43 that  $\text{Sr}$  increases in the vein margin relative to the wall rocks and remains quite high in the fractured vein, decreasing sharply in the unfractured part of the vein.  $\text{Rb}$  decreases steadily through the wall rocks and vein margins, and into the vein where it is absent.  $\text{Nb}$  shows slight variance when moving in toward the vein, and is also absent in the quartz vein.  $\text{Y}$  decreases toward the vein from the wall rocks adjacent to the vein margin and is absent in the unfractured part of the vein. The pattern of variation of  $\text{Zr}$  is similar to that of  $\text{Nb}$  with the exception that  $\text{Zr}$  is present in much greater amounts.  $\text{Sn}$  is low in the wall rocks and in the vein but peaks in the vein margin.  $\text{W}$  varies slightly in the traverse and is present in very small amounts.

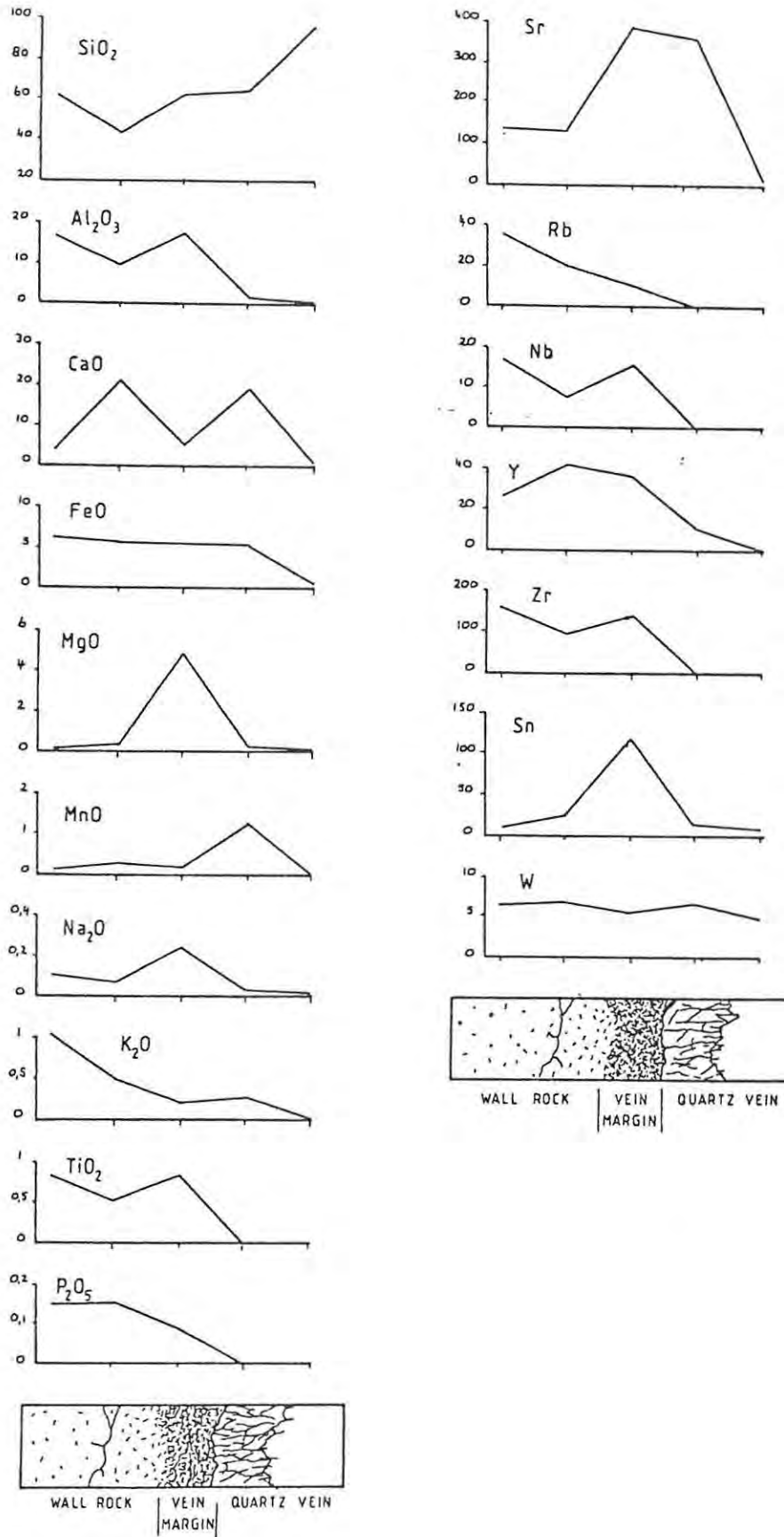
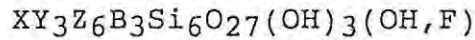


Fig. 43: Geochemical variations from the wall rocks into the vein margins and quartz veins.

### 7.1.5. Tourmaline composition

The general formula for tourmaline may be given as:



where X = (Na, Ca), Y = (Mg, Fe, Mn, Li, Al) and Z = (Al, Mg, Fe<sup>3+</sup>, Cr) (Deer *et al.*, 1986). The more common compositional end members are the magnesium tourmalines (dravites) where the Y site is predominantly Mg, and the iron-rich tourmalines (schorl) where the Y site is predominantly Fe<sup>2+</sup>. Alkali tourmalines (elbaite) also exist where Li becomes dominant in the Y site. A continuous solid solution series exists between dravite and schorl (Mg = Fe<sup>2+</sup>) and between schorl and elbaite (Fe<sup>2+</sup> = Li<sup>+</sup>) but there is an immiscibility gap between elbaite and dravite (Deer *et al.*, *op. cit.*).

Electron microprobe analyses were performed on tourmalines from the vein margins, the wall rocks and from the marbles. The analyses are presented in Tables VIII, IX and X. Below the partial analyses are the calculated structural formulae for the mineral which were based on approximated amounts for B<sub>2</sub>O<sub>3</sub> and H<sub>2</sub>O taken from tourmaline analyses in the literature (Deer *et al.*, 1986) (B<sub>2</sub>O<sub>3</sub> = 10,5%; H<sub>2</sub>O = 3,6%), since these could not be determined on the microprobe. The tourmalines at Gamigab are all Mg-rich (i.e. dravitic) although differences occur depending on their locality. On the basis of the substitution between Fe<sup>2+</sup> and Mg<sup>2+</sup> variation diagrams are plotted using the iron-number (Fe#):

$$Fe\# = \frac{FeO}{(FeO + MgO)}$$

Fig. 44 shows a plot of Fe# against MgO for the tourmalines in the vein margin, in the wall rocks approximately 1 m from the vein and also 2 m from the vein. The vein margin tourmalines have low Fe#'s whereas the tourmalines in the wall rocks become increasingly Fe-rich further away from the vein.

Tourmalines from altered vein margins in the marble plot in the same area as those in the schistose vein margins (Fig. 45).

TABLE VIII: Partial analyses of tourmalines from tourmalinised vein margins in altered schist.

GC	33A	33D	41A	41B	41C	41D	45C	45D	45E
SiO <sub>2</sub>	36,88	37,01	36,49	36,61	36,99	36,89	37,14	37,39	37,24
TiO <sub>2</sub>	0,54	1,00	0,55	0,88	0,53	0,92	0,62	0,59	0,91
Al <sub>2</sub> O <sub>3</sub>	29,99	29,82	30,16	30,13	29,65	30,10	31,03	30,68	30,71
FeO	3,35	3,47	3,36	3,02	3,54	3,20	3,21	3,24	3,48
MnO	0,06	0,05	0,09	0,07	0,12	0,08	0,08	0,04	0,06
MgO	10,06	10,07	9,50	9,53	9,72	9,55	9,41	9,19	9,45
CaO	1,87	1,90	1,55	1,46	1,63	1,44	1,37	1,51	1,69
Na <sub>2</sub> O	1,84	1,83	1,88	1,76	1,96	1,95	1,81	1,76	1,76
TOTAL	84,60	85,14	83,59	83,48	84,13	84,14	84,66	84,41	85,29
Fe#	0,25	0,26	0,26	0,24	0,27	0,25	0,25	0,26	0,27

TABLE IX: Partial analyses of tourmalines from the sericitised schist wall rocks. Distance measured from vein margin.

Dist. GC	2m 35B	2m 35C	1m 36B	1m 36C	1m 36D	1m 36E	1m 44A	1m 44C	1m 44D
SiO <sub>2</sub>	36,27	35,86	36,33	36,51	36,23	36,79	36,40	38,21	36,53
TiO <sub>2</sub>	0,45	0,90	0,72	0,53	1,15	0,35	0,83	0,73	0,80
Al <sub>2</sub> O <sub>3</sub>	31,64	29,97	29,88	30,99	29,06	30,45	30,46	29,31	30,17
FeO	6,28	5,78	3,85	4,09	4,13	3,60	3,79	3,55	3,58
MnO	0,06	0,01	0,05	0,06	0,04	0,05	0,03	0,03	0,05
MgO	7,20	7,69	9,34	8,70	9,44	9,19	9,22	8,99	9,52
CaO	0,72	1,26	1,69	0,95	1,76	1,20	1,52	1,49	1,67
Na <sub>2</sub> O	1,85	1,86	1,81	1,82	1,70	2,06	1,76	1,78	1,84
TOTAL	84,46	83,32	83,68	83,63	83,51	83,69	84,01	84,08	84,17
Fe#	0,47	0,43	0,29	0,32	0,30	0,28	0,29	0,28	0,27

TABLE X: Partial analyses of tourmalines from vein margins in altered marble.

	FW136/A	B	C	D	E	FW142/A	B	C	D	E
SiO <sub>2</sub>	37,00	37,09	37,22	37,02	36,83	37,20	36,79	37,50	37,26	36,89
TiO <sub>2</sub>	0,61	0,60	0,31	0,60	0,66	0,48	0,50	0,58	0,46	0,71
Al <sub>2</sub> O <sub>3</sub>	30,58	31,03	31,68	30,61	30,20	31,10	31,13	30,86	31,11	29,83
FeO	2,91	3,02	2,84	2,80	3,15	4,38	4,02	3,63	4,16	4,31
MnO	0,12	0,08	0,12	0,10	0,12	0,07	0,05	0,04	0,07	0,06
MgO	9,89	9,75	9,62	10,09	10,00	8,96	9,07	9,74	9,13	9,57
CaO	1,66	1,20	1,25	1,67	1,71	1,04	1,24	1,45	1,22	1,57
Na <sub>2</sub> O	1,84	1,96	1,85	1,80	1,82	2,27	2,08	2,01	2,17	1,98
TOTAL	84,61	84,73	84,88	84,69	84,48	85,49	84,88	85,82	85,60	84,91
Fe#	0,23	0,24	0,23	0,22	0,24	0,33	0,31	0,27	0,31	0,31

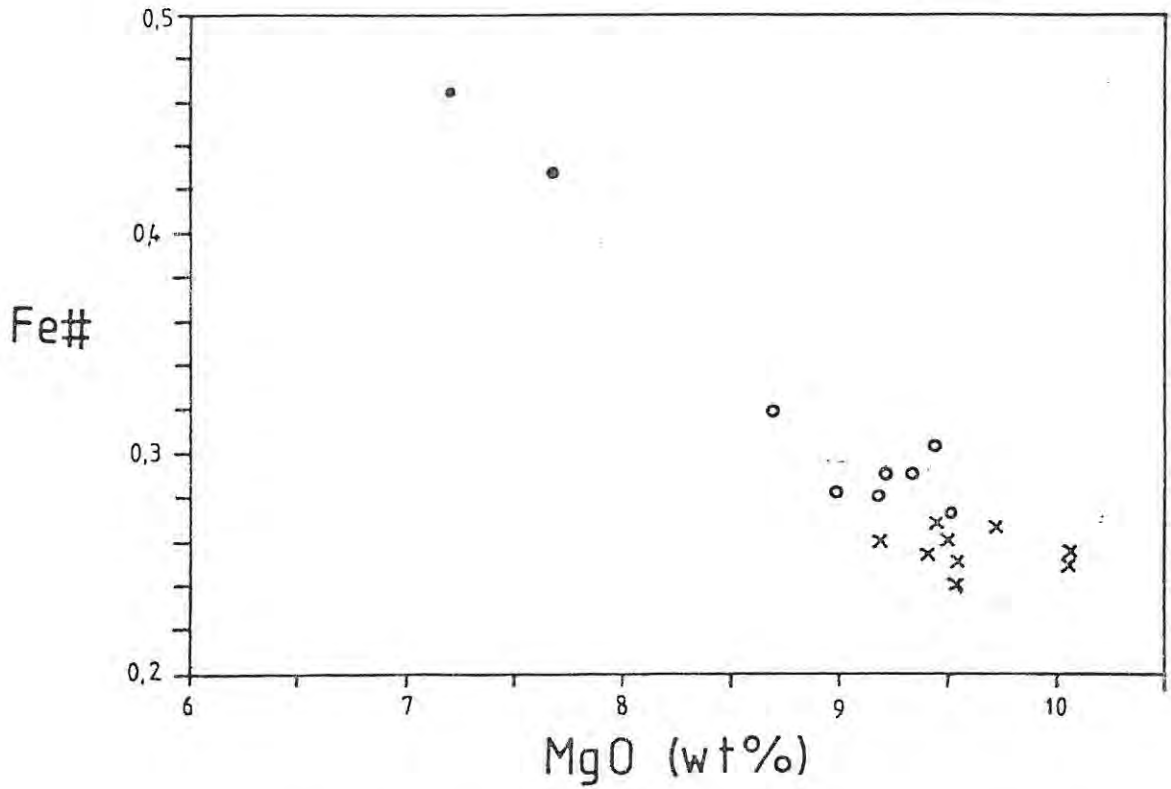


Fig. 44: Fe# vs MgO for tourmalines in the schistose vein margin (x), wall rocks 1m away (o) and 2m away (•) from the quartz vein.

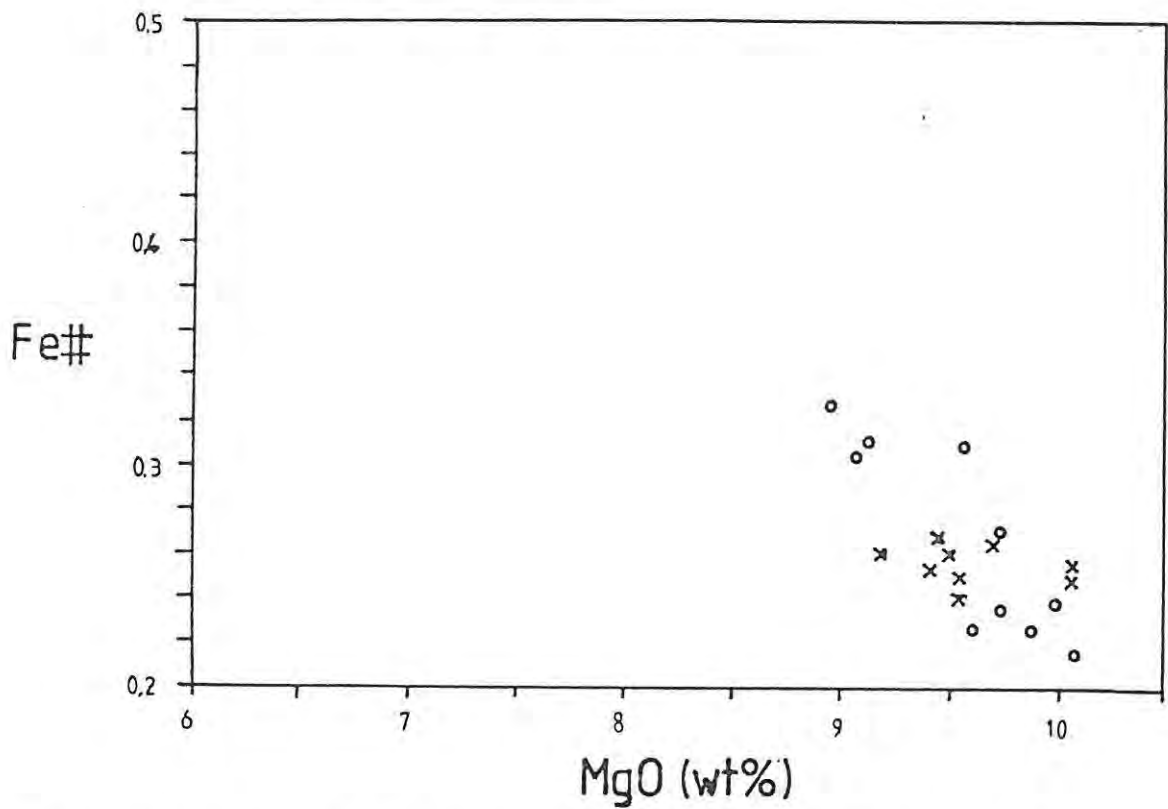


Fig. 45: Fe# vs MgO for tourmalines in schistose vein margin (x), and vein margin in marble (o).

## 7.2. Brecciation in the Karibib Formation

Some twenty breccias were identified and mapped in the Gamigab area. The surface expression of the breccias is variable from body to body. Generally they occur on a small scale with a surface area of 2 - 3 m<sup>2</sup> although much larger breccias are located 1 km south of, and 500 m south-east of the mineralisation. Another large breccia occurs in the vicinity of the igneous intrusions 500 m north-east of the mineralised area although it is not very well exposed.

The smaller breccias tend to be circular to oval in shape whereas the larger ones are more irregular and are longer and thinner parallel to the main F2 fold axis. In all cases the breccias are cross-cutting and are located within, or adjacent to, the apical parts of antiforms. They also occur close to the contact between the Karibib Formation and the underlying Orusewa Formation. An ubiquitous feature with the breccias is a halo of altered country rock. This alteration is essentially ferruginous and may be quite pervasive or fracture controlled.

### 7.2.1. Fragments

The fragments are commonly angular in shape and may be variable in size ranging from a few cm up to about 1 m (Fig. 46). Fragment composition is dependant on the country rock. Where the breccia occurs in blue-grey marble, the fragments are the same blue-grey marble and no other rock fragments were seen in any of the breccias. Minor fold structures are preserved in several of the fragments indicating that brecciation occurred after the deformation. It is also clear from field evidence that in some places the fragments did not move any great distance from their original position since they may be fitted back together like a jig-saw puzzle if the breccia matrix was removed.

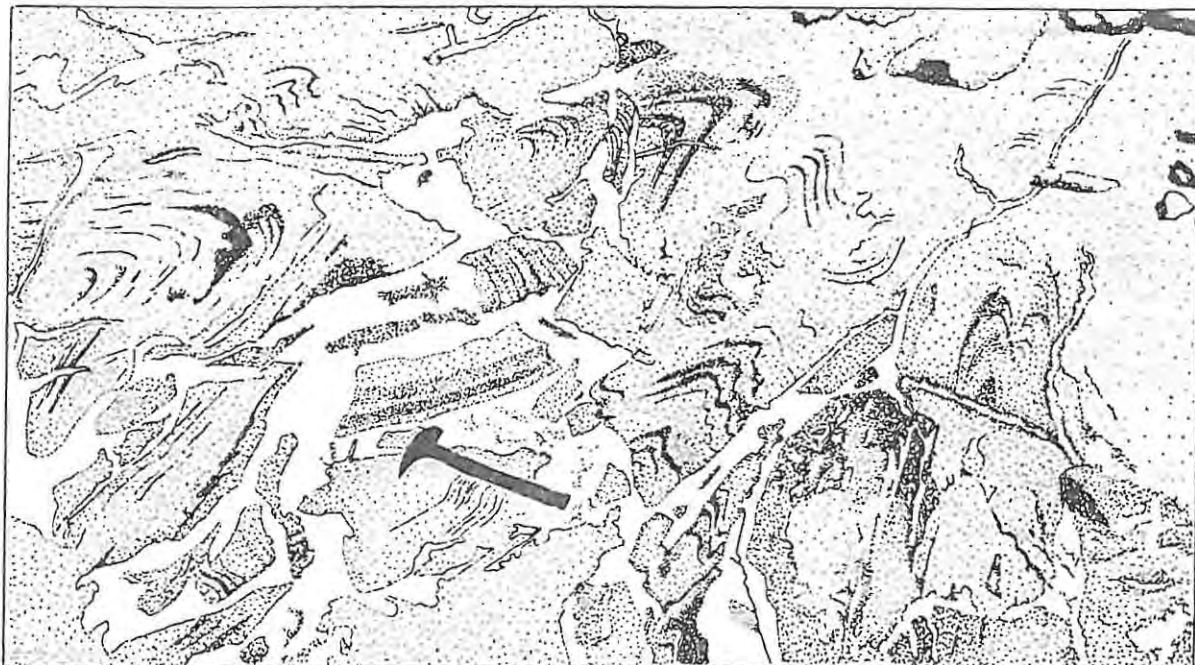


Fig. 46: Sketch (taken from photograph) of a breccia body at Gamigab, showing angular, partly rotated fragments, several with remnant fold structures.

#### 7.2.2. Matrix

The matrix cementing the fragments together generally consists of coarse-grained, white calcite which can be locally pervasively ferruginised. It is within these altered breccias that the fragments have well developed alteration rims (1-2 cm thick). Locally very small pink (hematitic) veinlets cross-cut the unaltered coarse calcite matrix.

The matrix can become quite siliceous in places as is seen in the southern parts of the large breccia body to the south of the mineralisation (Fig. 47). This dark resistant matrix is only developed on a local scale and the fragments which it cements tend to be slightly more rounded than usual. When viewed in thin section the siliceous nature is exemplified by the abundant quartz (0,25 mm) although calcite and accessory tourmaline are also present. Careful study under high power magnification reveals the presence of angular, stubby and very fine-grained (0,1 mm) grains of topaz. Although the inter-

ference colours are identical, the topaz may be distinguished from the quartz by its moderate relief and other optical properties. Hematite is found in conjunction with calcite, usually in the form of cross-cutting veinlets. Accessory amounts of muscovite occur interstitially to the quartz grains.



Fig. 47: Photograph of breccia with siliceous matrix.

Whole-rock and trace-element analyses of four samples of the matrix are presented in Table XI. Two of the samples (R759 and GC 109) are more siliceous as indicated by the high amounts of  $\text{SiO}_2$ , whereas the remaining samples (R758 and GC106F) are examples of the more calcite-rich matrix. All the samples contain several percent  $\text{Al}_2\text{O}_3$  due to the presence of topaz and/or tourmaline. Sn appears to be anomalously high in all the samples ranging from 10 - 47 ppm, whereas W ranges between 6 - 23 ppm.

TABLE XI: Major and trace element analyses of carbonate breccia and siliceous breccia matrix. Major elements are expressed in weight percent and trace elements in parts per million.

Sample No	CARBONATE		SILICEOUS	
	GC 106F	R758	R759	GC 109
SiO <sub>2</sub>	26,16	29,93	80,85	77,26
TiO <sub>2</sub>	0,30	0,11	0,12	0,29
Al <sub>2</sub> O <sub>3</sub>	6,03	2,76	2,84	7,10
Fe <sub>2</sub> O <sub>3</sub>	5,18	3,11	0,96	0,49
MnO	0,42	0,33	0,12	0,02
MgO	3,79	0,08	0,00	0,89
CaO	28,24	31,17	7,90	7,76
Na <sub>2</sub> O	1,76	2,48	0,00	0,01
K <sub>2</sub> O	0,08	0,00	0,01	0,09
P <sub>2</sub> O <sub>5</sub>	0,17	1,67	2,00	2,80
H <sub>2</sub> O <sup>+</sup>	8,07	8,85	3,45	2,71
CO <sub>2</sub>	19,72	17,88	1,77	0,58
<b>TOTAL</b>	<b>99,92</b>	<b>98,37</b>	<b>100,02</b>	<b>100,00</b>
Rb	169	180	9	5
Sr	463	366	725	884
Y	25	28	24	29
Zr	81	86	72	70
Nb	9	7	6	6
Sn	47	15	11	10
W	7	8	6	23

Total Fe expressed as Fe<sub>2</sub>O<sub>3</sub>.

### 7.2.3. Geochemistry of the porphyry plug

Although the intrusion occurs some distance from the mineralisation, it is thought that it may be related to the igneous activity responsible for the mineralisation. The field and thin section characteristics of the plug were described previously in section 4.4.1., whereas the geochemistry is presented in Table XII.

TABLE XII: Major and trace element analyses and calculated Norms of the porphyry plug. Major elements are expressed in weight percent; trace elements in parts per million.

Sample	GC12F	R748	R749
SiO <sub>2</sub>	63,54	64,02	62,88
TiO <sub>2</sub>	0,93	0,93	1,01
Al <sub>2</sub> O <sub>3</sub>	11,83	11,60	12,14
Fe <sub>2</sub> O <sub>3</sub> *	7,48	7,01	6,77
MnO	0,13	0,10	0,13
MgO	0,51	0,66	0,44
CaO	4,74	4,65	4,83
Na <sub>2</sub> O	1,33	1,08	1,19
K <sub>2</sub> O	3,98	4,32	4,29
P <sub>2</sub> O <sub>5</sub>	0,28	0,27	0,29
H <sub>2</sub> O <sup>+</sup>	3,11	4,47	4,11
CO <sub>2</sub>	2,86	2,16	2,09
TOTAL	100,71	101,27	100,17
Sr	216	218	200
Rb	99	105	86
Nb	22	42	34
Y	43	37	45
Zr	259	230	219
Sn	12	12	12
W	6	5	6

Calculated CIPW Norms

Q	27,80	28,91	27,46
or	24,82	26,95	27,01
ab	11,85	9,65	10,75
an	15,39	14,87	16,06
di	6,55	6,64	6,52
hy	11,06	10,47	9,47
il	1,86	1,86	2,03
ap	0,71	0,69	0,73

CIPW Norms recalculated from volatile free analyses. Total Fe expressed as Fe<sub>2</sub>O<sub>3</sub>\*

The plug is characterised by having SiO<sub>2</sub> contents between 65-67%, about 12% Al<sub>2</sub>O<sub>3</sub> and CaO > K<sub>2</sub>O > Na<sub>2</sub>O. MgO is typically low whereas Fe is quite high but this may be as a result of later ferruginisation. The high amounts of H<sub>2</sub>O and CO<sub>2</sub> are also an indication of alteration. The trace element determinations show that the rocks have high Sr and Zr (340 - 360 ppm and 250 - 270 ppm respectively) and lesser amounts of Nb (20 - 30 ppm),

Y (30 -45 ppm) and Rb (70 - 100 ppm). Sn can be considered to be anomalous considering the average content of felsic igneous rocks is between 2 - 3 ppm.

A way to distinguish igneous rocks is to plot their CIPW Norms on diagrams such as Ab-Or-An. For the purposes of comparison Table XIII lists major element analyses and CIPW norms of other rocks from the literature.

TABLE XIII: Average major element analyses and Norms for various igneous rocks.

	1	2	3	4	5	6	7
SiO <sub>2</sub>	65,01	71,30	61,25	68,98	69,28	68,27	67,33
TiO <sub>2</sub>	0,58	0,31	0,81	0,86	0,88	0,67	0,65
Al <sub>2</sub> O <sub>3</sub>	15,91	14,32	16,01	13,02	13,35	13,13	13,62
FeO*	4,73	2,85	5,35	5,39	5,42	7,38	6,39
MnO	0,09	0,05	0,09	0,09	0,09	0,16	0,14
MgO	1,78	0,71	2,22	1,22	1,17	0,34	0,41
CaO	4,32	1,84	4,34	2,47	3,49	1,74	2,03
Na <sub>2</sub> O	3,79	3,68	3,71	2,88	3,45	2,98	3,64
K <sub>2</sub> O	2,17	4,07	3,87	4,80	2,56	5,32	4,71
P <sub>2</sub> O <sub>5</sub>	0,15	0,12	0,33	0,29	0,30	0,19	0,17

Calculated CIPW Norms

Q	22,71	29,06	14,26	24,05	27,52	21,22	19,12
or	12,82	24,50	22,85	28,36	15,13	31,44	27,83
ab	32,07	31,13	31,38	34,37	29,19	25,22	30,80
an	19,99	8,04	15,64	8,42	13,38	6,74	6,91
di	0,07	-	2,05	1,66	1,69	0,58	1,80
hy	5,83	3,37	4,57	10,83	10,71	13,29	11,00
mt	3,52	1,75	3,91	-	-	-	-
il	1,10	0,58	1,54	1,63	1,67	1,27	1,23
ap	0,36	0,28	0,79	0,69	0,71	0,45	0,40

FeO\* = Total Fe

Analyses recalculated volatile free

Key to Samples

- 1 Average Dacite (Le Maitre, 1976)
- 2 Average Granite (Le Maitre, 1976)
- 3 Average Latite (Le Maitre, 1976)
- 4 Devitrified Etendeka Quartz Latite (Milner, 1987)
- 5 Pitchstone Etendeka Quartz Latite (Milner, 1987)
- 6 Main granite (Brandberg) (Pirajno, unpublished data)
- 7 Main granite (Brandberg) (Pirajno, unpublished data)

As can be seen in Fig. 48, the porphyry plug at Gamigab plots toward the Or-An line relative to the other igneous rocks. The field and thin-section characteristics show that the plug has been altered which could account for the plotted position. Igneous activity in the region is represented by the Brandberg alkaline complex and the Etendeka quartz latites. It is clear from Fig. 48 that the porphyry plug plots away from the latites and Brandberg granite. When comparing the major elements of the quartz latite, Brandberg granite and the porphyry plug the latter is lower in  $\text{SiO}_2$ ,  $\text{Al}_2\text{O}_3$  and  $\text{Na}_2\text{O}$  but has significantly higher  $\text{CaO}$ .  $\text{K}_2\text{O}$  is approximately the same among the rocks.

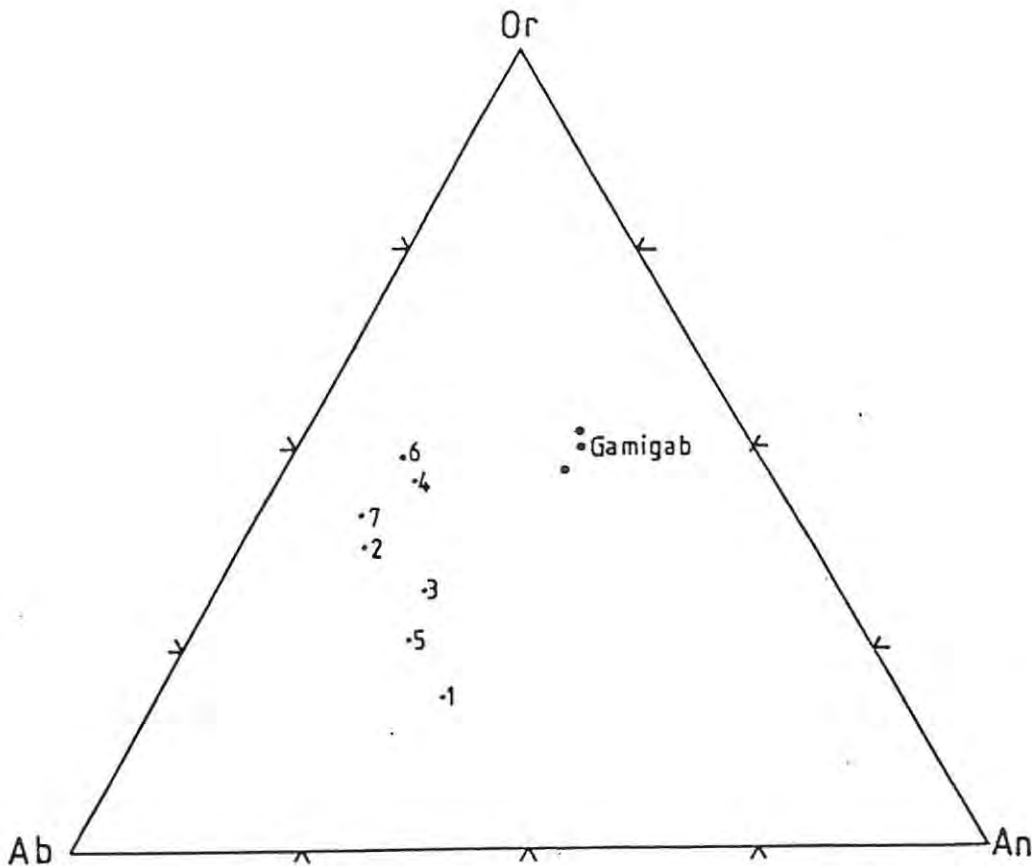


Fig. 48: Ab-Or-An normative diagram showing the distribution of the rocks represented in Table XIII and comparing them to the Gamigab Porphyry plug.

This discrepancy in the geochemistry may be explained by the fact that the porphyry plug intruded into carbonate rich rocks and has subsequently been altered. The assimilation of

carbonate-rich material (evidenced by marble xenoliths) could account for an increase in the amount of CaO. A late stage carbonatisation of the plug may also account for an increase in CaO by alteration of the albite feldspars (i.e. Na-rich) and replacement of Na by Ca. The differences in SiO<sub>2</sub> and Al<sub>2</sub>O<sub>3</sub> may also be as a result of the alteration. It is likely that a combination of assimilation and alteration is responsible for the difference in geochemistry.

## 8. MODEL FOR HYDROTHERMAL DEPOSITS

In order to understand the processes of the hydrothermal activity at Gamigab it is important to consider the models behind the formation of such hydrothermal deposits. In the sections that follow these ideas are presented first followed by a discussion on the hydrothermal activity at Gamigab and how the features there fit into the hydrothermal model.

### 8.1. Magma Characteristics

Many tin deposits occur adjacent to or within granitic bodies (Taylor, 1979; Plimer, 1983). These tin-bearing granites are supposedly specialised, with a specific compositional range (Tischendorf, 1977) and trace element abundance (Taylor *op. cit.*). Plimer (1983) suggests that 'A-type' granites are associated with hard rock tin deposits. These high temperature, low viscosity melts are commonly found in anorogenic terrains and crystallise to form alkali ring complexes, biotite adamellites and biotite granites.

Other granite 'types' have also been recognised. M-type granites occur in narrow belts and are associated with subduction zones. I-type granitoids are derived from pre-existing igneous material and S-type granites which are derived from a sedimentary source (Plimer, 1983). The M-type granites are not associated with economic ore deposits whereas the I-type may be related to porphyry Cu and Mo deposits as well as W-Mo-Cu skarns. S-type granitoids have similarities with the A-type granites and are associated with some economic Sn deposits. Geochemically the A-type granites are characteristically high in  $\text{SiO}_2$ ,  $\text{Na}_2\text{O}$ ,  $\text{K}_2\text{O}$ ,  $\text{Rb/Sr}$ ,  $\text{Li}$ ,  $\text{B}$ ,  $\text{Sn}$  and  $\text{Zn}$  and low  $\text{Fe}_2\text{O}_3$ ,  $\text{FeO}$ ,  $\text{MgO}$  and  $\text{CaO}$ , whereas S-type granites have high  $\text{SiO}_2$  and high  $\text{K}_2\text{O/Na}_2\text{O}$  ratios.

Plimer (1983) suggests that those granites spatially associated with Sn mineralisation are two mica granites (biotite and muscovite) with both or one of the micas generally of

metasomatic origin. A review on the formation of these magmas is given by Clemens *et al.* (1986), who suggest that these melts formed through a complex process of partial melting and fractionation coupled with volatile interaction. The recycling of ancient sedimentary crust for the origin of S-type granites is supported by the spatial association of younger granite-related deposits with much older (generally Proterozoic) metasediments (Plimer, 1983). This provides for the possibility that the ancient crust could serve as a source for several of the more unusual elements, including Sn.

Holland (1972, p281) provides support for the classical hypothesis that "*many ore metals are derived from magmas, that they are transported in hydrothermal solutions and that they are deposited at higher levels in the crust*". The formation of a hydrothermal solution requires that volatiles be present in the melt. The presence of hydrous minerals such as micas is a clear indication that magmas carry several percent H<sub>2</sub>O. Also present as volatiles in felsic magmas are H<sub>2</sub>S, CO<sub>2</sub>, HCl, HF and H<sub>2</sub>, although H<sub>2</sub>O is singly the most important (Burnham, 1979). Experimental work by Holloway and Lewis (1974) has shown that the amount of CO<sub>2</sub> in a melt is proportional to the amount of H<sub>2</sub>O. Of the other volatiles commonly present in granitic melts H<sub>2</sub>S, HCl and HF are able to behave similarly to H<sub>2</sub>O.

The presence of H<sub>2</sub>O in a melt has the effect of lowering the viscosity (Henderson, 1982), and if the magmas are able to intrude into near surface environments, retrograde boiling can occur if the initial concentration of volatiles is high (Best, 1982). If the system remains closed (i.e. no loss of elements) a hydrothermal solution may be produced which is able to form ore deposits and/or alter pre-existing rocks (Best *op. cit.*). The behaviour of elements in a crystallising melt is dependent on their fluid-melt partition coefficient (Strong, 1981). Elements such as F, Li, B, Sn, W, U and Mo remain in the residual melt during fractionation whereas Cl and CO<sub>2</sub> will be concentrated in the aqueous phase and separate from the melt before significant differentiation (Strong, *op. cit.*).

In his classical model (Fig. 49) Burnham (1979) suggests that crystallisation occurs in a closed system, and as crystallisation proceeds the aqueous phase collects at the top of the intrusion forming a H<sub>2</sub>O-saturated 'carapace'. The carapace serves as a barrier to the migration of volatiles either into, or out of, the magma. With continual crystallisation of the anhydrous minerals, H<sub>2</sub>O becomes more concentrated in the melt and a stage may be reached whereby the H<sub>2</sub>O solubility in the melt is exceeded and secondary or retrograde boiling occurs. The effect of this resurgent boiling is to increase the internal volume of the magma chamber and so with continued crystallisation the internal pressure also increases. The increase in internal pressure may reach a stage where the chilled margins of the chamber and the enclosing country rocks will fracture and hydrothermal fluids are able to move into the country rocks. Breccia pipes and dykes may also form in these regions.

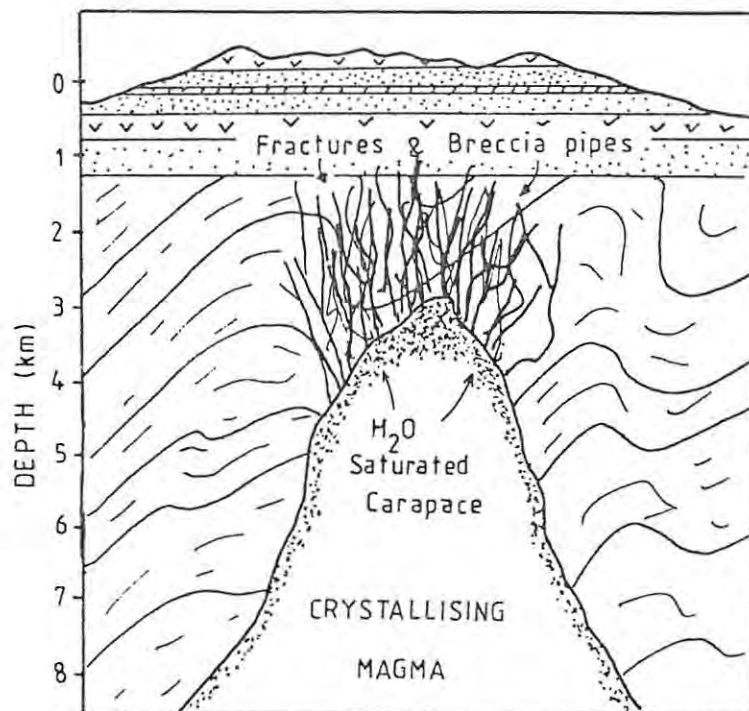


Fig. 49: Schematic model of crystallising hydrous magma (Adapted from Burnham, 1979).

## 8.2. Hydrothermal Alteration

The hydrothermal fluids may move considerable distances into the country rocks or may remain in close proximity to the granite source. In either case, the interaction of these hot aqueous fluids with the rocks results in hydrothermal alteration. Pirajno (1987a) defines hydrothermal alteration as a process of mineralogical, chemical and textural change induced in the rocks as a result of changing physio-chemical conditions in the presence of H<sub>2</sub>O and other volatiles. The physio-chemical conditions include fluid composition, fluid temperature, wall rock composition, pressure and the residence time of the fluid (Siems, 1984). Rose and Burt (1979) visualise the process of alteration as involving relatively large amounts of fluid which are able to move into the country rocks through fractures or connected pore spaces.

The extent of the alteration effect is dependent on the water to rock ratio (Henley and Ellis, 1983) and for extensive alteration to take place, the value for the ratio needs to be high. Alteration effects may be described as being pervasive or non-pervasive (the latter being sub-divided into selectively pervasive and vein or veinlet controlled) (Pirajno, 1987a). In aluminosilicate rocks, the major alteration types are albitisation, chloritisation, argillic alteration, greisenisation, tourmalinisation, silicification, hematitisation, fensitisation and carbonatisation (Siems, 1984).

A paragenetic sequence in alteration events may be recognised (Fig. 50), the first of these being alkali metasomatism (Pirajno, 1987a), in which there is replacement of Na by K or K by Na in magmatic feldspars. Alkali metasomatism is a common feature with the anorogenic alkaline ring complexes of Namibia (Potgieter, 1987).

If the alteration environment is allowed to mature, the next stage in the sequence may be reached; greisenisation. Greisen assemblages characteristically contain mica, quartz, topaz, tourmaline, fluorite, Sn, W and Mo (Burt, 1981; Štemprok,

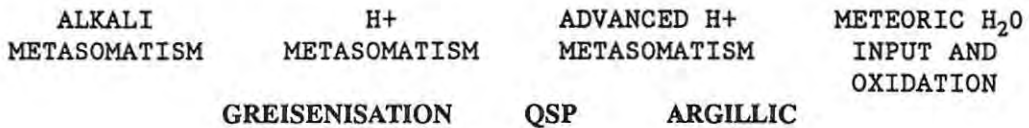


Fig. 50: Idealised paragenetic sequence during alteration  
(Adapted from Pirajno, 1987).

1987). Greisens generally occur at the contact zones of metalliferous plutons (endogreisens) or in their immediate envelope (exogreisens) (Štemprok, *op. cit.*). The deposition of silica and ore metals (oxides and sulphides) usually follows the metasomatic event in fractures within and outside the granite (Pirajno, 1987a). This generally starts with the precipitation of oxides (cassiterite, wolframite-scheelite) followed by sulphides (pyrite, pyrrhotite, chalcopyrite, arsenopyrite, molybdenite), lower temperature sulphosalts of Pb, Ag or Bi and finally a carbonate stage during which calcite, siderite, ankerite, fluorite, and pyrite precipitates out (Pirajno, *op. cit.*).

Advanced hydrogen ion (H<sup>+</sup>) metasomatism results in the further breakdown of rock forming minerals into a Quartz-Sericite-Pyrite (QSP) assemblage. The original composition of the country rocks can play an important role in the mineralogy of the greisen and QSP alteration zones (Scherba, 1970). In metapelitic rocks, tourmaline, white micas (muscovite and sericite) and albite assemblages may occur along prominent fractures and may be associated with metalliferous quartz veins. In mafic rocks, the greisenisation process leads to the formation of chlorite, talc and actinolite. In carbonate rocks, acidic greisenisation fluids are typically neutralised and the marbles and skarns are seen to contain phlogopite, topaz, fluorite and microcline.

Contact metamorphic effects, which normally precede the alteration (Pirajno, 1987a), may be seen in a narrow zone

enveloping the granite. In these zones biotite and cordierite may develop.

It is generally accepted that elements such as Sn are highly insoluble in aqueous fluids and so it is suggested that these elements may become soluble by forming complex ions (Taylor, 1979). The complex by which the Sn is transported in the hydrothermal fluid is a function of the geological environment (Taylor, 1979). Probably the two most important complexing agents are sulphur and chlorine (Pirajno, 1987a) although there several others (Taylor, *op. cit.*).

Once in the form of a complex, the Sn can be carried away from the source granite and precipitated in veins or replacement-type bodies. Various mechanisms can cause the precipitation of Sn (and other elements) from the hydrothermal fluid. They include temperature and pressure changes, boiling, reaction between the hydrothermal fluid and wall rocks or chemical changes due to the mixing of fluids (Pirajno, 1987a). It seems unlikely that any one to these processes alone will be responsible for the precipitation of elements from the hydrothermal fluid (Pirajno, *op. cit.*).

### 8.3. The Hydrothermal Environment at Gamigab

#### 8.3.1. Alteration-mineralisation

The alteration assemblages present at Gamigab (tourmaline, muscovite, sericite) indicate a QSP-type of alteration. Although not present in fresh form, the evidence for pyrite is seen in the ferruginous spots commonly found in the altered country rocks. Minerals such as topaz and fluorite which are typical to greisens are conspicuously absent from the wall rocks and vein margins.

Contact relationships between minerals indicate that the first stage in the alteration of the schists was sericitisation. During this process the unaltered quartz-biotite-feldspar

schists were altered to a fine-grained quartz-sericite rock dispersed with pyrite. The crystal lattice of biotite is known to be a source for metals and during its breakdown iron and sulphur could have been released so forming the pyrite grains. Replacing the fine-grained QSP minerals are coarser grained muscovite grains. Formation of the muscovite requires the introduction of potassium which could have been derived from the alteration of the alkali feldspars during the late stages of alteration.

The next stage in the alteration of the schistose rocks was tourmalinisation. Haloes of tourmaline-rich rocks are found along the margins of nearly all the veins suggesting that the hydrothermal fluids were able to move up into fractures probably initiated during D2. The high angle of the veins to the foliation indicates that these fractures may have been a-c joints (Hobbs *et al.*, 1976). The pervasive nature of the tourmalinised vein margins suggests massive replacement assisted by the foliation since the tourmalines in thin section still show a preferred orientation.

The first tourmalines to form were the Mg-rich dravites and during the initial stages the composition of the country rocks did not have a great influence in the composition of the tourmaline since those found in the marbles have the same composition as those in the vein margins. This implies that either the B-rich hydrothermal fluids were charged in Mg as well or that the Mg was liberated during the metasomatism of dolomite in the marbles. The tourmalines in the wall-rocks, adjacent to the vein margins, progressively become more Fe-rich the further away from the vein. B and Mg were able to diffuse into the country rocks but became progressively depleted and so Fe was scavenged from the country rocks and resulted in the formation of the schorl-type tourmalines. This is an indication of compositional control on the tourmaline composition.

The following pulse of hydrothermal fluid was saturated in SiO<sub>2</sub> and was responsible for the formation of the quartz veins. Detailed mapping of the veins in the exploration trenches shows

that only a single set of veins was emplaced. In places the veins have been fractured and these fractures infilled with calcite and/or siderite and hematite. Concurrent with the vein emplacement was ore deposition which commonly occurs at a late stage. Fluid inclusion studies (Table XIV) have shown that homogenisation temperatures during cassiterite deposition was about 245°C.

TABLE XIV: Results of fluid inclusion studies on a sample of cassiterite from Gamigab (Pirajno and Smithies, unpublished data).

	HOMOGENISATION TEMPERATURE (°C)	FREEZING TEMPERATURE (°C)	
		1st	2nd
GT 1	245 245	-13,8	-7

FLUID COMPOSITION: KCl+H<sub>2</sub>O  
SALINITY : 10 weight % NaCl equivalent

The homogenisation temperature may represent the true temperature of entrapment provided the pressure of the solution did not exceed the lithostatic pressure. If the pressure at the time of entrapment is higher, then a temperature correction needs to be applied (Potter, 1977). The age of mineralisation at Gamigab is not clearly known but may either be post-Damara or Karoo in age. If the mineralisation is of Damara age then the correction is unknown, but may be approximately 2 kbars since metamorphic pressures are in this range.

The top of the Brandberg Granite Complex is some 2000 m above the surrounding plains. On its top surface are volcanic rocks suggesting extrusion onto the Karoo surface, therefore, if the height of the Brandberg is used as a minimum thickness for the Karoo sediments and lavas, then a pressure correction of approximately 44°C needs to be added to the homogenisation temperatures making the temperature during mineralisation 289°C.

### 8.3.2. Brecciation

Breccias are not uncommon with hydrothermal activity (Gates, 1959; Norton and Cathles, 1973; Allman-Ward *et al.*, 1982; Burnham, 1985 and Sillitoe, 1985, to mention but a few). Sillitoe (*op. cit.*) provides an extensive overview on the different possible mechanisms for breccia formation. The major mechanism required is for a high temperature, high pressure hydrothermal fluid to interact explosively with the country rocks. This activity may take place at depth or even near surface as is seen with epithermal deposits.

At Gamigab, several important field characteristics are associated with the breccias. They occur in the apical parts of the main folds; they contain mono-mineralic fragments whose sizes and shapes are variable within and between breccias; in some instances the fragments are unrotated and can be fitted together if the matrix was removed; the fragments and country rocks associated with the breccias can also be altered. These features together suggest *in situ* fracturing of the country rock by a hydrothermal fluid.

The mechanism for the formation of the hydrothermal breccias is diagrammatically presented in Fig. 51. The fluids are generated at depth in a cooling granitic magma and collect in the apical parts of the chamber together with any incompatible elements. A point is reached when the fluids are released from the chamber and travel through the country rocks, via joints and fractures. The pathways for fluid movement may have been generated by the explosive release of the fluids or by the regional deformation, more than likely a combination of the two. Fluid movement, physically through the cracks or by slow chemical diffusion, follows a pressure, temperature or chemical gradient.

In this model the important gradient to consider is the temperature and more importantly the pressure gradient. The fluids will move into zones where the temperature and pressure is lower i.e. as close to the surface as possible. This being the case the fluids will rise through the country rocks and

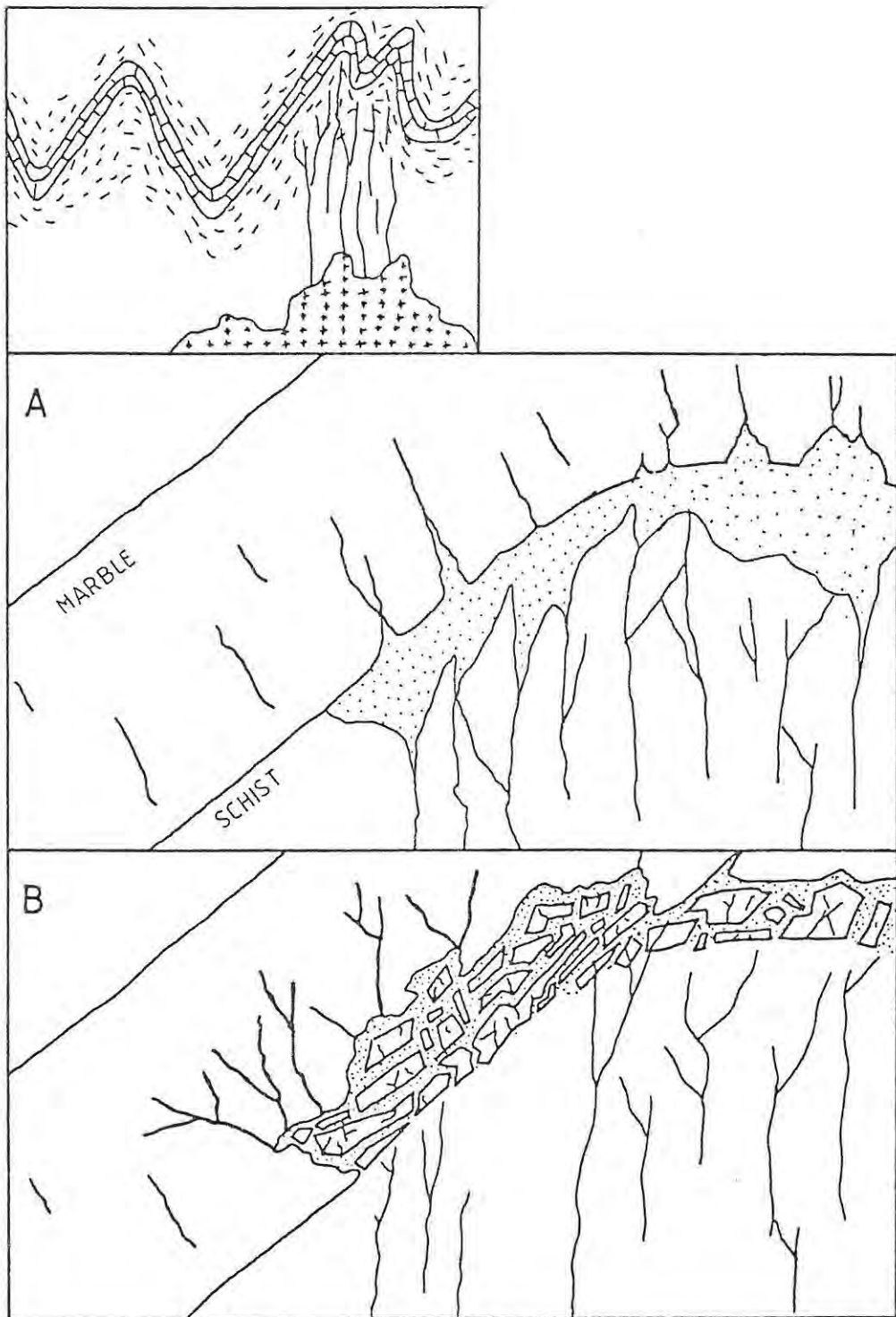


Fig. 51: Proposed model for breccia formation at Gamigab. A: Hydrothermal fluids dam up at the contact between the marble and schist. Replenishment from below assists in increasing fluid pressure until it exceeds the lithostatic pressure. B: Hydraulic fracturing of the marble to form the hydrothermal breccia.

collect in the antiforms. Whilst moving through the country rocks it is very likely that some sort of element exchange occurs between the schist and the fluid. For instance the Fe concentration of the fluids can build up from the release of Fe from the biotite which the fluid comes into contact with. Alternatively meteoric water charged with elements may mix with the hydrothermal fluids depending on the depth of emplacement.

Movement in the country rocks is also facilitated by the foliated nature of the schist and the fluids are able to move quite freely until the contact with the marble is reached. The permeability of the marble is very much less than the schist since it is not as strongly foliated and it is more competent. Upon reaching the contact the fluid's movement is drastically reduced and with the replenishment from below the fluids begin to dam up at the contact (Fig. 52).



Fig. 52: Photograph of quartz veins in schist damming up at the contact with the marble. (Rhinowash - lower Ugab region).

Initially these resevoirs would be quite small but as more fluid is fed into them they will grow and in some instances resevoirs can merge and become quite large (e.g. in the region south of the mineralisation). This resevoir can build up internal fluid pressure ( $P_f$ ). The lithostatic pressure ( $P_L$ ) exerted by the overlying country would be greater than  $P_f$  for the initial stages but as more fluid is fed into the resevoir the  $P_f$  would start to increase.

It can be expected that as  $P_f$  increases a point could be reached where  $P_f$  exceeds  $P_L$ . Depending on the strength of the rocks explosive fracturing could occur at the contact. The sudden decrease in pressure causes the fluids to cool fairly quickly thereby cementing the fragments together before any large amounts of rotation and movement of the fragments could occur. In most instances the breccia fragments, matrix and surrounding country rocks have been altered, specifically ferruginised. These Fe-rich fluids were introduced during and after brecciation because some of the breccias are not altered but their matrix is transected by numerous Fe veinlets.

The hydraulic breccias at Gamigab have a calcite matrix and are ferruginised in places suggesting that if the fluids responsible for the brecciation are related to the mineralisation then the brecciation event post-dated the mineralisation.

Based on the observations, a summary of the suggested paragenetic sequence of events during hydrothermal activity at Gamigab is presented in Table XV and diagrammatically in Fig. 53.

### 8.3.3. Age of mineralisation

The age of mineralisation is debatable and could be either of post-tectonic Damara or Karoo age. Igneous activity during post-tectonic times is indicated by the Salem-type granites which contain anomalously high Sn, and the Brandberg complex

TABLE XV: Paragenetic sequence of hydrothermal events at Gamigab.

STAGE	DESCRIPTION
1	Emplacement of volatile-rich granitic magma and subsequent crystallization
2	Release of fluids into the country rocks
3	Sericitisation of Orusewa Formation schist (QSP assemblage) with late-stage potassic metasomatism
4	Tourmalinisation adjacent to fractures in the Orusewa Formation
5	Crystallisation of quartz in the fractures
6	Brecciation in the apical parts of the F2 folds in the Karibib marble
7	Carbonatisation in both the Karibib and Orusewa Formations
8	Mineralisation in the quartz veins
9	Carbonatisation with ferruginisation in the mineralised area and breccias.

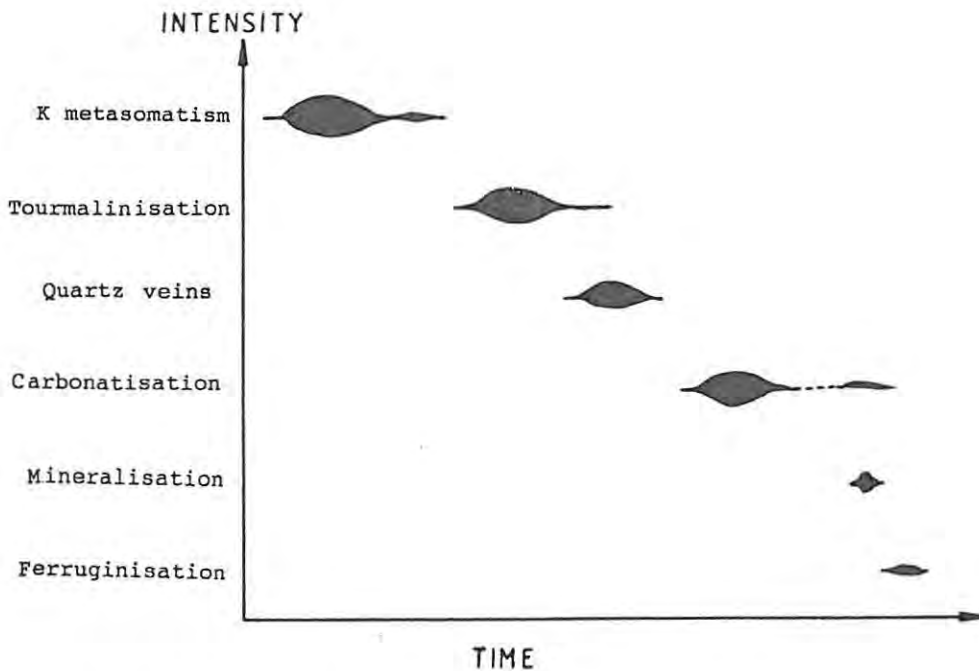


Fig. 53: Timing and intensity of the alteration-mineralisation at Gamigab.

is also known to contain high Sn (Pirajno, unpublished data). The field relationships at Gamigab indicate clearly that the alteration-mineralisation is post-tectonic and in some instances a Karoo-age is indicated by the alteration of the porphyry plug whereas the intrusion of a dolerite dyke across a hydraulic breccia suggests pre-Karoo hydrothermal activity. Preliminary Rb/Sr dating (F.J. Kruger, unpublished data) on samples of muscovite and calcite from the veins gives a three point isochron age of  $509 \pm 11$  Ma ( $R_0 = 0,71037 \pm 0,00021$ ).

## 9. METALLOGENESIS IN THE SOUTHERN KAOKO ZONE

The central and north-western parts of the Damara Orogen contain several "granite-related" Sn and Sn-W deposits. Three groups of deposits have been recognised by Pirajno and Jacob (1987a).

- (a) Northern Group. These include the vein- and replacement-type deposits at Brandberg West, Frans Prospect, Goantagab Mining Area, Gamigab and the syn-tectonic Ousis pegmatites,
- (b) Central Group which comprises the syn- to post-tectonic pegmatites at Strathmore, Uis, Neneis and Kohero,
- (c) Southern Group is in the Erongo-Karibib area and consists of W-dominated greisen deposits and Sn ± Ta ± W mineralisation in zoned pegmatites.

Fig. 2 shows the limits of the Northern and Central Groups. Apart from the Ousis pegmatites all the remaining deposits are characterised by features suggesting that alteration-mineralisation is post-tectonic to the metamorphic fabric (Pirajno and Jacob, 1987a). It is suggested by these workers that partial melting of the basement rocks during the Pan-African event produced syn- to late-tectonic granites which after differentiation produced residual pegmatitic liquids that were emplaced into the Damara sediments along zones of weakness. A second event during the break-up of Gondwanaland is thought to be responsible for the alteration-mineralisation in the vein- and replacement-hosted deposits of the Northern Group and the alteration of the Damara-aged pegmatites of the other two groups.

Of interest to this work are the vein- and replacement-type deposits in the Northern Group. The mineralisation is characterised by Sn and Sn-W hosted in quartz veins and replacement bodies which seem to occur adjacent to circular structures which are considered to be a product of degassing of igneous intrusions at depth (Pirajno and Jacob, 1987a;

Gableman, 1984). The characteristics of the various deposits in the northern SKZ has led Pirajno and Jacob (1987b) to propose a model which envisages the mineralised centres existing at different levels with respect to their source (Fig. 54). However, in order to understand the model the hydrothermal features of each deposit need to be considered.

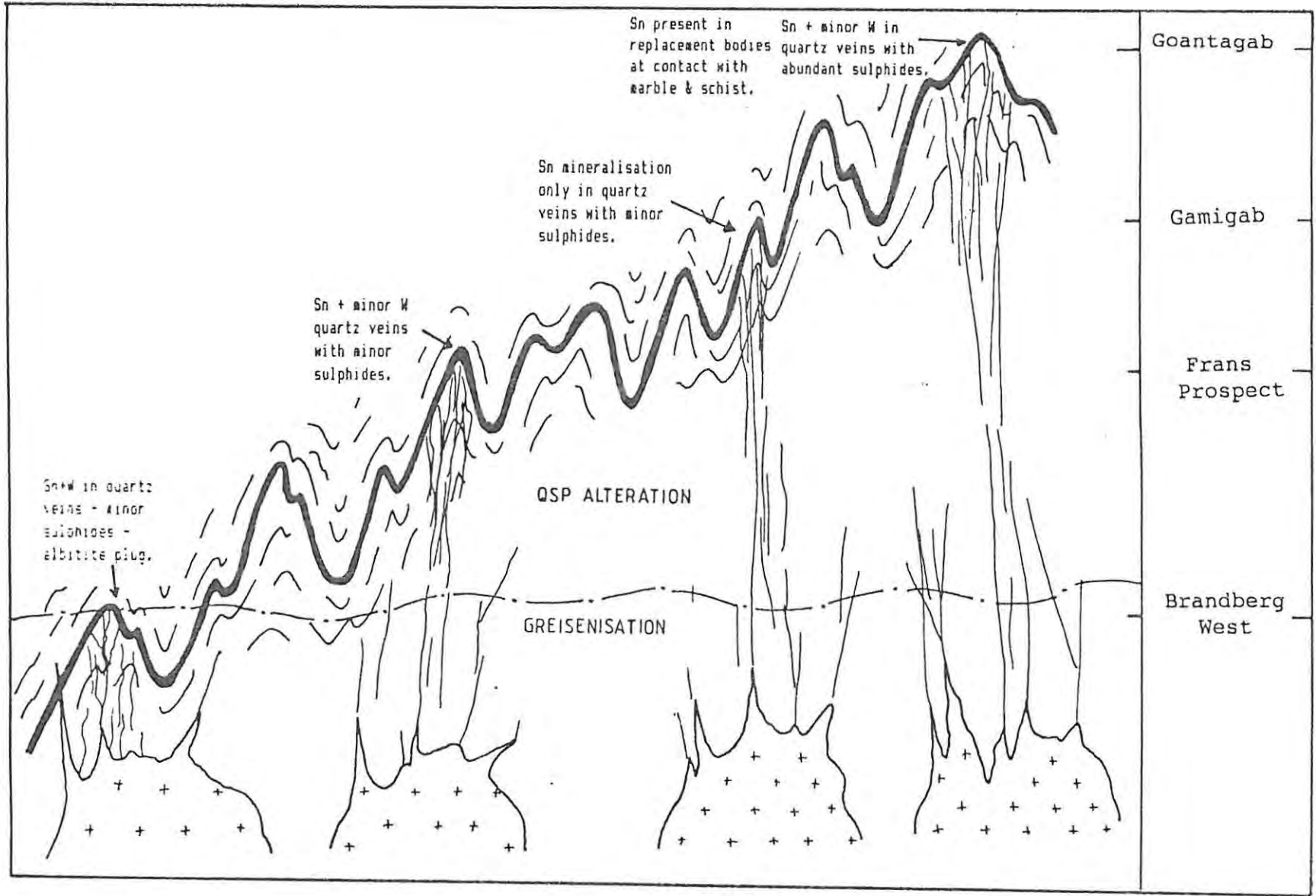
#### 9.1. The Brandberg West Sn-W Deposit

Mining started at Brandberg West in the early 1950's, initially as an underground operation but changed to an open cast operation from about 1957 onwards, until it finally closed down in 1980. The Sn and Sn-W mineralisation is hosted in an anastomosing system of quartz veins which have intruded, within a mega-anticlinorium, into quartz-biotite schist. The mineralised areas are located close to the intersection of two ring structures and a north north-west trending fracture zone (Pirajno *et al.*, 1987).

A quartz-albitite plug crops out some 2 km north-west of the open pit. It consists of a felted mass of albite and anhedral quartz with perthitic K-feldspar which has been largely replaced by albite. Mirolitic vugs containing K-feldspar along the margins and cores of calcite and quartz are abundant in the plug and indicate Na-metasomatism followed by CO<sub>2</sub>-rich volatile activity (Pirajno *et al.* 1987).

Up to four sets of quartz veins have been identified in the open pit (Townshend, 1985) and a fifth set to the north-east and south-west was identified by Bowen and Evers (1985). The veins are fractured and infilled with later material indicating more than one pulse of fluid movement (Pirajno *et al.*, 1987). Both cassiterite and wolframite occur in the veins with the wolframite commonly found along the vein margins. Sulphides are also present in the veins as pyrite, chalcopyrite, sphalerite, stannite, pyrrhotite and marcasite (Petzel, 1986).

Fig. 54: Model for the deposits in the Northern Group.



The wall rocks adjacent to the veins are pervasively altered (Elliot, 1985). Immediately adjacent to the vein margins is a muscovite selvage which grades outwards from the vein into a zone rich in tourmaline with lesser amounts of quartz. Tourmaline laths are generally pokiloblastic and constitute up to 90% of the volume. Adjacent to the tourmaline halo is a zone rich in muscovite and quartz with only minor amounts of tourmaline, biotite, fluorite and chlorite. The third zone of alteration associated with the veins is one in which biotite porphyroblasts are developed overprinting finer-grained biotite and quartz. This alteration zone grades out into the unaltered country rocks. The marbles are not as pervasively altered as the schist but where the veins have intruded localised alteration into talc, tremolite and hematite has occurred (Pirajno *et al.*, 1987).

Several dolerite dykes cross-cut the Damara sediments and are in general unaltered, although one, in the north-west of the pit has been highly altered. Field evidence indicates that this dyke was emplaced early on in the hydrothermal history and probably intruded into the metasediments after a stage of greisenisation.

Pirajno *et al.* (1987) recognise three alteration-types in the pit i.e. greisen, quartz-sericite and hematitic types. Greisenisation has affected most of the rocks in the south, east and northern parts whereas the quartz-sericite alteration assemblage and the hematite are developed in the east, north and north-west.

## 9.2. Frans Prospect

The Sn-W mineralisation at Frans Prospect is hosted in a vein system which has intruded the Swakop Group rocks on the eastern limb of a tight anticlinal fold (Petzel, 1986, Pirajno and Jacob, 1986; Kilroe, 1986). There are three vein systems trending north, north-north-east and north-west respectively (Potgieter, 1984). The vein sets form two zones, one on either

side of the marble (Kilroe, 1986). The veins consist predominantly of quartz and are fractured and contain cassiterite and wolframite with lesser amounts of pyrite and chalcopyrite. Where the veins have intruded into the marble, usually over small distances, the marble is locally ferruginised.

An ubiquitous feature of the veins is a halo of altered wall rock adjacent to the veins. Alteration-types include tourmalinisation, sericitisation, hematitisation and carbonatisation (Kilroe, 1986). Immediately adjacent to the veins is a narrow zone of silicified schist which grades into a tourmaline-rich halo. The tourmaline laths range in length from 0,2 - 0,5 mm, they are generally randomly orientated and occur with quartz and plagioclase feldspar. Adjacent to the tourmalinised halo the wall rocks have been pervasively sericitised, obliterating the pre-alteration metamorphic fabric. In these rocks the main alteration assemblage consists of quartz, sericite and pyrite.

Ferruginisation of the altered country rocks has occurred in all the alteration zones but especially in the sericitic zone and is characterised by replacement along grain boundaries and micro-fractures of the biotite and tourmaline. Ferruginous veinlets also cross-cut the rocks in places. The last pulse of hydrothermal alteration is indicated by calcite veinlets which appear to be concentrated near the quartz veins. Hematite occurs in the veinlets especially in the sericitised wall rocks.

### 9.3. Goantagab Mining Area

Mineralisation is contained in quartz veins in the schist as well as replacement bodies in the marble. The mineralisation appears to be spatially associated with two circular structures.

Cassiterite in the mining area occurs in quartz veins within

the schist and in replacement bodies at the contact between the marble and schist (Pirajno and Jacob, 1987b). The quartz veins underlie the replacement bodies suggesting that they may have acted as feeder systems to the replacement bodies. Cassiterite occurs in the veins together with tourmaline, sericite, chlorite, calcite, pyrite, pyrrhotite, sphalerite and galena.

In the replacement bodies the cassiterite mineralisation is associated with hematite and lesser amounts of quartz and calcite. Some of the replacement bodies carry small ferruginised breccia bodies. In these breccias fragments of altered and unaltered marble are cemented together by a ferruginous matrix which in places has been cut by iron-silica veins (de Klerk, 1985) which can carry significant amounts of cassiterite. The cassiterite is commonly brecciated and cemented by hematite.

The wall rocks adjacent to the veins are intensely altered and zoned. A zonation from tourmalinisation (with graphite) and silicification, close to the veins, to sericitisation away from the veins is evident (Pirajno and Jacob, 1987b). Late-stage carbonate veinlets are associated with a phase of ferruginisation.

In the replacement bodies hematite is the main alteration mineral although minor sericitisation, chloritisation and tourmalinisation effects are seen to pre-date the main ferruginisation event (de Klerk, 1985).

#### 9.4. Discussion

When considering the model of Pirajno and Jacob (1987b), it is evident that the mineralisation at Brandberg West is interpreted as being the most proximal of all the deposits. This is because of the greisenisation, the association of W with Sn, the absence of abundant sulphide mineralisation and the intrusion of the albitite plug close to the mineralisation. The most distal of the deposits is considered to be Goantagab,

since at Goantagab the main alteration-type present is QSP, only minor amounts of W mineralisation are found, sulphides are quite abundant and apart from occurring in quartz veins the cassiterite mineralisation is present within replacement bodies at the contact between the marble and the schist.

The alteration-mineralisation at Gamigab has several characteristics in common with that at Goantagab and so is thought to possibly represent a slightly lower level than Goantagab (i.e. closer to the granite source) and the characteristics at Frans indicate that it may be at a similar level as Gamigab but closer to the source.

More recent work on the various mineralised centres, including this work at Gamigab, support the earlier ideas of Pirajno and Jacob (1987b). The more recent results include microprobe analyses of the tourmalines from the alteration haloes, fluid inclusion work on samples of the quartz veins and sulphur isotope determinations on the sulphides from the quartz veins.

#### 9.4.1. Tourmaline composition

Tourmaline composition has been used in the study of other related deposits as an indication of the position of that deposit in relation to its source granite (Pirajno, unpublished data, Smithies, 1987). The change in composition is a reflection of the exchange between  $Fe^{2+}$  and  $Mg^{2+}$  in the schorl-dravite solution series.

A review of the literature suggests that granite related tourmalines are overwhelmingly Fe-rich (Neiva, 1974). Tourmalines that were generated during hydrothermal activity can span the full range between schorl and dravite although it is possible to relate the composition of these hydrothermal tourmalines to their distance from their source.

In his work in the north-west Cape at the Van Rooi's Vley W/Sn

deposit, Smithies (1987) found that the hydrothermal tourmalines in the metasediments are more Mg-rich than those tourmalines which are found as pods within the source granite. Smithies (*op. cit.*) was also able to show this relationship for tourmalines at the Zaaipplaats and Rooiberg Sn mines where the granite-hosted tourmalines are distinctly Fe-rich compared to those some distance from the source granite. Pirajno (unpublished data) has also recognised the change in tourmaline composition with increasing distance from the source in New Zealand.

The compositions of tourmalines from the deposits in the northern SKZ were analysed by microprobe and the results are shown in Table XVI. Using the Fe # (as defined earlier), Fig.55 shows a plot of compositions of the tourmalines from the various deposits together with magmatic and sedimentary tourmalines taken from the literature for comparison (Neiva, 1974; Taylor and Slack, 1984).

The tourmalines from Brandberg West and Frans Prospect have higher Fe #'s and plot in the vicinity of granite-related tourmalines, whereas those from Gamigab and Goantagab have lower Fe #'s and plot in the area of sedimentary tourmalines. Relating tourmaline composition to the model of Pirajno and Jacob (1987b) it is apparent that the tourmalines at Brandberg West and Frans Prospect indicate that these deposits may occur close to their source granite. Tourmalines from Gamigab and Goantagab have lower Fe#'s which is probably due to the fact that these deposits occur somewhat further from their granitic source.

#### 9.4.2. Fluid inclusion determinations

Fluid inclusion determinations on primary inclusions on samples of quartz vein and cassiterite from Goantagab and Frans are shown in Table XVII whereas those for Gamigab are shown in Table XIV. As described in section 8.3.1. a pressure correction needs to be allocated to the homogenisation

TABLE XVI: Partial quantitative analyses of tourmalines from Brandberg West, Frans Prospect and Goantagab.

	BRANDBERG WEST					FRANS PROSPECT				
	87892/4	5	2	1	6	882A/T5	T4	T3	T2	T6
SiO <sub>2</sub>	35,99	36,24	37,11	36,34	36,83	35,70	37,83	36,32	36,07	36,09
TiO <sub>2</sub>	1,01	0,56	0,22	0,62	0,18	0,76	0,18	0,72	0,51	0,67
Al <sub>2</sub> O <sub>3</sub>	30,81	32,02	34,19	31,15	34,12	30,29	31,93	30,53	31,19	30,12
FeO	11,65	11,21	10,91	10,04	11,23	11,57	8,50	10,86	11,15	10,41
MnO	0,31	0,28	0,22	0,26	0,25	0,37	0,33	0,29	0,36	0,41
MgO	3,48	3,51	2,46	4,67	2,37	3,84	4,68	4,41	3,63	4,73
CaO	0,17	0,14	0,04	0,29	0,04	0,08	0,03	0,13	0,05	0,07
Na <sub>2</sub> O	2,37	2,27	1,42	2,34	1,49	2,61	2,09	2,55	2,43	2,75
<b>TOTAL</b>	<b>85,77</b>	<b>86,22</b>	<b>86,58</b>	<b>85,71</b>	<b>86,51</b>	<b>85,22</b>	<b>85,57</b>	<b>85,82</b>	<b>85,39</b>	<b>85,25</b>
Fe#	0,77	0,76	0,82	0,68	0,83	0,75	0,64	0,71	0,75	0,69

GOANTAGAB

	RJT/1	2	3	5	6
SiO <sub>2</sub>	37,61	37,79	37,82	37,24	37,62
TiO <sub>2</sub>	0,52	0,34	0,49	0,64	0,25
Al <sub>2</sub> O <sub>3</sub>	31,28	32,81	32,11	30,90	31,83
FeO	3,20	2,95	3,19	3,21	2,92
MnO	0,00	0,03	0,01	0,01	0,00
MgO	9,83	9,21	9,29	9,91	9,58
CaO	1,03	0,84	0,95	1,57	0,81
Na <sub>2</sub> O	2,10	2,11	2,17	1,77	2,13
<b>TOTAL</b>	<b>85,58</b>	<b>86,08</b>	<b>86,03</b>	<b>85,26</b>	<b>85,16</b>
Fe#	0,25	0,24	0,26	0,24	0,23

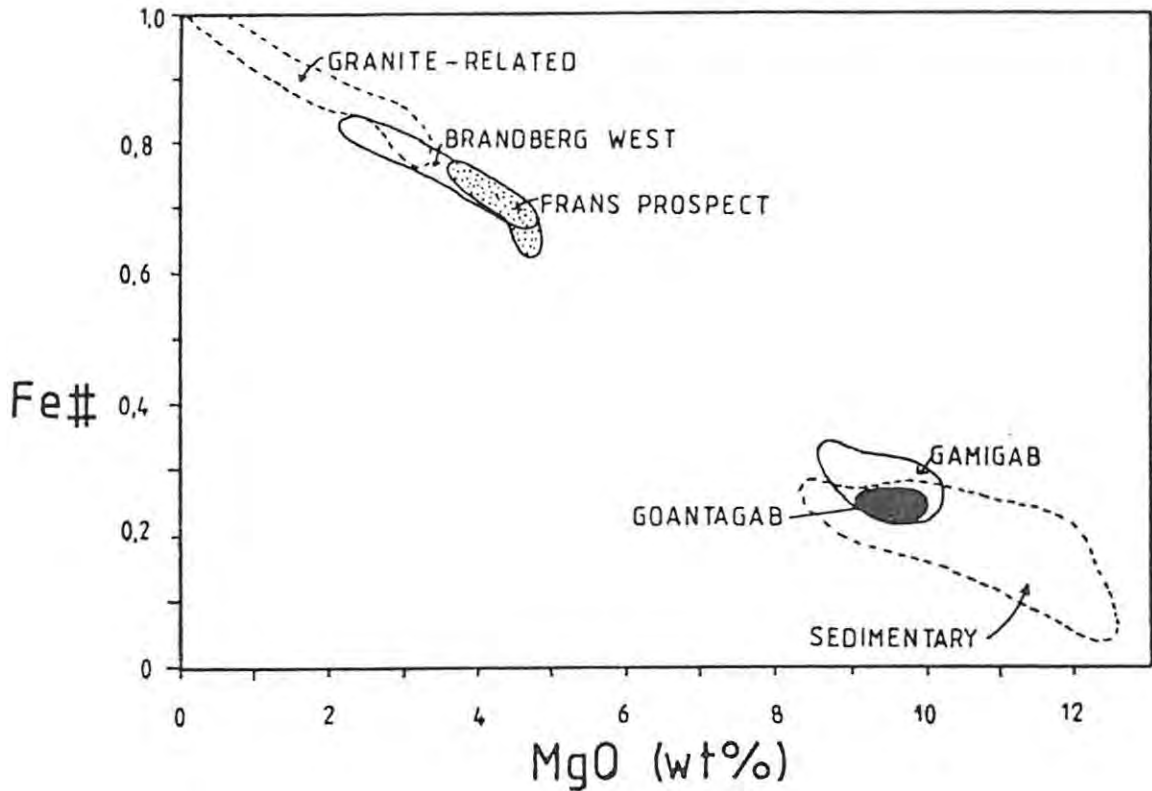


Fig. 55: Variation in tourmaline composition in the deposits of the Northern Group.

temperatures if the age of mineralisation is Karoo. A correction of 45°C and 57°C needs to be applied to the homogenisation temperatures at Frans and Goantagab respectively. The results show that homogenisation temperatures (and corrected temperatures) at Frans are higher than those at Gamigab which in turn are higher than those at Goantagab (Fig. 56).

#### 9.4.3. Sulphur isotope measurements

Sulphur isotopes may be used in the understanding of genesis of ore deposits. With sulphur three important isotopes may be recognised;  $^{32}\text{S}$ ,  $^{33}\text{S}$  and  $^{34}\text{S}$ . The variation in the amount of the isotope is expressed as  $\delta^{34}\text{S}$  which by definition is the ratio of  $^{34}\text{S}/^{32}\text{S}$  between the sample and the universal standard;

i.e.

$$\delta^{34}\text{S} = \left( \frac{(^{34}\text{S}/^{32}\text{S})_{\text{SAMPLE}}}{(^{34}\text{S}/^{32}\text{S})_{\text{STANDARD}}} - 1 \right) \times 1000$$

TABLE XVII: Results of fluid inclusion studies on samples from Frans Prospect and Goantagab Mining Area

	HOMGENISATION TEMPERATURE (°C)	FREEZING TEMPERATURE (°C)	
		1st	2nd
<b>Frans Prospect</b>			
AZ 8796	250	-22	-11
	249	-24,8	-13,7
	290	-17,8	- 9,8
	247	-21,1	-12,2
	264		
	296	-17	- 9
	299	-20,4	-11,2
	273	-16	- 7,3
	293		
Average	270°C	Fluid : NaCl + KCl + H <sub>2</sub> O	
Corrected Temperature	315°C	Salinity: 15% weight NaCl equivalent	
<b>Goantagab</b>			
R456	150	-16	-9.8
	183	-21	-9
	189	-20	-9
	193		
	189		
	193		
Average	183°C	Fluid : NaCl + H <sub>2</sub> O	
Corrected Temperature	240°C	(+ minor KCl)	
		Salinity: 15% weight NaCl equivalent	

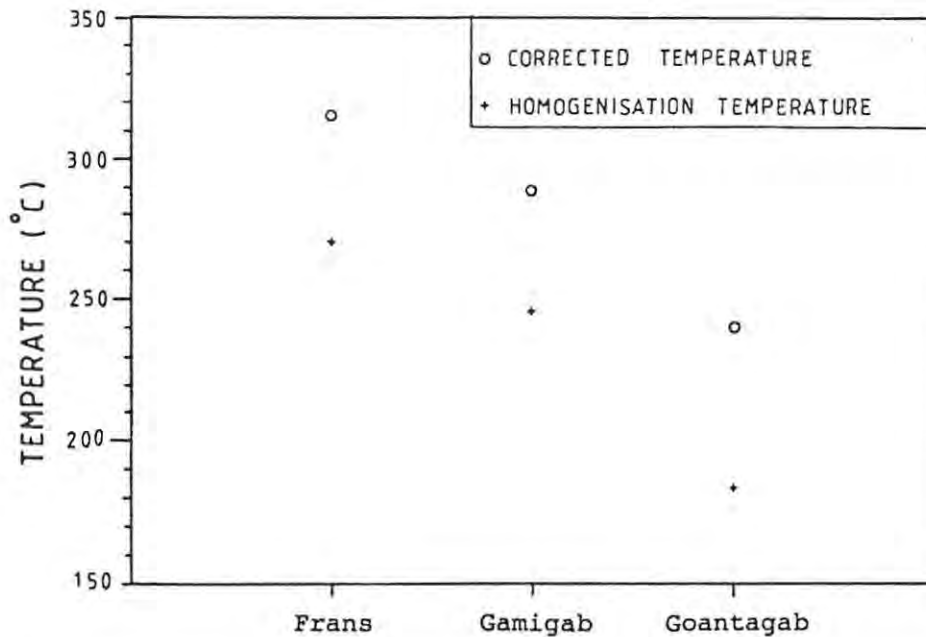


Fig. 56: Variation in homogenisation and corrected temperatures for the deposits in the Northern Group.

and is expressed as ‰ (per mil). Ohmoto and Rye (1979) determined the differences in  $\delta^{34}\text{S}$  from various environments. Sulphides from igneous rocks are isotopically similar to those found in meteorites ( $\delta^{34}\text{S}$  close to 0‰), whereas sedimentary and sea water sulphates are more enriched in the heavy isotope (10 - 30‰). Sedimentary sulphides have a wide range of  $\delta^{34}\text{S}$  values from -70 through to +70‰ but in general the values are in the lower part of the range. The average  $\delta^{34}\text{S}$  value for acid igneous rocks as well as the crust is  $0 \pm 3$ ‰.

Some preliminary  $\delta^{34}\text{S}$  measurements have been done on samples of sulphides from Brandberg West and Goantagab and are presented in Table XVIII. The sulphides from Goantagab are somewhat more enriched in the heavy isotope when compared to the sulphides from Brandberg West (average +5,47‰ vs +1,33‰). If the origin of the sulphur and not the chemistry of the solution is the most important, then the  $\delta^{34}\text{S}$  values for Brandberg West suggest a magmatic origin. The higher values for Goantagab may be an indication of contamination from sedimentary sulphur as the hydrothermal fluids moved upwards through the crust away from the source magma.

TABLE XVIII: Results of  $\delta^{34}\text{S}$  measurements on sulphide samples from Brandberg West and Goantagab (Pirajno, unpublished data).

Sample	Sulphide	$\delta^{34}\text{S}$ (‰)	
DM3	pyrite	+1,27	Brandberg West (Average = +1,33)
AZ7839	pyrite	+1,35	
AZ7839	chalcopyrite	+1,36	
R589	sphalerite	+6,31	Goantagab (Average = +5,47)
R589	pyrite	+5,86	
R330	pyrite	+5,15	
R557	pyrite	+4,79	
R559	pyrite	+5,50	
R559	pyrrhotite	+5,22	

(Analyses performed at the University of St. Andrews, courtesy of P. Bowden)

#### 9.4.4. Concluding remarks

Results from the tourmaline analyses, fluid inclusion determinations and sulphur isotope work all support the model of Pirajno and Jacob (1987b) in that the deposits in the Northern Group represent different levels of deposition relative to the source granite.

## 10. SUMMARY

The Gamigab prospect is the eastern-most member of a group of tubidite-hosted deposits termed the Northern Group (Pirajno and Jacob, 1987), in the Southern Kaoko Zone of the Damara Orogen. The other deposits include the vein-hosted Sn-W deposit at Brandberg West, the vein-hosted Sn prospect at Frans and the vein- and replacement-hosted Sn deposit at Goantagab.

The base metal mineralisation at Brandberg West, Frans and Goantagab have been the centre of recent studies (Pirajno and Jacob, 1987; Pirajno *et al.*, 1987; Petzel, 1985; Elliot 1985; Townshend, 1985; and Kilroe, 1986), whereas the mineralisation at Gamigab has not been fully documented. Early exploration at Gamigab was started in 1953 by SWACO (South West African Company) who excavated three exploration trenches perpendicular to the east-west trending Sn-bearing quartz veins. Further exploration by percussion drilling and detailed geological mapping was undertaken by the Trekkopje Mining Company (Le Roux, 1982). The results from the drilling and surface sampling indicated a sub-economic deposit.

The quartz veins at Gamigab have intruded into a thick sequence of quartz-biotite schist within an antiformal structure. Accompanying the mineralisation was hydrothermal alteration, brecciation and minor igneous activity, the latter in the form of a feldspar porphyry plug. This study was undertaken to determine the relationship between the mineralisation, alteration, brecciation, igneous activity and regional structure.

Detailed (1:2000) and regional (1:10 000) geological mapping of the prospect and surrounding area has shown that the stratigraphy of the area consists of two schist units separated by a thick banded marble unit. The lithologies have been assigned to the Swakop Group, in particular to the Orusewa Formation, the Karibib Formation and the Kuiseb Formation respectively. The Orusewa Formation is defined by a well foliated, fine-grained and dark-brown quartz-biotite schist.

Overlying this is the Karibib Formation which consists of a banded calcitic marble unit (which in places contains tremolite needles) interbedded with numerous thin dolomite-rich layers. Minor lenses of quartz-biotite schist occur toward the top of the formation. The banded nature of the marble is exemplified by different coloured layers ranging between pale-yellow, blue-grey, yellow-brown, black and white. The calcite-rich marble is seen in places to carry poikiloblastic tremolite grains. Lenses of "streaky marble" occur inbetween bands of calcite-rich and dolomite-rich marble. The lenses are fairly persistent along strike but are seen eventually to pinch out.

The Kuiseb Formation in the area consists of a well foliated, fine-grained green quartz-biotite-chlorite schist containing numerous actinolite-bearing calc-silicate lenses and marble interbeds.

An altered feldspar porphyry plug has intruded into the Karibib Formation about 500 m north-east of the mineralised quartz veins. The intrusion has been ferruginised and brecciated and in places is amygdaloidal. In the same area of the porphyry plug is a weathered dolerite sill which contains xenoliths of underformed conglomerate and feldspathic greywacke.

The Gamigab area was subjected to four phases of ductile deformation. D1 produced an axial planar transpositional banding in the Karibib Formation and a penetrative regional axial planar foliation in the metapelitic rocks ( $S_1$ ). F1 folds are only locally preserved in the marbles as small intrafolial folds. The F2 folds are megascopic, almost north-south trending folds which plunge between  $30^\circ$  and  $50^\circ$  toward the south. In some places in the fold closures local transposition into the  $S_2$  direction is seen. In section the folds are "M" shaped having open anticlines and tight synclines and are in general upright although some verge slightly to the west. The third phase of deformation was responsible for the change in strike of the lithologies between Goantagab to the north-west and Gamigab. At Goantagab the main structures strike south-south-east whereas those at Gamigab strike south-south-west.

those at Gamigab strike south-south-west. The mechanism for this change in strike is interpreted as an anticlockwise rotational event causing drag folding along a sinistral shear zone. The final phase of folding is seen by flexuring about a north-west trending axis. In the field it is expressed as kink folds in the schist and as small open folds in the marble.

Cross-cutting the folded lithologies in the area around the mineralisation are several east-west trending faults. The amount of displacement with the faults is difficult to determine because of the association of extensive alteration (ferruginisation) around the fault plane. Several other much larger faults occur to the north-west of the mineralisation. One such fault transects the schists in a north-west trend and defines the contact between the Orusewa Formation and the Karibib Formation.

In the Gamigab area the rocks underwent a single phase of low-grade regional metamorphism. Study of the relationship between the mineral assemblages in the metapelitic rocks, marbles and calc-silicate lenses suggest that temperatures were in the range between 420°C and 500°C with pressures less than 2 kbars. The effects of contact metamorphism are seen south-east and south-west of Gamigab in the form of cordierite porphyroblasts and biotite porphyroblasts respectively. Contact relationships between minerals suggest that the tremolite was formed by the reaction between dolomite and quartz and the grossularite in the calc-silicate lenses formed through the reaction of zoisite with quartz.

The alignment of the phyllosilicates is a clear indication that metamorphism started during the first phase of deformation. The decussate nature of the tremolite porphyroblasts suggests post-tectonic growth, probably after D2. The actinolite porphyroblasts show a strained extinction when viewed in thin section indicating a late- to post-tectonic growth. The effects of contact metamorphism started during the late stages of D4 as evidenced by partial alignment of coarse-grained biotite laths but continued after D4. This syn- to post-tectonic contact

metamorphism is also shown up by the growth of the cordierite porphyroblasts in the regional  $S_1$  or  $S_2$  foliation but which are generally decussate relative to one another.

Hydrothermal activity at Gamigab was responsible for the Sn-mineralisation, alteration and brecciation. Cassiterite ( $\text{SnO}_2$ ) is present as brecciated nuggets found within the fractured quartz veins which intruded into the Orusewa Formation. Accessory amounts of pyrite and chalcopyrite are also present in the veins. Adjacent to the veins is a halo of pervasively tourmalinised wall rock which grades out into altered rocks which have a quartz-sericite-pyrite (QSP) assemblage.

Some 20 veins intruded the metasediments and detailed mapping along exploration trenches dug by SWACO identified a single set of veins. In general the veins trend almost east-west and are sub-vertical, dipping steeply either to the north or south and could have been emplaced along zones of weakness generated during D2 (i.e. along a-c joints).

Fluid inclusion studies, although limited, indicate that homogenisation temperatures were about  $245^\circ\text{C}$  and the fluid composition was  $\text{K}_2\text{O} + \text{NaCl} + \text{H}_2\text{O}$  and had a salinity of 10 weight percent NaCl equivalent. Pressure correction of 2 kbars indicates mineralisation temperature of about  $289^\circ\text{C}$ .

The tourmalinised vein margins consist of fine-grained tourmaline laths which are aligned probably parallel to the regional foliation. Quartz is also present as a fine-grained unstrained mosaic. The wall rocks further away from the vein have been pervasively sericitised. Weathered ferruginous spots are developed almost everywhere and are thought to have initially been pyrite grains, but which have been completely weathered out. Coarse-grained muscovite laths are seen in places replacing the fine-grained sericitic assemblage.

Microprobe analyses on samples of tourmalinised wall rocks show that the tourmaline is Mg-rich (dravite) whereas those further away in the altered wall rocks are slightly more Fe-rich. The

composition of the country rocks does not appear to have a great effect on the composition of the tourmaline since those that are found in altered portions of the marble are also Mg-rich.

Breccias, of probable hydrothermal origin, occur scattered about the prospect. They vary in size and are all located within or adjacent to the axial parts of F2 antiformal structures. The breccias are only found within the Karibib Formation and only contain fragments of the calcitic- and dolomitic-marble which can in places be fitted back together if the matrix was removed. The matrix cementing the fragments is usually calcite although in some breccias it can become siliceous. Surrounding the breccias is a halo of ferruginised country rock. The characteristics of the breccias suggest *in situ* fracturing of the marble in response to pressure release from the build up of hydrothermal fluids at the contact between the schists and the impermeable marble in the apical portions of the main folds. This hydrothermal fluid was probably also responsible for the alteration of the country rocks and fragments.

Although it crops out some 500 m from the mineralisation, it was initially thought that the porphyry plug may in some way be related to the igneous activity responsible for the alteration-mineralisation. Major and trace element analysis suggest that it may represent an altered feeder pipe to a latite flow as seen further north in the Etendeka. The two main differences are an increase in the CaO and decrease in the Na<sub>2</sub>O which could have resulted in the combined effect of assimilation of Ca during intrusion into the marbles and a late-stage carbonatisation alteration. The samples also show anomalous amounts of Sn.

Preliminary Rb/Sr dating on a sample of muscovite and calcite from the alteration zone suggests an age of 509 ± 11 Ma.

A paragenetic sequence of hydrothermal events at Gamigab may be recognised:

1. Emplacement of volatile-rich granitic magma and subsequent crystallization
2. Release of fluids into the country rocks
3. Sericitisation of Orusewa Formation schist (QSP assemblage) with late-stage potassic metasomatism
4. Tourmalinisation adjacent to fractures in the Orusewa Formation
5. Crystallisation of quartz in the fractures
6. Brecciation in the apical parts of the F2 folds in the Karibib marble
7. Carbonatisation in both the Karibib and Orusewa Formations
8. Mineralisation in the quartz veins
9. Carbonatisation with ferruginisation in the mineralised area, breccias and porphyry plug.

A model for the hydrothermal deposits of the Northern group is presented by Pirajno and Jacob (1987b). Their model is built on the alteration assemblages and mineralisation types which are characteristic of the various deposits and suggests that the mineralisation at Brandberg West is the most proximal deposit to the source granite. Frans Prospect is somewhat further away and Gamigab and Goantagab are the distal members. Additional work during the course of this study provides evidence to support the model.

The use of tourmaline composition as an indicator on the relative position of the alteration environment to its source has been identified at other hydrothermal deposits (Smithies, 1987). The composition of tourmaline in the deposits of the Northern Group are seen to change from being Mg-rich at Gamigab and Goantagab to Fe-rich at Brandberg West and Frans, the latter overlapping with the field of "granite-related" tourmalines.

Preliminary fluid inclusion studies on samples from Frans and Goantagab show that temperatures during hydrothermal activity are higher at Frans (315°C - corrected) than at Goantagab (240°C - corrected). Considering the temperature of 289°C for Gamigab it seems that Frans was probably closer to the source than Gamigab and Goantagab respectively.

Sulphur isotope results appear to support the model. The sulphides from Goantagab are somewhat more enriched in the heavy isotope ( $\delta^{34}\text{S}$ ) compared to Brandberg West (5,47 ‰ cf 1,33 ‰). The higher values for Goantagab may be an indication of contamination of sedimentary sulphur derived from a granitic magma.

#### ACKNOWLEDGEMENTS

*There have been a number of persons who have either directly or indirectly influenced the course of this study. In particular, I wish to extend my sincere appreciation to the following:*

*To the Geological Survey of Namibia, in particular Dr. Roy Miller, for the financial assistance without which this study would not have taken place.*

*Mr. Pat Vickers of Gold Fields South Africa, and the geological staff of Gold Fields, Namibia, for permission to work at Gamigab and also for assistance during field work. Alan and Lex Lyons must be thanked for their friendship and hospitality during my stay in the field.*

*To my supervisor, Professor Roger Jacob, for his encouragement and assistance throughout the course of this study. Professor Franco Pirajno is also thanked for guidance and discussion on numerous occasions.*

*Appreciation is extended to Billy de Klerk for his assistance with XRF analyses, Rob Skae for electron microprobe work and to my fellow students, namely Hugh Smithies and Julian Misiewicz, for constant companionship and numerous discussions.*

*Finally my heartfelt thanks to my wife, Lynne, for all her assistance in the typing and proof reading of this thesis. Her encouragement and patience throughout the course of this study are greatly appreciated.*

REFERENCES

- Ahrendt, H., Behr, H.J. and Clauer, N. (1983). The northern branch: depositional development and timing of the structural and metamorphic evolution within the framework of the Damara Orogen, 723-743. In: Martin, H. and Eder, F.W. (Eds): *Intracontinental fold belts*, Springer Verlag, Berlin. 945pp.
- Allman-Ward, P., Halls, C., Rankin, A. and Bristow, C.M. (1982). An intrusive hydrothermal breccia body at Wheal Remfry in the western part of the St. Austell granite pluton, Cornwall, England, 1-28. In: Evans, A.M. (Ed): *Metallisation associated with acid magmatism*, John Wiley and Sons, London, 385pp.
- Allsopp, H.L., Bristow, J.W., Logan, C.T., Eales, H.V. and Erlank, A. (1984). Rb-Sr Geochronology of three Karoo-related Intrusive Complexes. *Special Publication of the Geological Society of South Africa*, 13, 281-287.
- Barnes, S.J. and Sawyer, E.W. (1980). An alternative model for the Damara Mobile Belt: Ocean crust subduction and continental convergence. *Precambrian Research*, 13, 297-336.
- Best, M.G. (1982). *Igneous and metamorphic petrology*. W.H. Freeman and Co, New York, 630pp.
- Botha, B.J.V., Gunter, C.J., Koornhof, J.C., Schoeman, P.J., Tordiffe, E.A.W. and Van Reenen, D.D. (1971). Die sisteem Damara in die gebied tussen Uis en Kaap Kruis, Suidwes-Afrika. *Annals of the Geological Survey of South Africa*, 9, 57-67.
- Botha, B.J.V. and Hodgson, F.D.I. (1976). Karoo Dolerites in north-western Damaraland. *Transactions of the Geological Society of South Africa*, 79, 186-190.

- Bowen, M.P. and Evers, T. (1985). Report on detailed mapping and lithogeochemistry, Brandberg West Mine. Unpublished Gold Fields Internal Report.
- Bowden, P. (1985). The geochemistry and mineralisation of alkaline ring complexes in Africa (A review). *Journal of African Earth Sciences*, 3, 17-39.
- Bristow, J.W. and Saggerson, E.P. (1983). A review of Karoo vulcanicity in Southern Africa. *Bulletin of Volcanology*, 46, 135-159.
- Burnham, C.W. (1979). Magmas and hydrothermal fluids, 71-136. In: Barnes, H.J. (Ed): *Geochemistry of Hydrothermal Ore Deposits*, New York, Wiley, 798pp.
- Burnham, C.W. (1985). Energy release in subvolcanic environments: Implications for breccia formation. *Economic Geology*, 80, 1515-1522.
- Burt, D.M. (1981). Acidity-salinity diagrams - application to greisen and porphyry deposits. *Economic Geology*. 76, 832-843.
- Clemens, J.D., Holloway, J.R. and White, A.J.R. (1986). Origin of an A-Type granite: Experimental constraints. *American Mineralogist*, 71(3,4), 317-324.
- Coward, M.P. (1983). The tectonic history of the Damaran belt. *Special Publication of the Geological Society of South Africa*, 11, 409-421.
- Deer, W.A., Howie, R.A. and Zussman, J. (1986). *Rock forming minerals, Volume 1B. Disilicates and ring structures*. Longman Scientific and Technical, London, 629pp.

- De Klerk, I. (1985). *An investigation of iron-rich alteration and associated mineralisation in marbles from the Brandberg north region, South West Africa/Namibia*. BSc (Honours) Project (Unpublished) Rhodes University, Grahamstown, 23 pp.
- Elliot, L. (1985). *The wall rocks of the Brandberg West Mine, Namibia*. BSc (Honours) project (Unpublished), Rhodes University, Grahamstown, 40pp.
- Erlank, A.J., Marsh, J.J., Duncan, A.R., Miller, R.Mc.G., Hawkesworth, C.J., Betton, P.J. and Rex, D.C. (1984). *Geochemistry and petrogenesis of the Etendeka volcanic rocks from South West Africa/Namibia*. *Special Publication of the Geological Society of South Africa*, 13, 195-245.
- Finnemore, S.H. (1974). *Geology of the Elisenheim area, Windhoek district, South West Africa, with specific reference to the 'Matchless' amphibolite belt*. MSc. Thesis (Unpublished) Rhodes University, Grahamstown, 72pp.
- Finnemore, S.H. (1978). *The geochemistry and origin of the matchless amphibolite belt, Windhoek district, South West Africa*. *Special Publication of the Geological society of South Africa*, 4, 433-477.
- Frets, D.C. (1969). *Geology and structure of the Huab-Welwitschia area, South West Africa*. *Bulletin of the Precambrian Research Unit, University of Cape Town*, 5, 235pp.
- Freyer, E.E. and Hälbich, I.W. (1983). *A note on the Ogden Rocks Formation: a protomylonite belt in the Damara Orogen*. *Special Publication of the Geological Society of South Africa*. 11, 173-174.
- Freyer, E.E. (In Preparation). *Structural and metamorphic geology of the Damara Sequence along the Lower Ugab River*. Msc thesis, University of Stellenbosch.

- Gabelman, J.W. (1984). Circular geomorphic features permissive to interpretation as conduits of mantle degassing. *Global Tectonics and Metallogeny*, 2, 151-168.
- Gates, O. (1959). Breccia pipes in the Shoshone Range, Nevada. *Economic Geology*, 54, 790-815.
- Gevers, T.W. (1931). An ancient tillite in South West Africa. *Transactions of the Geological Society of South Africa*, 34, 1-17.
- Gordon, T.M. and Greenwood, H.J. (1971). The stability of grossularite in H<sub>2</sub>O-CO<sub>2</sub> mixtures. *American Mineralogist*, 56, 1674-1688.
- Groen, C. (1986). Progress report on the local structural setting and controls of cassiterite mineralisation in the Gaontagab Mining Area, central Damaraland, South West Africa/Namibia. Unpublished Gold Fields Internal Report, 15pp.
- Groves, D.I. (1972). The geochemical evolution of tin-bearing granites in the Blue Tier Batholith, Tasmania. *Economic Geology*, 67, 445-457.
- Guj, P. (1970). The Damara mobile belt in south-western Kaokoveld, South West Africa. *Bulletin of the Precambrian Research Unit, University of Cape Town*, 18, 168pp.
- Hälbich, I.W. and Freyer, E.E. (1985). Structure and metamorphism of Damaran rocks in the Ugab Profile, Progress Report for 1982/83. *Communications of the Geological Survey of South West Africa/Namibia*, 1, 97-99.
- Hartmann, O., Hoffer, E. and Haack, U. (1983). Regional metamorphism in the Damara Orogen: Intereaction of crustal motion and heat transfer. *Special Publication of the Geological Society of South Africa*, 11, 233-243.

- Hartnady, C.J. (1978). Tectonic evolution of the south-eastern part of the Hakos-Auas Mountain Zone in the Damara Orogenic Belt. *14/15th Annual Report, Precambrian Research Unit, University of Cape Town*, 171-182.
- Hawkesworth, C.J., Gledhill, A.R., Roddick, J.C., Miller, R.McG. and Kröner, A. (1983). Rb/Sr and Ar/Ar studies bearing on models for the thermal evolution of the Damara belt, Namibia. *Special Publication of the Geological Society of South Africa*. 11, 323-338.
- Hawkesworth, C.J., Menzies, M.A. and van Calsteren, P. (1986) Geochemical and tectonic evolution of the Damara Belt, Namibia, 305-319. In: Coward, M.P. and Ries, A.C. (Eds): *Collision tectonics*, Geological Society Special Publication, 19, 415pp.
- Henderson, P. (1982). *Inorganic geochemistry*, Pergamon Press, Oxford, 353pp.
- Henley, R.W. and Ellis, A.J. (1983). Geothermal systems, ancient and modern: A geological review. *Earth Science Reviews*, 19, 1-50.
- Henry, G., Stanistreet, I.G. and Maiden, K.J. (1986). Preliminary results of a sedimentological study of the Chuos formation in the central zone of the Damara Orogen: Evidence for mass flow processes and glacial activity. *Communications of the Geological Survey of South West Africa/Namibia*, 2, 75-92.
- Hobbs, B.E., Means, W.D. and Williams, P.F. (1976). *An outline of structural geology*. John Wiley and Sons, New York, 571pp.
- Hodgson, F.D.I. (1972). *The geology of the Brandberg-Aba Huab area, South West Africa*. DSc. thesis (Unpublished), University of the Orange Free State, South Africa, 174pp.

- Hodgson, F.D.I. (1973). Petrology and evolution of the Brandberg intrusion, South West Africa. *Special Publication of the Geological Society of South Africa*, 3, 339-343.
- Hodgson, F.D.I. and Botha, B.J.V. (1974). The Doros Complex, South West Africa. *Neues Jahrbuch für Mineralogie Monatshefte*, 9, 398-418.
- Hoffer, E. (1983). Compositional variations of minerals in metapelites involved in low to medium-grade isograd reactions in the Southern Damara Orogen, South West Africa/Namibia, 745-765. In: Martin, H. and Eder, F.W. (Eds): *Intracontinental Fold Belts*, Springer-Verlag, Berlin, 945pp.
- Hoffman, K.H. (1983). Lithostratigraphy and facies of the Swakop Group of the Southern Damara Belt. *Special Publication of the Geological Society of South Africa*, 11, 43-63.
- Holland, H.D. (1972). Granites, solutions and base metal deposits. *Economic Geology*, 67, 281-301.
- Holloway, J.R. and Lewis, C.F. (1974). CO<sub>2</sub> solubility in hydrous albite liquid at 5 kbar (abstract). *Transactions of the American Geophysical Union*, 55, 483pp.
- Jacob, R.E. (1974). Geology and metamorphic petrology of part of the damara orogen along the lower Swakop river, South West Africa. *Bulletin of the Precambrian Research Unit*, University of Cape Town, 17, 185pp.
- Jacob, R.E., Snowdon, P.A. and Bunting, F.J.L. (1983). Geology and structural development of the Tumas Basement dome and its cover rocks. *Special Publication of the Geological Society of South Africa*, 11, 157-172.

- Jeppé, J.F.B. (1952). *The geology of the area along the Ugab River, west of the Brandberg*. DSc. thesis (Unpublished), University of the Witwatersrand, 224pp.
- Kasch, K.W.A. (1979). A continental collision model for the tectonothermal evolution of the (southern) Damara belt. *16th Annual Report, Precambrian Research Unit, University of Cape Town*, 101-107.
- Kasch, K.W. (1983a). Regional P-T variations in the Damara Orogen with particular reference to early high pressure metamorphism along the southern margin. *Special Publication of the Geological Society of South Africa*, 11, 243-253.
- Kasch, K.W. (1983b). Tectonothermal evolution of the southern Damara Orogen. *Special Publication of the Geological Society of South Africa*, 11, 255-265.
- Kasch, K.W. (1986). Delamination and suture progradation in the southern Damara Orogen of central South West Africa/Namibia. *Transactions of the Geological Society of South Africa*, 89, 215-222.
- Kennedy, W.Q. (1964). The structural differentiation of Africa in the Pan African ( $\pm$  500 Ma) tectonic episode. *8th Annual Report, Research Institute of African Geology, University of Leeds*, 48.
- Kilroe, T. (1986). *Hydrothermal alteration and structural development of Frans Prospect, Namibia*. BSc (Honours) Project (Unpublished), Rhodes University, Grahamstown, 42pp.
- Korn, H. and Martin, H. (1954). The Messum Igneous Complex in South West Africa. *Transactions of the Geological Society of South Africa*, 57, 83-124.

- Kröner, A. (1977). Precambrian mobile belts of southern and eastern Africa - ancient sutures or sites of insialic mobility? A case for crustal evolution toward plate tectonics. *Tectonophysics*, 40, 101-135.
- Kröner, A. (1982). Rb/Sr geochronology and tectonic evolution of the Pan African Damara Belt of Namibia, south-western Africa. *American Journal of Science*, 282, 1471-1507.
- Le Maitre, R.W. (1976). The chemical variability of some common igneous rocks. *Journal of Petrology*, 17, 589-637.
- Le Roux, D.L. (1982). Brandberg North Prospect - progress report on the work done at Gamigab. Unpublished report, Trekkopje Exploration and Mining Company, 10pp.
- Manton, W.I. and Siedner, G. (1967). Age of the Paresis Complex, South West Africa. *Nature*, 216, 1197-1198.
- Marsh, J.S. (1973). Relationships between transform directions and alkaline igneous rock lineaments in Africa and South America. *Earth and Planetary Science Letters*, 18, 317-323.
- Martin, H. (1965). The precambrian geology of South West Africa and Namaqualand. *Precambrian Research Unit*, University of Cape Town, 159pp.
- Martin, H. (1983). Alternative geodynamic models for the Damara Orogeny. A critical discussion, 913-945. In: Martin, N. and Eder, F.W. (Eds): *Intracontinental Fold Belts*, Springer Verlag, Berlin, 945pp.
- Martin, H., Mathias, M. and Simpson, E.S.W. (1960). The Damaraland sub-volcanic ring complexes in South West Africa. *International Geological Congress, XXI Session*, 156-174.
- Martin, H. and Porada, H. (1977). The intracratonic branch of the Damara Orogen in South West Africa. I: Discussion of geodynamic models. *Precambrian Research*, 5, 311-338.

- Metz, P. (1970). Experimental investigations of the metamorphism of siliceous dolomites II. The conditions of diopside formation. *Contributions to Mineralogy and Petrology*, 28, 221-250.
- Metz, P. and Tromsdorff, V. (1968). On phase equilibrium in metamorphosed siliceous dolomites. *Contributions to Mineralogy and Petrology*, 18, 305-309.
- Miller, R.McG. (1972). *The geology of a portion of southern Damaraland, South West Africa, with particular reference to the petrogenesis of the Salem granite.* PhD thesis (Unpublished), University of Cape Town, 246pp.
- Miller, R.McG. (1973a). Geological Map 2013 - Cape Cross, Scale 1:250 000. Geological Survey South West Africa/Namibia (Unpublished).
- Miller, R.McG. (1973b). The Salem granite suite South West Africa: Genesis by partial melting of the Khomas schist. *Memoirs of the Geological Survey of South Africa*, 64, 106pp.
- Miller, R.McG. (1979). The Okahandja Lineament, a fundamental tectonic boundary in the Damara Orogen of South West Africa/Namibia. *Transactions of the Geological Society of South Africa*, 82, 349-361.
- Miller, R.McG. (1980). Geology of a portion of central Damaraland, South West Africa/Namibia. *Memoirs of the Geological Survey of South Africa.* (South West Africa Series), 6, 78pp.
- Miller, R.McG. (1983). The Pan-African Damara Orogen of South West Africa/Namibia. *Special Publication of the Geological Society of South Africa*, 11, 431-515.

- Miller, R.McG. and Burger, A.J. (1983). U-Pb zircon ages of members of the Salem granitic suite along the northern edge of the central Damaran granite belt. *Special Publication of the Geological Society of South Africa*, 11, 273-280.
- Miller, R.McG., Freyer, E.E. and Hälbich, I.W. (1983). A turbidite succession equivalent to the entire Swakop group. *Special Publication of the Geological Society of South Africa*, 11, 65-73.
- Milner, S.C. (1988). *The geology and geochemistry of the Etendeka Formation quartz latites, Namibia*. PhD thesis (Unpublished), University of Cape Town, 263pp.
- Neiva, A.M.R. (1974). Geochemistry of tourmaline (schorlite) from granites, aplites and pegmatites from northern Portugal. *Geochemica et Cosmochimica Acta*, 38, 1307-1317.
- Norton, D.L. and Cathles, L.M. (1973). Breccia pipes - products of exsolved vapour from magmas. *Economic Geology*, 68, 540-546.
- Ohle, E.L. (1985). Breccias in Mississippi Valley-Type Deposits. *Economic Geology*, 80, 1736-1752.
- Ohmoto, H. and Rye, R.O. (1979). Isotopes of sulphur and carbon, 509-567. In: Barnes, H.L. (Ed): *Geochemistry of Hydrothermal Ore Deposits*, 2nd edition. Wiley Interscience, New York, 798pp.
- Osborn, R.I. (1985). Regional mapping Brandberg north (portions of grants 1068, 1299 and 1300). Gold Fields internal report (Unpublished), 16pp.
- Petzel, V.F.W. (1984). Final report on the first phase of exploration on Area 1, Goantagab Mining Area. Unpublished Gold Fields Internal Report, 23pp.

- Petzal, V.F.W. (1986). *Vein and replacement type Sn and Sn-W mineralisation in the Southern Kaoko zone, Damara Province, South West Africa/Namibia*. MSc. (Exploration Geology) Thesis (Unpublished) Rhodes University, Grahamstown, 141pp.
- Pirajno, F. (1987a). Hydrothermal mineral deposits and wall rock alteration. Exploration Geology course notes (Unpublished), Rhodes University, Grahamstown, 293pp.
- Pirajno, F. (1987b). A fossil hot-spring system in the Brandberg complex, Damara Province, South West Africa/Namibia. *South African Journal of Geology*, 90, 509-513.
- Pirajno, F. and Jacob, R.E. (1986). Sn-W metallogeny in the Damara Orogen, Namibia. Unpublished Rhodes University Internal Report
- Pirajno, F. and Jacob, R.E. (1987a). Sn-W metallogeny in the Damara Orogen, South West Africa, Namibia. *South African Journal of Geology*, 90, 239-255.
- Pirajno, F. and Jacob, R.E. (1987b). Hydrothermal tin-tungsten mineralisation in the Brandberg West-Goantagab area of the Damara Orogen, South West Africa/Namibia. *Communications of the Geological Survey of South West Africa/Namibia*, 3, 99-103.
- Pirajno, F., Petzel, V.F.W. and Jacob, R.E. (1987). Geology and alteration-mineralisation of the Brandberg West Sn-W deposits, Damara Orogen, South West Africa/Namibia. *South African Journal of Geology*, 90, 256-269.
- Plimer, I.R. (1983). The geology of tin and tungsten deposits. Course Handbook, Institute of Mining and Petrology, Mining University Leoben Austria.

- Porada, H. (1973). Tektonisches Verhalten und geologische Bedeutung von Kalksilikatfels - lagen und -spindeln im Damara Orogen Südwest-Afrikas. *Geologische Rundschau*, 62, 918-938.
- Porada, H. (1979). The Damara-Ribeira orogen of the Pan-African Braziliano cycle in Namibia (South West Africa) and Brazil as interpreted in terms of continental collision. *Tectonophysics*, 57, 237-265.
- Porada, H. (1983). Geodynamics model for the geosynclinal development of the Damara Orogen, Namibia, 503-543. In: Martin, H. and Eder, F.W. (Eds): *Intracontinental fold belts*. Springer-Verlag, Berlin, 945pp.
- Porada, H. (1985). Stratigraphy and facies in the upper proterozoic Damara Orogen, Namibia, based on a geodynamic model. *Precambrian Research*, 29, 235-264.
- Porada, H. (1989). Pan-African rifting and orogenesis in southern to equatorial Africa and eastern Brazil. *Precambrian Research*, 44, 103-136.
- Porada, H., Ahrendt, H., Behr, H.J. and Weber, K. (1983). The join of the coastal and intracontinental branches of the Damara Orogen, Namibia, South West Africa, 901-912. In: Martin, H. and Eder, F.W. (Eds): *Intracontinental fold belts*, Springer-Verlag, Berlin, 945pp.
- Porada, H. and Wittig, R. (1983). Turbidites in the Damara Orogen, 543-571. In: Martin, H and Eder, F.W. (Eds): *Intracontinental fold belts*, Springer-Verlag, Berlin, 945pp.
- Potgieter, J.E. (1984). Progress report on exploration conducted on the Frans Prospect during the period October 1982 and May 1983. Unpublished Goldfields Internal Report.

- Potgieter, J.E. (1987). *Anorogenic alkaline ring-type complexes of the Damaraland province, Namibia, and their economic potential*. MSc. (Exploration Geology) Dissertation (Unpublished) Rhodes University, Grahamstown, 150pp.
- Potter, R.W. (1977). Pressure corrections for fluid inclusion homogenisation temperatures based on the volumetric properties of the system NaCl-H<sub>2</sub>O. *Journal of Research of the United States Geological Survey*, 5, 603-607.
- Prins, P. (1981). The geochemical evolution of the alkaline and carbonatite complexes of the Damaraland igneous province, South West Africa. *Annale van Universiteit Stellenbosch Series A1*, 3, 145-278.
- Puhan, D. (1983). Metamorphism of siliceous dolomites of the Central and southern part of the Damara Orogen, 767-784. In: Martin, H. and Eder, F.W. (Eds): *Intracontinental fold belts*. Springer-Verlag, Berlin, 945pp.
- Puhan, D. and Hoffer, E. (1973). Phase relations of talc and tremolites in metamorphic calcite-dolomite sediments in the southern portion of the Damara belt (South West Africa). *Contributions to Mineralogy and Petrology*, 40, 207-214.
- Ramsay, J.G. (1967). *Folding and Fracturing of Rocks*. McGraw-Hill Book Company, London, 568pp.
- Reeves, C.V. (1978). Interpretation of the reconnaissance aeromagnetic survey of Botswana. *Report of the Geological Survey of Botswana*, 199pp.
- Richards, T.E. (1986). Geological characteristics of rare-metal pegmatites of the Uis type in the Damara Orogen, south West Africa/Namibia, 1845-1862. In: Anhaeusser, C.R. and Maske, S. (Eds): *Mineral Deposits of Southern Africa, Volume II*, Geological Society of South Africa, Johannesburg.

- Rose, A.W. and Burt, D.M. (1979). Hydrothermal alteration, 173-235. In: Barnes, H.L. (Ed): *Geochemistry of Hydrothermal Ore Deposits*, 2nd Edition, Wiley Interscience, New York, 798pp.
- Sawyer, E.W. (1981). Damaran structural and metamorphic geology of an area south-east of Walvis Bay, South West Africa/Namibia. *Geological Survey of South West Africa Memoirs*, 7, 94pp.
- Schemerhorn, L.J.G. (1974). Late precambrian mixtites: Glacial and/or non-glacial? *American Journal of Science*, 274, 673-824.
- Scherba, G.N. (1970). Greisens. *International Geological Reviews*, 12, 114-151.
- Schmidt, A. and Wedepohl, K.H. (1983). Chemical composition and genetic relations of the matchless amphibolite, Damara Orogenic belt, 139-145. *Special Publication of the Geological Society of South Africa*, 11, 945pp.
- Seidner, G. and Miller, J.A. (1968). K-Ar age determination on basaltic rocks from South West Africa and their bearing on continental drift. *Earth and Planetary Science Letters*, 4, 451-458.
- Siems, P.L. (1984). Hydrothermal alteration for mineral exploration workshop. Lecture manual. University of the Witwatersrand, Johannesburg, 528pp.
- Sillitoe, R.H. (1985). Ore-related breccias in volcano-plutonic arcs. *Economic Geology*, 80, 1467-1514.
- Slaughter, J., Kerrick, D.M. and Wall, V.J. (1975). Experimental and thermodynamic study of the equilibria in the system CaO-MgO-SiO<sub>2</sub>-H<sub>2</sub>O-CO<sub>2</sub>. *American Journal of Science*, 275, 143-162.

- Smithies, H. (1987). *The geology and alteration-mineralisation of the Van Rooi's Vlei W-Sn deposit, Namaqua Metamorphic Complex, South Africa.* MSc (Economic Geology) Thesis (Unpublished), Rhodes Univeristy, Grahamstown, 124pp.
- South African Committee for Stratigraphy (SACS) (1980). *Stratigraphy of South Africa. Part 1: Lithostratigraphy of the Republic of South Africa, South West Africa/Namibia, and the Republics of Bophuthaswana, Transkei and Venda. Handbook of the Geological Survey of South Africa , 8, 415-423.*
- South West Africa Company (SWACO) (1953). *Gamigab, Brandberg North, Assay Plan.* Unpublished Company map.
- Štemprok, M. (1987). *Greisenisation (A review).* *Geologische Rundschau, 76, 169-175.*
- Stone, M. (1982). *The behaviour of tin and some other trace elements during granite differentiation, West Cornwall, England, 339-355.* In: Evans, A.M. (Ed): *Metallisation Associated with Acid Magmatism.* John Wiley and Sons Ltd., 395pp.
- Storre, B. and Nitsch, K.H. (1983). *Experimental investigation of the stability conditions of a petrological significant calc-silicate assemblage observed in originally marly rocks in the Kuiseb Formation of the Damara Orogen, 795-801.* In: Martin, H. and Eder, F.W. (Eds): *Intracontinental Fold Belts,* Springer-Verlag, Berlin, 945pp.
- Strong, D.F. (1981). *Ore deposit models - 5. A model for granophile mineral deposits.* *Geoscience Canada, 8, 155-161.*
- Swart, R. (In Preparation). *The sedimentology of the Zerrissenes turbidite system, Southern Kaoko Zone, Namibia.* PhD Thesis, Rhodes University, Grahamstown.

- Swart, R. (1987). The Brandberg West Formation-A late Proterozoic carbonate turbidite?. *Communications of the Geological Survey of South West Africa/Namibia*, 3, 19-23.
- Tankard, A.J., Jackson, M.P.A., Eriksson, K.A., Hobday, D.K., Hunter, D.R. and Minter, W.E.L. (1982). *Crustal evolution of Southern Africa. 3,8 Billion years of earth history*. Springer-Verlag, New York, 523pp.
- Taylor, R.G. (1979). *Geology of Tin Deposits*. Elsevier, Amsterdam, 543pp.
- Taylor, B.E. and Slack, J.F. (1984). Tourmalines from Appalachian - Caledonian massive sulphide deposits: textural, chemical and isotopic relationships. *Economic Geology*, 79, 1703-1726.
- Tischendorf, G. (1977). Geochemical and petrographic characteristics of silicic magmatic rocks associated with rare-element mineralisation, 41-96. In: Štemprok, M., Burnol, L. and Tischendorf, G. (Eds): *Metallisation Associated With Acid Magmatism (MAWAM)*, 2, 166pp.
- Townshend, M. (1985). *Some aspects of the geology of the vein systems at the Brandberg West Mine, South West Africa/Namibia*. BSc (Honours) project (Unpublished) Rhodes University, Grahamstown, 27pp.
- Turner, F.J. (1968). *Metamorphic Petrology: Mineralogical and Field Aspects*, McGraw-Hill, New York, 403pp.
- Walraven, F.C. (1985). *A petrographic study of the Goantagab amphibolite and an attempt to determine its possible origin. Marl or mafic?* BSc (Honours) project (Unpublished), Rhodes University, Grahamstown, 24pp.

- Weber, K., Ahrendt, H. and Hunziker, J.C. (1983). Geodynamic aspects of structural and radiometric investigations on the northern and southern margins of the Damara Orogen, South West Africa/ Namibia, 307-319. *Special Publication of the Geological Society of South Africa*, 11, 945pp.
- Windley, B.F. (1984). *The Evolving Continents* (2nd Edition), John Wiley and Sons, New York, 399pp.
- Winkler, H.G.F. (1979). *Petrogenesis of Metamorphic Rocks*. (5th Edition). Springer-Verlag, New York, 348pp.
- Wolf, K.H., Easton, A.J., and Warne, S. (1967). Techniques of examining and analyzing carbonate skeletons, minerals and rocks, 253-341. In: Chilingar, G.V., Bissell, H.J. and Fairbridge, R.W. (Eds): *Carbonate Rocks, Physical and Chemical Aspects*, Elsevier, Amsterdam, 413pp.

APPENDIX 1

DETERMINATION OF MAJOR ELEMENTS BY X-RAY FLUORESCENCE

Major element analyses at Rhodes University are made according to the method outlined by Norrish and Hutton (1969).

Sample preparation is outlined below:

1. Rock splitter:

Used to break up large pieces into match-box size blocks and to remove weathered and stained surfaces.

2. Motorised Jaw Crusher:

Used to reduce blocks to fragments ranging in size from less than 1 cm downwards.

3. Swing Mill:

Fine grinding of crushed samples in Mn-steel vessel.

Pellet and fusion disc preparation:

1. 7,0 g of rock powder from fine-grinding transferred to motorised agate mortar. Sample is ground to a fineness of -300 mesh.
2. 5,0 g of powder pressed into pellet using pressing pressure of approximately 13 tonnes. High silica samples require internal binder (2% solution "Mowiol").
3. Remaining 2,0 g was weighed, heated in furnace at 1000°C for 8 hours, and reweighed to determine LOI. Of this material,  $0,2800 \pm 0,01$  g was weighed and added to 1,500 g flux. This mixture was then heated in Pt crucibles and

pressed while still molten into fusion discs.

X-ray Fluorescence Procedure:

The instrumental settings used on the Philips 1410 X-ray spectrometer are summarised in the table below. Mass absorption coefficients were determined using the Mo-Compton/FE-K-alpha technique described by Nesbitt *et al.*, 1976. Standard calibration and data reduction was achieved by using computer programmes available on XRFFILE on the Rhodes University Mainframe. These programmes allow for position, dead time and background corrections, instrumental drift and spectral line interferences.

Running conditions for x-ray fluorescence

ELEMENT	TUBE	KV	MA	CRYSTAL	TIME (SECS)	COUNTER	COLLIMATOR	SPECIMEN
Si	Cr	55	40	PET	40	flow	coarse	fusion disc
Ti	Cr	55	40	LiF(200)	10	flow	fine	fusion disc
Al	Cr	55	40	PET	40	flow	coarse	fusion disc
Fe	Cr	55	40	LiF(200)	20	flow	fine	fusion disc
Mn	Cr	55	40	LiF(200)	20	flow	coarse	fusion disc
Mg	Cr	55	40	TLAP	100	flow	fine	fusion disc
Ca	Cr	55	40	LiF(200)	10	flow	fine	fusion disc
Na	Cr	55	40	TLAP	100	flow	fine	powder pellet
K	Cr	55	40	LiF(200)	10	flow	fine	fusion disc
P	Cr	55	40	Ge	20	flow	coarse	fusion disc
Sr	W	55	40	LiF(220)	200	scint.	fine	powder pellet
Rb	W	55	40	LiF(220)	200	scint.	fine	powder pellet
Zr	W	55	40	LiF(220)	200	scint.	fine	powder pellet
Y	W	55	40	LiF(220)	200	scint.	fine	powder pellet

Calibration curves were determined from the following international and in-house standards:

- Major elements - NIM-N, BCR, GSP, AGV, DTS, NIM-D.
- Na - G-2, PCC, BCR, AGV, GSP, NIM-G.
- Rb, Sr, Zr, Y - BCR, S-12, AGV, SDC, BHVO.
- MAC's - DTS, BHVO, GSP, BCR, AGV, S-12.

## APPENDIX 2

A Jeol Superprobe 733 wavelength dispersive electron microprobe was used to determine the composition of tourmaline. Highly polished thin sections, that were coated with C under vacuum, were used. Accelerating voltage was 15 kv with a current of 25 nA. Natural silicate standards were used and data reduction was carried out automatically.

### CO<sub>2</sub> DETERMINATIONS

CO<sub>2</sub> determinations were carried out at the Zimbabwe Geological Survey, Harare. A standard method was used in which a pre-determined weight of sample (0,5 - 2,0 g) was digested in concentrated HCl ( $\pm$  10 ml). The gases emitted during reaction were channelled through a system of U-tubes containing Mg-perchlorate (to remove H<sub>2</sub>O), concentrated H<sub>2</sub>SO<sub>4</sub> (to remove any additional H<sub>2</sub>O) and a mixture of copper phosphate and manganese dioxide (to remove sulphur). The CO<sub>2</sub> gas was collected in a U-tube containing a pre-determined weight of "Carbosorb" (soda-lime). The percentage CO<sub>2</sub> in the sample was calculated using the difference in mass of the carbosorb (i.e. before and after the CO<sub>2</sub> was introduced).

### REFERENCES

- Nesbitt, R.W., Mastings, H., Stolz, G.W. and Bruce, D.R. (1976). Matrix corrections in trace element analysis by x-ray fluorescence; an extension of the Compton scattering technique to long wavelengths. *Chemical Geology*, 18, 203-213.
- Norrish, K. and Hutton, J.T. (1969). An accurate x-ray spectrographic method for the analysis of a wide range of geological samples. *Geochemica Cosmochimica Acta*, 38, 1549-1577.